LOCALIZATION AND THE FLOER HOMOLOGY OF STRONGLY INVERTIBLE KNOTS

AAKASH PARIKH

Abstract. We establish two spectral sequences in knot Floer homology associated to a directed strongly invertible knot K: one from the knot Floer homology of K to a two dimensional vector space, and one from the singular knot Floer homology of a singular knot associated to K to the knot Floer homology quotient knot of K. The first of these spectral sequences is used to define a numerical invariant of strongly invertible knots.

Contents

The author was partially supported by NSF CAREER Grant DMS-2019396.

1. Introduction

1.1. **Main results.** A *symmetric knot* $(\widetilde{K},\tau)$ is a knot $\widetilde{K}\subset S^3$ along with a finite order diffeomorphism $\tau:(S^3,\widetilde{K})\to(S^3,\widetilde{K})$. A symmetric knot $\widetilde{K}$ is *strongly invertible* if τ is order 2, orientation preserving, and $|\mathrm{Fix}(\tau)\cap\widetilde{K}|=2$. The study of strongly invertible knots was initiated by Sakuma [Sak86].

The purpose of this paper is to establish two new spectral sequences in knot Floer homology for strongly invertible knots.

Theorem 1.1. *Given $\widetilde{K}$ a strongly invertible knot, there is a spectral sequence with E_1 page equal to $\widehat{HFK}(\widetilde{K},0)\otimes\mathbb{F}[\theta,\theta^{-1}]$ and E_∞ page isomorphic to $\widehat{HF}(S^3)\otimes\mathbb{F}[\theta,\theta^{-1}]$. Every page of this spectral sequence is an invariant of $\widetilde{K}$.*

From Theorem 1.1 we extract a numerical invariant s_τ of strongly invertible knots constructed similarly to many concordance invariants including Rasmussen's s invariant [Ras04], and Hendricks-Lipshitz-Sarkar's $q_\tau(\widetilde{K})$ and $d_\tau(\widetilde{K},m)$ [HLS16], and conjecture that this invariant is an equivariant concordance invariant.

Let $(\widetilde{K},\tau,\widetilde{A})$ be a *directed* strongly invertible knot (DSI) with quotient knot K as in Definition 2.1 and Figure 1.

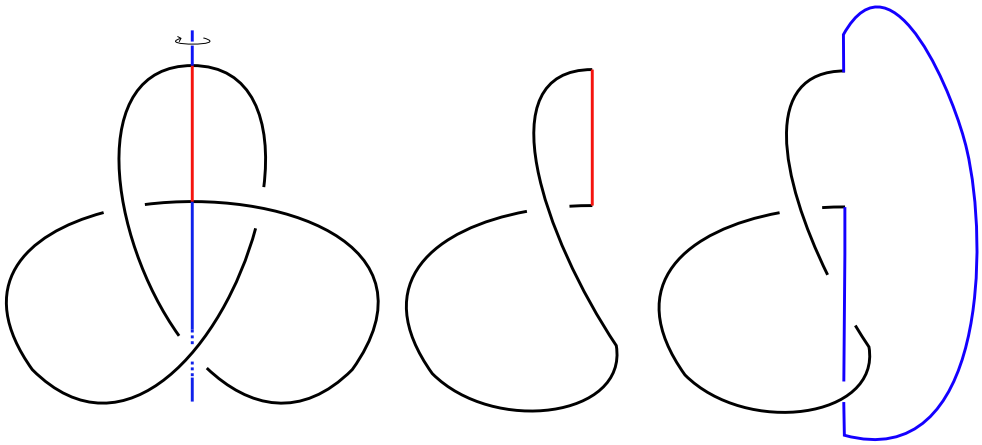

Figure 1. Left: The left handed trefoil 3_1 with strong inversion given by a π-radian rotation about the vertical symmetry axis. Middle: The quotient unknot of the directed strong inversion on 3_1 denoted 3_1^+ with the short vertical red segment chosen as the distinguished half axis. Right: The quotient trefoil of the directed strong inversion on 3_1 denoted 3_1^- with the opposite choice of distinguished half axis.

The next spectral sequence makes use of

- *singular* knot Floer homology, a Floer homology group associated to a singular knot due to Ozsváth, Szabó and Stipsicz [OSS09], [OS09], and
- a singular knot $S_b(\widetilde{K})$ constructed from Boyle and Issa's *butterfly link* $L_b(\widetilde{K})$, and also their *axis linking number* $\widetilde{lk}(\widetilde{K})$ [BI22].

Section 2 contains the definitions of $L_b(\widetilde{K})$, $S_b(\widetilde{K})$ and $\widetilde{lk}(\widetilde{K})$, and Section 3.3 is a brief review of singular knot Floer homology.

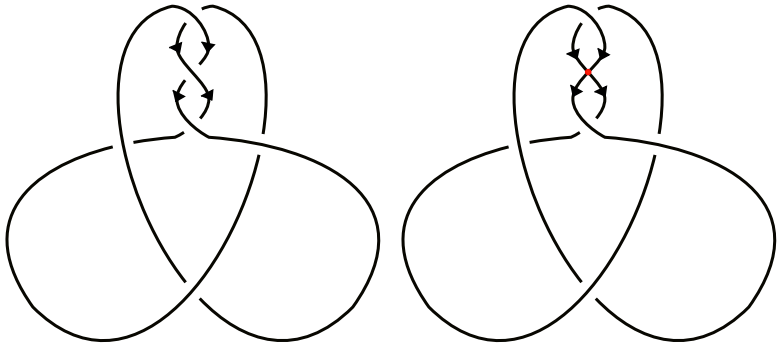

FIGURE 2. Left: The butterfly link $L_b(3_1^+)$. Right: The singular butterfly link $S_b(3_1^+)$.

Theorem 1.2. *Let $(\widetilde{K}, \tau, A)$ be a DSI with quotient knot K and axis linking number $\widetilde{lk}(\widetilde{K}) < 0$. There is a spectral sequence with E_1-page equal to*

$$\widehat{HFK}(S_b(\widetilde{K})) \otimes \mathbb{F}[\theta, \theta^{-1}]$$

and E_∞-page isomorphic to

$$\widehat{HFK}(K) \otimes \mathbb{F}[\theta, \theta^{-1}].$$

Furthermore, this spectral sequence splits along Alexander gradings:

- *For each $a \in \mathbb{Z}$ there is a spectral sequence with E_1 page equal to*

  $$\widehat{HFK}(S_b(\widetilde{K}), 2a + \widetilde{lk}(\widetilde{K}) + \frac{3}{2}) \otimes \mathbb{F}[\theta, \theta^{-1}]$$

  and E_∞ page isomorphic to

  $$\widehat{HFK}(K, a + \widetilde{lk}(\widetilde{K}) + 1) \otimes \mathbb{F}[\theta, \theta^{-1}].$$

- *For any Alexander grading A which cannot be written as $A = 2a + \widetilde{lk} + \frac{3}{2}$, there is spectral sequence with E_1 page equal to $\widehat{HFK}(S_b(\widetilde{K}), A) \otimes \mathbb{F}[\theta, \theta^{-1}]$ and E_∞ page equal to 0.*

Every page of this spectral sequence is an invariant of $\widetilde{K}$.

Remark 1.3. The condition $\widetilde{lk}(\widetilde{K}) < 0$ is not restrictive; if $\widetilde{lk}(\widetilde{K}) > 0$ then $\widetilde{lk}(m(\widetilde{K})) < 0$. Alternatively, there is a slightly different grading shift formula for positive $\widetilde{lk}(\widetilde{K})$. The condition $\widetilde{lk}(\widetilde{K}) < 0$ is chosen for simplicity.

1.2. **Background.** There has been a recent burst of activity in the study of strongly invertible knots and their relation to 3- and 4-dimensional topology. For instance, Boyle–Issa studied equivariant versions of 3- and 4-genera [BI22], and Hirasawa–Hiura–Sakuma computed the equivariant 3-genus for all 2-bridge strongly invertible knots [HHS23]; Alfieri–Boyle introduced an equivariant knot signature [AB21] and used it to give a lower bound on the *butterfly* 4-genus; Di-Prisa showed that the equivariant concordance group is non-abelian [Pri22]; Dai–Mallick–Stoffregen introduced equivariant concordance invariants derived from knot Floer homology and used them to give lower bounds on the equivariant 4-genus [DMS22]; Dai–Kang–Mallick–Park–Stoffregen studied the $(2,1)$-cable of 4_1 and proved that is not slice by showing that the branched double cover $\Sigma((4_1)_{2,1}) \cong S_{+1}(4_1 \# 4_1^r)$ does not bound an equivariant $\mathbb{Z}/2\mathbb{Z}$ homology ball, in part by studying the swapping strong inversion on $4_1 \# 4_1^r$; Lobb–Watson constructed a spectral sequence involving a refinement of Khovanov homology in the presence of an involution for a strongly invertible knot

[LW21]; Lipshitz-Sarkar constructed another spectral sequence involving Khovanov homology of a DSI [LS22] and the annular Khovanov homologies of its two annular quotients, and also used it to distinguish exotic slice disks; and, Hendricks-Mak-Raghunath constructed the analog of the Lipshitz-Sarkar spectral sequence using symplectic Khovanov homology and symplectic annular Khovanov homology [HMR24].

Theorems 1.1 and 1.2 are in part inspired by Lipshitz and Sarkar's spectral sequence. An annular link is a link in a thickened annulus $D^2 \times S^1$, or equivalently a link in S^3 along with a choice of unknotted axis. Given an intravergent diagram as in Definition 2.2 $\widetilde{D}_n$ for a DSI $(\widetilde{K}, \tau, \widetilde{A}')$, there are two naturally associated annular quotient knots, K_0 and K_1 – the quotients of the 2-periodic 0 and 1 resolutions of the central crossing of $\widetilde{D}_n$. The subscript n in $\widetilde{D}_n$ is the winding number of the annular knot K_0 or equivalently the linking number of K_0 with the symmetry axis A. Lipshitz and Sarkar define an *axis moving map*

$$f^+ : \Sigma^{0,0,1} ACKh(K_1) \to ACKh(K_0)$$

on the annular Khovanov chain complexes of K_1 and K_0. Here $\Sigma^{0,0,1}$ denotes a degree shift of $(0,0,1)$ on the triply graded complex $ACKh(K_1)$. With these ingredients in place they prove the following theorem, stated below with small tweaks to conform with terminology used in this paper.

Theorem 1.4. [LS22] *Given an intravergent diagram $\widetilde{D}_n$ for a DSI $\widetilde{K}$ with annular quotient knots K_0 and K_1, there is a spectral sequence with the following properties:*

1. *The E^1 page is $Kh(\widetilde{K}, \mathbb{F}) \otimes \mathbb{F}[\theta, \theta^{-1}]$ with d^1 differential the map $\theta(Id + \tau_*)$ where τ_* is induced by the strong inversion.*
2. *The d^r differential preserves the quantum grading and increases the θ power by r.*
3. *The spectral sequence converges to $AKh(K_0, K_1) \otimes \mathbb{F}[\theta, \theta^{-1}]$, where*

$$ACKh(K_0, K_1) := Cone(\Sigma^{0,0,1} ACKh(K_0) \xrightarrow{f^+} ACKh(K_1)). \tag{1.1}$$

By property (2) above, the spectral sequence splits along quantum gradings; specifically the summand of the spectral sequence in quantum grading $\widetilde{j}$ converges to

$$\bigoplus_{\substack{i,j,k \in \mathbb{Z} \\ i+j=\widetilde{j}-1-3(n-2\cdot \widetilde{lk}(\widetilde{K}))}} H_* Cone(ACKh_{i,j,k-1}(K_1, \mathbb{F}) \xrightarrow{f^+} ACKh_{i,j,k}(K_0, \mathbb{F})) \otimes \mathbb{F}[\theta, \theta^{-1}]. \tag{1.2}$$

Our techniques are inspired by Hendricks' work concerning localization spectral sequences for link Floer homology of doubly periodic knots [Hen15]. A *doubly periodic link* is a link $\widetilde{P} \subset S^3$ equipped with an order 2 orientation preserving diffeomorphism $\tau : (S^3, \widetilde{P}) \to (S^3, \widetilde{P})$ that preserves the orientation of $\widetilde{P}$. The fixed point set of τ is an unknot $\widetilde{A}$ disjoint from $\widetilde{P}$ called the *axis of symmetry*. The *quotient link* of $(\widetilde{P}, \tau)$ is the link P which is the image of $\widetilde{P}$ under the quotient map $q : S^3 \to S^3/\tau \cong S^3$, and $A := q(\widetilde{A})$ is the quotient axis.

Theorem 1.5. [Hen15, HLS16] *There is a spectral sequence with E_1 page equal to $\widehat{HFK}(\widetilde{P}) \otimes V \otimes W \otimes \mathbb{F}[\theta, \theta^{-1}]$ and E_∞ page isomorphic to $\widehat{HFK}(P) \otimes W \otimes \mathbb{F}[\theta, \theta^{-1}]$. Furthermore this spectral sequence splits along Alexander gradings:*

- *For any $a \in \mathbb{Z}$ there is a spectral sequence with E_1 page equal to*

$$\widehat{HFK}(\widetilde{P}, 2a + \frac{1-\lambda}{2}) \otimes V \otimes W \otimes \mathbb{F}[\theta, \theta^{-1}]$$

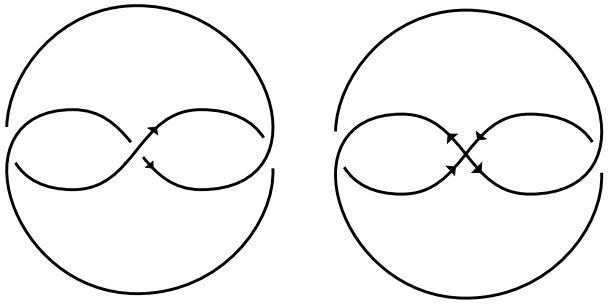

FIGURE 3. Left: An intravergent diagram for 3_1^+. Right: An intravergent diagram for $S_b^1(3_1^+)$.

and E_∞ page isomorphic to

$$\widehat{HFK}(P, a + \frac{1-\lambda}{2}) \otimes W \otimes \mathbb{F}[\theta, \theta^{-1}].$$

- *For any Alexander grading A which cannot be written as $A = 2a + \frac{1-\lambda}{2}$, there is a spectral sequence with E_1 page equal to $\widehat{HFK}(\widetilde{P}) \otimes V \otimes W \otimes \mathbb{F}[\theta, \theta^{-1}]$ and E_∞ page equal to 0.*

where V and W are bigraded two dimensional vector spaces over $\mathbb{F}$ and $\lambda = lk(\widetilde{P}, \widetilde{A}) = lk(P, A)$. Every page of this spectral sequence is an invariant of $(\widetilde{P}, \tau)$.

The spectral sequences of Theorems 1.1, 1.2 and 1.5 are constructed via the following procedure:

(1) Construct a τ-equivariant Heegaard diagram $\widetilde{\mathcal{H}}$ for the symmetric knot.
(2) Identify the fixed point sets of the symmetric product and tori associated to $\widetilde{\mathcal{H}}$ with the symplectic manifold associated to Heegaard data $\mathcal{H} = \widetilde{\mathcal{H}}/\tau$ for the quotient.
(3) In this setting verify the symplectic hypotheses for a *localization isomorphism* in $\mathbb{Z}/2\mathbb{Z}$-equivariant Floer homology are met.

In Hendricks' work the result used for (3) is Seidel-Smith's localization isomorphism [SS10], and in this paper we make use of Large's more general localization isomorphism [Lar19]. The equivariant Heegaard diagrams constructed in [Hen15] have underlying surface S^2 and multiple basepoints because this is the setting in which one of the restrictive hypotheses required by Seidel-Smith's localization theorem – the existence of a *stable normal trivialization* – can be met. The flexibility afforded by the analogous weaker hypothesis in Large's localization theorem – a *stable tangent normal isomorphism* – allows us to make use of higher genus equivariant Heegaard diagrams with minimal basepoints. This is of particular relevance in Theorem 1.1, because an equivariant Heegaard diagram for a DSI with more than 2 basepoints induces a spectral sequence that abuts to 0. For the benefit of the expert reader, we include an example of the symmetric Heegaard diagrams associated to an intravergent diagram for 3_1^+ and $S_b^1(3_1^+)$ in Figures 3 and 4. For the definition of $S_b^n(\widetilde{K})$ we refer the reader to Definition 2.14. The Heegaard diagram for $S_b^1(3_1^+)$ induces a spectral sequence that is identical to the one from Theorem 1.2 besides an Alexander grading shift; it is used as the illustrating example in this paper instead of a Heegaard diagram for $S_b(3_1^+)$ because it is simple.

Organization. This paper is organized as follows. In Section 2 we recall background on strongly invertible knots and singular links. Section 3 is background on Heegaard Floer homology, link Floer homology and singular link Floer homology. In Section 4.2 we introduce Large's localization isomorphism and use it to prove Theorems 1.1 and 1.2, deferring the verification of Large's hypotheses

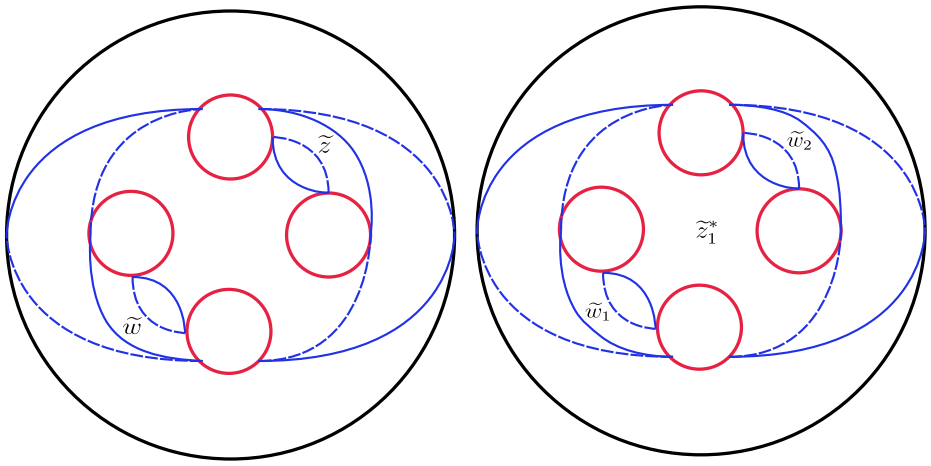

FIGURE 4. Left: A symmetric Heegaard diagram for 3_1^+. Right: A symmetric Heegaard diagram for $S_b^1(3_1^+)$.

to later Sections. Section 5 contains examples of Theorems 1.1 and 1.2 along with a computation of s_τ for all Floer $\delta-$thin and L-space strongly invertible knots. We study the homotopy type and cohomology of the symmetric product of punctured surfaces in Section 6. Section 7 contains a proof of the existence of a *stable tangent normal isomorphism* of the polarization data associated to the fixed point sets of τ. Appendix A is an exposition of a grid diagram based proof of the skein exact triangle for singular knot Floer homology, and an explanation of how this proof pins down absolute Alexander gradings for singular knot Floer homology.

Acknowledgments. The author would like to thank Kristen Hendricks for suggesting this project and providing guidance and support throughout. The author is also grateful to Akram Alishahi, Anna Antal, Keegan Boyle, Jen Hom, Tye Lidman, Robert Lipshitz, Abhishek Mallick, Danielle O'Donnol and Sriram Raghunath for helpful conversations.

2. Topological preliminaries

In this Section we recall basics about strongly invertible knots and singular links.

2.1. Strongly invertible knots.

Definition 2.1. A knot $\widetilde{K} \subset S^3$ is *strongly invertible* if there is an order 2 orientation preserving diffeomorphism $\tau : (S^3, \widetilde{K}) \to (S^3, \widetilde{K})$ that reverses the orientation on $\widetilde{K}$. The fixed point set of τ is an unknotted circle called the *axis of symmetry* that intersects $\widetilde{K}$ in exactly two points denoted by

$$\widetilde{A} := \{x \in S^3 | \tau(x) = x\}.$$

The two points of $\text{Fix}(\tau) \cap \widetilde{K}$ separate $\widetilde{A}$ into two pieces $\widetilde{A} = \widetilde{A}' \cup \widetilde{A}''$ called half-axes. The pair $(\widetilde{K}, \tau)$ along with the choice of an oriented half axis, without loss of generality say $\widetilde{A}'$, is called a *directed strongly invertible knot* (DSI). Say that $q : S^3 \to S^3/\tau \cong S^3$ is the quotient map induced by τ. Defining $A := q(\widetilde{A})$, and $A' = q(\widetilde{A}')$, we see that $q(\widetilde{K})$ is a (knotted) arc whose endpoints lie on the unknotted axis $A \subset S^3$. The *quotient knot* K of a DSI $(\widetilde{K}, \tau, \widetilde{A}')$ is the union of the knotted arc and the chosen half axis; $K := q(\widetilde{K}) \cup A'$.

It is useful to have diagrams for strongly invertible knots that display their symmetry.

Definition 2.2. [BI22, Definition 3.3] Let $(\widetilde{K},\tau)$ be a strongly invertible knot. A knot diagram for $\widetilde{K}$ is

(1) *transvergent* if τ acts as rotation around an axis contained in the diagram, and
(2) *intravergent* if τ acts as rotation around an axis perpindicular to the plane of the diagram.

Remark 2.3. Every strongly invertible knot admits both transvergent and intravergent diagrams. An intravergent diagram for a strongly invertible knot distinguishes a half-axis, namely the one that lies between the over and under strands of the central crossing.

The primary example that we use to illustrate our constructions is the directed strong inversion on the left-handed trefoil $\widetilde{K}=3_1^+$, depicted as a transvergent symmetry (rotation about the short red vertical half axis) in Figure 1, and as an intravergent symmetry in 5. Notice that this DSI has an unknotted quotient, $K=0_1$.

Definition 2.4. Strongly invertible knots $(\widetilde{K}_0,\tau_0)$ and $(\widetilde{K}_1,\tau_1)$ are *equivariantly isotopic* or *equivalent* if there is an orientation preserving diffeomorphism $\phi:S^3\to S^3$ such that $\phi(\widetilde{K}_0)=\widetilde{K}_1$ and $\phi\circ\tau_0=\tau_1\circ\phi$. If $\widetilde{K}_0$ and $\widetilde{K}_1$ are directed with oriented half axes $\widetilde{A_0}'$ and $\widetilde{A_1}'$ they are *equivalent as DSIs* if $\phi(\widetilde{A_0}')=\widetilde{A_1}'$ and ϕ preserves the chosen orientations on the half axes.

Remark 2.5. The data of a DSI consists of the knot $\widetilde{K}$ along with the involution τ and the choice of oriented half axis $\widetilde{A}'$. Indeed, the quotient knot of a directed strong inversion depends on the choice of half axis; for example the strong inversion on the trefoil yields quotient knots equal to the unknot or the trefoil depending on the choice of half axis as seen in Figure 1. However, once we fix a DSI $(\widetilde{K},\tau,\widetilde{A}')$, we abuse notation and refer to $\widetilde{K}$ as the DSI.

See the left hand side of Figure 1 for a transvergent diagram for the unique strong inversion on the trefoil, and the left hand side of Figure 5 for an intravergent diagram for the directed strong inversion on the trefoil 3_1^+.

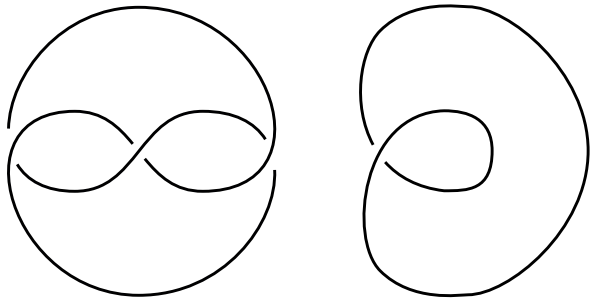

FIGURE 5. Left: An intravergent diagram for 3_1^+. Right: The quotient unknot of 3_1^+.

There is a family of two component 2-periodic links naturally associated to a DSI. The definition of $L_b(\widetilde{K})$ is given in [BI22, Section 1]. This definition is generalized to construct $L_b^n(\widetilde{K})$ for integer values of n in [Pri23, Definition 1.8].

Definition 2.6. [BI22][Pri23] The *n-butterfly link* $L_b^n(\widetilde{K})$ of a DSI $\widetilde{K}$ is the two component 2-periodic link with linking number n constructed by performing an equivariant band move on $\widetilde{K}$ along a band containing the chosen half axis. The 0-butterfly link is *the butterfly link* of $\widetilde{K}$ and is denoted $L_b(\widetilde{K}):=L_b^0(\widetilde{K})$.

See the left hand side of Figure 2 for an illustration of the butterfly link $L_b(3_1^+)$ or part (2) of Figure 6 for an illustration of the 1-butterfly link $L_b^1(3_1^+)$.

Definition 2.7. The *axis linking number* $\widetilde{lk}(\widetilde{K})$ is the linking number of either component of $L_b(\widetilde{K})$ with the symmetry axis $\widetilde{A}$.

We will need the following extension of the definition of $L_b^n(\widetilde{K})$ to half integer values of n.

Definition 2.8. Given $n \in \mathbb{Z}$ and c a negative crossing in the equivariant band used to construct $L_b^n(\widetilde{K})$ in Definition 2.6, then $L_b^{n+\frac{1}{2}}(\widetilde{K})$ is the oriented resolution $(L_b^n(\widetilde{K}))_0$ (c.f Figure 10) at c. If c is instead a positive crossing then $(L_b^n(\widetilde{K}))_0 =: L_b^{n-\frac{1}{2}}(\widetilde{K})$.

See part (4) of Figure 6 for an example of this construction with $\widetilde{K} = 3_1^+$ and $n = \frac{3}{2}$. The quotient knot of $L_b^n(\widetilde{K})$, considered as a doubly periodic link, for each value n is the *same* quotient knot K of the DSI $\widetilde{K}$. For integer values of m, the linking number of $L_b^m(\widetilde{K})$ with the symmetry axis $\widetilde{A}$ is $lk(L_b^m(\widetilde{K}), \widetilde{A}) = \widetilde{lk}(\widetilde{K}) + m$, and the linking number of $L_b^{m+\frac{1}{2}}(\widetilde{K})$ with the $\widetilde{A}$ is given by

$$lk(L_b^{m+\frac{1}{2}}(\widetilde{K}), \widetilde{A}) = \begin{cases} 2(\widetilde{lk}(\widetilde{K}) + m) - 1 & \text{if } \widetilde{lk}(\widetilde{K}) + m > 0 \\ 2(\widetilde{lk}(\widetilde{K}) + m) + 1 & \text{if } \widetilde{lk}(\widetilde{K}) + m < 0 \end{cases}. \tag{2.1}$$

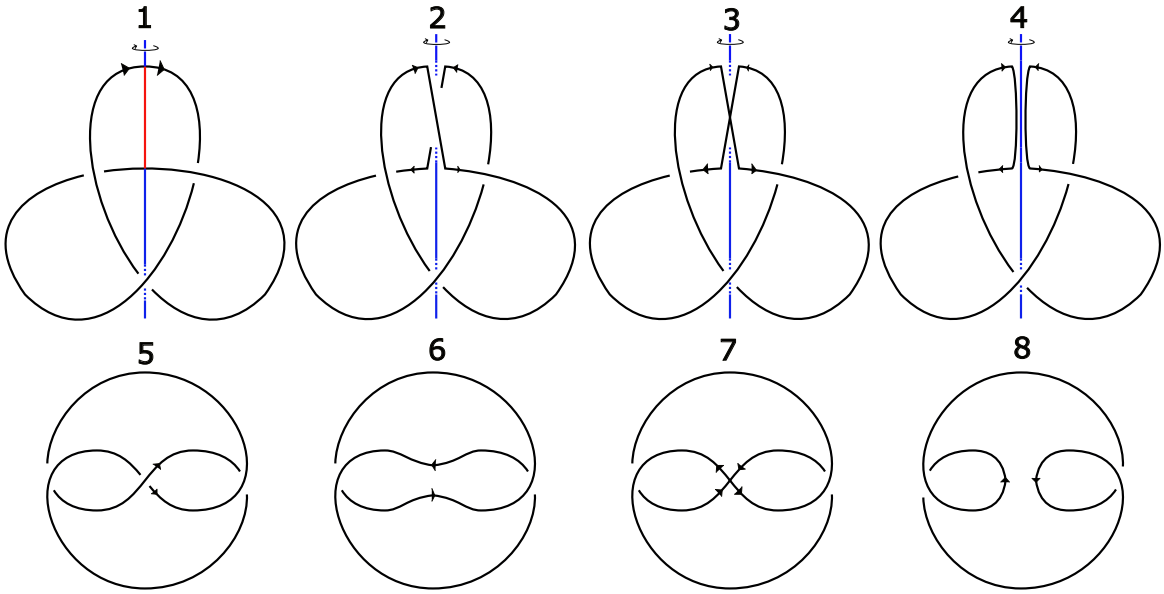

FIGURE 6. (1) A transvergent diagram showing the strong inversion on left handed trefoil 3_1. The symmetry axis is split into two halves corresponding to the DSIs 3_1^+ in red and 3_1^- in blue. (2) A transvergent diagram for $L_b^1(3_1^+)$, the positive Hopf link. (3) A transvergent diagram for the singular link $S_b^1(3_1^+)$, as in Definition 2.14, obtained from singularizing $L_b^1(3_1^+)$. (4) A transvergent diagram for $L_b^{\frac{3}{2}}(3_1^+)$, the unknot. Diagrams (5)-(8) display intravergent perspectives of (1)-(4) respectively.

2.2. **Singular links.** Because of the natural relationship of DSIs and trivalent graphs or equivalently singular knots via appending the distinguished half axis, we will also be interested in a family of singular links $S^n_b(\widetilde{K})$.

Definition 2.9. An *oriented singular link* is an immersion $K : \cup_{i=1}^k S^1 \hookrightarrow S^3$ with transverse double point singularities. Oriented singular links K and K' are *equivalent as oriented singular links* if there is an orientation preserving homeomorphism $h : (S^3, K) \to (S^3, K')$ that preserves a small rigid disk separating the incoming and outgoing strands at each singularity.

Definition 2.10 ([HO17])**.** An *oriented spatial graph* is an orientation preserving embedding f of a directed graph G in S^3,

$$f : G \to S^3.$$

A *transverse spatial graph* is an oriented spatial graph such that there is a small disk $D \subset S^3$ that separates the incoming edges and the outgoing edges for each vertex. Two transverse spatial graphs are equivalent if there is an ambient isotopy between them.

We associate a transverse spatial graph to a singular knot K by taking the vertex set V to be the transverse double point singularities of K and the oriented edges to be the connected components of $K - V$. Considering oriented singular links up to the weaker equivalence relation $\tilde{\ }$ that K and K' are $\tilde{\ }$-equivalent if there is an orientation preserving homeomorphism $h : (S^3, K) \to (S^3, K')$, then K and K' are $\tilde{\ }$-equivalent iff their associated transverse spatial graphs are equivalent.

Definition 2.11. If $f : G \to S^3$ is a transverse spatial graph, then a diagram for f is a projection $D : S^3 \to S^2$ such that if $x \in f(G)$, then $D^{-1}(D(x))$ contains one or two points, and if it contains two points then neither is a vertex of f. Diagrams are similarly defined for oriented singular links, replacing vertex with transverse double point singularity.

Let D be a diagram for a link, and let c be a positive or negative crossing in D. Below we describe two different singular links obtained by replacing the crossing c with a singularity. The first, $S_c(D)$, is the *singularization* of D at c, and the second, $IS_c(D)$, is the *intravergent singularization* of D at c.

Definition 2.12. The *singularization of D at c* is the diagram $S_c(D)$ obtained by performing the local modification seen in Figure 7 at c.

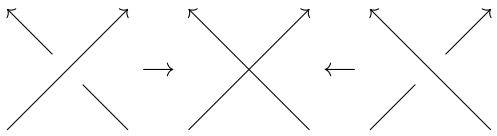

FIGURE 7. Singularizing a positive or negative crossing

Definition 2.13. The *intravergent singularization of D* at c is the diagram $IS_c(D)$ obtained by performing the local modification seen in Figure 8 followed by orientations changes on the rest of D that are forced by the new orientations at c.

It is worth emphasizing the diagrammatic difference between the singularization and intravergent singularization of a crossing. A transverse double point singularity has two incoming and two outgoing strands. In a singularization, the singularity is presented so that the plane of the diagram is transverse to a disk separating the incoming and outgoing arrows. In an intravergent singularization, the singularity is presented with the separating disk *in* the plane of the diagram.

We are now ready to give the definition of the singularized n-butterfly link $S^n_b(\widetilde{K})$.

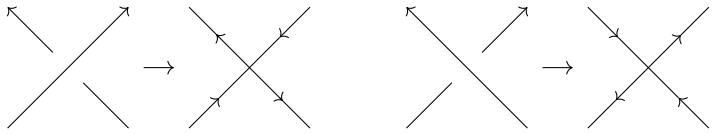

FIGURE 8. Intravergent singularization of a positive (left) or negative (right) crossing.

Definition 2.14. Let $\widetilde{D}$ be a transvergent diagram for a DSI $\widetilde{K}$, $\widetilde{D}_b^n$ be the diagram for $L_b^n(\widetilde{K})$ obtained by surgering in an equivariant band in $\widetilde{D}$, and c be a crossing in that band. Then the *singularlized n-butterfly link of* $\widetilde{K}$ is the singular link $S_b^n(\widetilde{K})$ represented by the diagram $S_c(L_b^n(\widetilde{K}))$. The *singular butterfly link of* $\widetilde{K}$, denoted $S_b(\widetilde{K})$, is the singularized 0-butterfly link $S_b^0(\widetilde{K})$.

In Figure 2 the butterfly link $L_b(3_1^+)$ and the singular butterfly link $S_b(3_1^+)$ are depicted.

Remark 2.15. There is a set of Reidemeister moves for singular link diagrams, analogous to the Reidemeister moves for classical link diagrams. An application of the move labeled $\Omega 5a$ in [BEHY18, Figure 2] shows that $S_b^n(\widetilde{K})$ is independent of the choice crossing c in a diagram for the equivariant band of $L_b^n(\widetilde{K})$, and the other Reidemeister moves guarantee that $S_b^n(\widetilde{K})$ is independent of chosen The Reidemeister move $\mathrm{R}\overline{V}$ in [HO17, Figure 4] further shows that the transverse spatial graph equivalence class of $S_b^n(\widetilde{K})$ is independent of n.

It will be helpful to explain how we can obtain a diagram for $S_b^n(\widetilde{K})$ from an intravergent diagram $\widetilde{D}$ for $\widetilde{K}$: we apply an intravergent singularization as in Definition 2.13 to the central crossing c of $\widetilde{D}$ to obtain a diagram $IS_c(\widetilde{D})$ for $S_b^n(\widetilde{K})$.

Remark 2.16. The value of n will depend on the intravergent diagram $\widetilde{D}$ that we choose. From here on out, we will label intravergent diagrams with a subscript n: if $\widetilde{D}_n$ is an intravergent diagram for $\widetilde{K}$ with central crossing c, then $IS_c(\widetilde{D}_n)$ is a diagram for $S_b^n(\widetilde{K})$. If one applies the equivariant Reidemeister move illustrated in [LS22, Figure 4.1] to the central crossing of a diagram $\widetilde{D}_n$, this has the effect of shifting n by a half integer.

Associated to an intravergent diagram $\widetilde{D}_n$ of $\widetilde{K}$ is a singular skein triple consisting of $S_b^n(\widetilde{K})$ and two 2-periodic resolutions as shown in Figure 9. If the central crossing of $\widetilde{D}_n$ is positive this is called

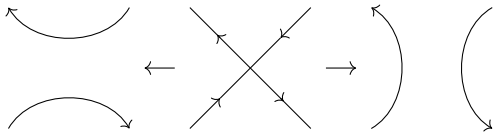

FIGURE 9. A singular skein triple from the intravergent perspective.

a positive singular skein triple, and we denote these 2-periodic resolutions as $S_b^n(\widetilde{K})_+ = L_b^n(\widetilde{K})$ and $S_b^n(\widetilde{K})_0 = L_b^{n-\frac{1}{2}}(\widetilde{K})$. If the central crossing of $\widetilde{D}$ is negative this is called a negative singular skein triple, and we denote these 2-periodic resolutions as $S_b^n(\widetilde{K})_0 = L_b^{n+\frac{1}{2}}(\widetilde{K})$ and $S_b^n(\widetilde{K})_- = L_b^n(\widetilde{K})$. These labeling conventions come from looking at Figure 9 from the transvergent perspective; this is illustrated in case of 3_1^+ in Figure 6.

3. Heegaard Floer homology

In Sections 3.1 and 3.2 we give brief reviews of Heegaard Floer homology and link Floer homology, mainly to set up notation. The original references for this standard material are [OS04c, OS04b, OS08b, Ras03]. In Subsection 3.3 we review singular link Floer homology and grid homology [OSS09, OS09, OSS15]. Equivariant Heegaard diagrams for $\widetilde{K}$, $L_b^n(\widetilde{K})$ and $S_b^n(\widetilde{K})$ are constructed in Section 3.5.

3.1. **Heegaard Floer homology.** Let X be a integer homology 3-sphere. A *Heegaard splitting* of X is a decomposition $X = U_{\boldsymbol{\alpha}} \cup_{\Sigma_g} U_{\boldsymbol{\beta}}$ into two genus g handlebodies glued along their common boundary Σ_g. The handlebodies $U_{\boldsymbol{\alpha}}$ and $U_{\boldsymbol{\beta}}$ are specified by systems of attaching curves $\boldsymbol{\alpha} = \{\alpha_1, \dots, \alpha_{g+n-1}\}$ and $\boldsymbol{\beta} = \{\beta_1, \dots, \beta_{g+n-1}\}$ on Σ_g. Given n basepoints $\boldsymbol{w} = \{w_1, \dots, w_n\} \subset \Sigma_g$ such that each connected component of $\Sigma_g - \boldsymbol{\alpha}$ and $\Sigma_g - \boldsymbol{\beta}$ contains exactly one w_i, the data $\mathcal{H} = (\Sigma_g, \boldsymbol{\alpha}, \boldsymbol{\beta}, \boldsymbol{w})$ defines an *$n-$pointed Heegaard diagram* for X. The α and β curves define two Lagrangians $\mathbb{T}_{\boldsymbol{\alpha}} := \alpha_1 \times \ldots \times \alpha_{g+n-1}$ and $\mathbb{T}_{\boldsymbol{\beta}} := \beta_1 \times \ldots \times \beta_{g+n-1}$ in the symplectic manifold $(\mathrm{Sym}^{g+n-1}(\Sigma_g \backslash \boldsymbol{w}), \omega_{\boldsymbol{\alpha},\boldsymbol{\beta}})$ where $\omega_{\boldsymbol{\alpha},\boldsymbol{\beta}}$ is a symplectic form which agrees with the product symplectic form away from the fat diagonal of the symmetric product as constructed in [Per08]. Then the Heegaard Floer homology of the diagram $\mathcal{H}$ is the Lagrangian Floer homology

$$\widetilde{HF}(\mathcal{H}) := HF(\mathbb{T}_{\boldsymbol{\alpha}}, \mathbb{T}_{\boldsymbol{\beta}}) \tag{3.1}$$

of $(\mathbb{T}_{\boldsymbol{\alpha}}, \mathbb{T}_{\boldsymbol{\beta}})$ computed in $\mathrm{Sym}^{g+n-1}(\Sigma_g \backslash \boldsymbol{w})$. Heegaard Floer homology admits a $\mathbb{Z}$-valued homological (or *Maslov*) grading which we denote by M:

$$\widetilde{HF}(\mathcal{H}) = \bigoplus_{M \in \mathbb{Z}} \widetilde{HF}_M(\mathcal{H}) \tag{3.2}$$

The version of Heegaard Floer homology defined above is not quite a three manifold invariant as it depends on the number of basepoints; if $\mathcal{H}'$ is a k-pointed Heegaard diagram for X and $\mathcal{H}$ is a singly pointed Heegaard diagram for X then

$$\widetilde{HF}(\mathcal{H}') \cong \widetilde{HF}(\mathcal{H}) \otimes (\mathbb{F} \oplus \mathbb{F}_{(-1)})^{\otimes(k-1)}. \tag{3.3}$$

where $\mathbb{F} \oplus \mathbb{F}_{(-1)}$ is the two dimensional vector space with generators in Maslov gradings 0 and -1. The isomorphism class of the homology $\widetilde{HF}(\mathcal{H})$ is independent of the choice of diagram $\mathcal{H}$ for X, and hence is a three manifold invariant denoted $\widehat{HF}(X)$.

3.2. **Link Floer homology.** Next we discuss a link invariant due to Ozsváth, Szabó and independently Rasmussen called link Floer homology, whose definition closely mirrors that of Heegaard Floer homology [OS08a, Ras03]. Given an ℓ-component link $L \subset S^3$, a $2n$-pointed *Heegaard diagram* for L is a quintuple

$$\mathcal{H} = (\Sigma_g, \boldsymbol{\alpha} = \{\alpha_1, \dots, \alpha_{g+n-1}\}, \boldsymbol{\beta} = \{\beta_1, \dots, \beta_{g+n-1}\}, \boldsymbol{w} = \{w_1, \dots, w_n\}, \boldsymbol{z} = \{z_1, \dots, z_n\})$$

such that

- The quadruples $(\Sigma_g, \boldsymbol{\alpha}, \boldsymbol{\beta}, \boldsymbol{w})$ and $(\Sigma_g, \boldsymbol{\alpha}, \boldsymbol{\beta}, \boldsymbol{z})$ are n-pointed Heegaard diagrams for S^3.
- The union of arcs ξ_i connecting each w_i to a z_j on $\Sigma_g - \cup_{i=1}^{g+n-1} \alpha_i$ that are then slightly pushed into the handlebody specified by $\boldsymbol{\alpha}$ and arcs ζ_i connecting each z_j to a w_i on $\Sigma_g - \cup_{i=1}^{g+n-1} \beta_i$ that are then slightly pushed into the handlebody specified by $\boldsymbol{\alpha}$ yields the link L: that is, $\bigcup_i \xi_i \cup \zeta_i = L$.

Then the link Floer homology is

$$\widetilde{HFL}(\mathcal{H}) := HF(\mathbb{T}_{\boldsymbol{\alpha}}, \mathbb{T}_{\boldsymbol{\beta}}) \tag{3.4}$$

where $\mathbb{T}_{\boldsymbol{\alpha}} := \alpha_1 \times \ldots \times \alpha_{g+n-1}$ and $\mathbb{T}_{\boldsymbol{\beta}} := \beta_1 \times \ldots \times \beta_{g+n-1}$, and the right hand side of the Equation (3.4) is the Lagrangian Floer homology $HF(\mathbb{T}_{\boldsymbol{\alpha}}, \mathbb{T}_{\boldsymbol{\beta}})$ computed inside of $\mathrm{Sym}^{g+n-1}(\Sigma_g \backslash (\boldsymbol{w} \cup \boldsymbol{z}))$, again with respect a suitable symplectic form [Per08]. Link Floer homology decomposes as a direct sum along two gradings – the $\mathbb{Z}$ valued homological/Maslov grading, and the *Alexander grading*. Write $L = K_1 \cup \ldots \cup K_\ell$ for a decomposition of L into its ℓ connected components. Define

$$a_i := \begin{cases} 0 & \text{if } \sum_{j \neq i} lk(K_i, K_j) \equiv 0 \pmod 2 \\ \frac{1}{2} & \text{if } \sum_{j \neq i} lk(K_i, K_j) \equiv 1 \pmod 2 \end{cases}$$

and $a := \sum_{i=1}^{\ell} a_i$. Then the Alexander grading takes values in $\mathbb{Z} + a$.

Remark 3.1. In some variations the Alexander grading of a multi-component link is a multi-grading, but we use the collapsed version of this grading defined by adding up all of the multi-gradings.

Link Floer homology in Maslov and Alexander gradings (M, A) is denoted $\widetilde{HFL}_M(\mathcal{H}, A)$:

$$\widetilde{HFL}(\mathcal{H}) = \bigoplus_{(M,A) \in \mathbb{Z} \oplus (\mathbb{Z}+a)} \widetilde{HFL}_M(\mathcal{H}, A). \tag{3.5}$$

This version of link Floer homology depends on the number basepoints; if we let $V := \mathbb{F}_{(0,0)} \oplus \mathbb{F}_{(-1,-1)}$ be the two dimensional vector space with generators in gradings $(0,0)$ and $(-1,-1)$, $\mathcal{H}'$ be a $2k$-pointed Heegaard diagram for L for some $k \geq \ell$, and $\mathcal{H}$ be a 2ℓ pointed Heegaard diagram for L, then

$$\widetilde{HFL}(\mathcal{H}') \cong \widetilde{HFL}(\mathcal{H}) \otimes V^{\otimes(k-\ell)}. \tag{3.6}$$

The isomorphism class of the homology $\widetilde{HFL}(\mathcal{H})$ is independent of the choice of 2ℓ pointed diagram $\mathcal{H}$ for L, and hence is a link invariant denoted $\widehat{HFL}(L)$. We recall the relationship of link Floer homology and the Alexander polynomial $\Delta_L(t) \in \mathbb{Z}[t^{\frac{1}{2}}, t^{-\frac{1}{2}}]$ defined by normalization on the unknot U

$$\Delta_U(t) = 1 \tag{3.7}$$

and the *skein relation*

$$\Delta_{L_+}(t) - \Delta_{L_-}(t) = (t^{\frac{1}{2}} - t^{-\frac{1}{2}})\Delta_{L_0}(t) \tag{3.8}$$

where L_+, L_- and L_0 are as in Figure 10.

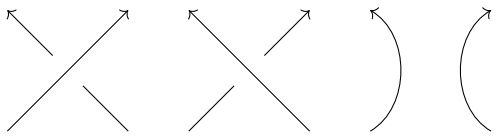

FIGURE 10. L_+, L_- and L_0.

An important property of link Floer homology is that it recovers the Alexander polynomial as its bigraded Euler characteristic [OSS15, Proposition 8.2.10]:

$$\chi(\widehat{HFL}(L)) := \sum_{d,s} t^s \dim(\widehat{HFL}_d(L, s)) = \Delta_L(t) \cdot (t^{\frac{1}{2}} - t^{-\frac{1}{2}})^{\ell-1}. \tag{3.9}$$

3.3. **Singular link Floer homology.** In [OSS09] and [OS09], a variant of Heegaard Floer homology is established for singular links. Here we review this construction. In this Section a singular link will refer to a singular link with exactly one transverse double point singularity and one component. The conventions and equations for singular link Floer homology described below reflect this specialization, but can be easily generalized at the cost of additional notation.

Remark 3.2. We follow the basepoint conventions of [OS09] for singular link Floer homology with the understanding that our $\boldsymbol{w}$ basepoints are their $\mathbb{O}$ basepoints and our $\boldsymbol{z}$ basepoints are their $\mathbb{X}$ basepoints.

Definition 3.3. A *multipointed Heegaard diagram for a singular link* S is a quintuple

(3.10)
$$\mathcal{H} = (\Sigma_g, \boldsymbol{\alpha} = \{\alpha_1, \dots, \alpha_{g+n-1}\}, \boldsymbol{\beta} = \{\beta_1, \dots, \beta_{g+n-1}\}, \boldsymbol{w} = \{w_1, \dots, w_{n+1}\}, \boldsymbol{z} = \{z_1^*, z_2, \dots, z_n\})$$

such that

- The sets of attaching curves $\boldsymbol{\alpha}$ and $\boldsymbol{\beta}$ specify a handlebody decomposition of S^3.
- In each region R of $\Sigma_g - \cup_{i=1}^{g+n-1}\alpha_i$ or $\Sigma_g - \cup_{i=1}^{g+n-1}\beta_i$, $|R \cap \boldsymbol{z}| = 1$ and either $z_1^* \notin R \cap \boldsymbol{z}$ and $|R \cap \boldsymbol{w}| = 1$, or $z_1^* \in R \cap \boldsymbol{z}$ and $|R \cap \boldsymbol{w}| = 2$.
- If one connects w's to z's by arcs ξ_i on $\Sigma_g - \cup_{i=1}^{g+n-1}\alpha_i$ that are then slightly pushed into the $\boldsymbol{\alpha}$ handlebody, and connects z's to w's by arcs ζ_i on $\Sigma_g - \cup_{i=1}^{g+n-1}\beta_i$ that are then slightly pushed into the $\boldsymbol{\beta}$ handlebody, then the union of the ξ and ζ_i recovers the singular link S:
$$(\bigcup \xi_i) \cup (\bigcup \zeta_i) = S.$$

Then the singular link Floer homology of $\mathcal{H}$ is the Lagrangian intersection Floer homology

$$\widetilde{HFK}(\mathcal{H}) := HF(\mathbb{T}_{\boldsymbol{\alpha}}, \mathbb{T}_{\boldsymbol{\beta}}) \tag{3.11}$$

where $\mathbb{T}_{\boldsymbol{\alpha}} := \alpha_1 \times \ldots \times \alpha_{g+n-1}$, $\mathbb{T}_{\boldsymbol{\beta}} := \beta_1 \times \ldots \times \beta_{g+n-1} \subset \mathrm{Sym}^{g+n-1}(\Sigma_g \backslash (\boldsymbol{w} \cup \boldsymbol{z}))$ and the ambient symplectic manifold is $\mathrm{Sym}^{g+n-1}(\Sigma_g \backslash (\boldsymbol{w} \cup \boldsymbol{z}))$ equipped with an appropriate symplectic form [Per08]. Singular link Floer homology also decomposes as a bigraded sum on a Maslov (homological) and Alexander grading:

$$\widetilde{HFK}(\mathcal{H}) = \bigoplus_{(d,s) \in \mathbb{Z} \oplus (\mathbb{Z}+a)} \widetilde{HFK}_d(\mathcal{H}, s) \tag{3.12}$$

where $a = \frac{1}{2}$ if resolving the singularity of S yields a 2 component link and $a = 0$ if desingularizing S yields a knot; refer to Figure 7 for a reminder of what is meant by (de)singularization. Singular link Floer homology again depends on the number of basepoints. If $\mathcal{H}'$ is a Heegaard diagram for S with $|\boldsymbol{z}| = |\boldsymbol{w}| - 1 = k$ then and $\mathcal{H}$ is a Heegaard diagram for S with $|\boldsymbol{z}| = |\boldsymbol{w}| - 1 = 1$ then

$$\widetilde{HFK}(\mathcal{H}') \cong \widetilde{HFK}(\mathcal{H}) \otimes V^{\otimes(k-1)} \tag{3.13}$$

where $V = \mathbb{F}_{(0,0)} \oplus \mathbb{F}_{(-1,-1)}$ is as in the last Section. The homology $\widetilde{HFK}(\mathcal{H})$ is independent of choice of triply pointed Heegaard diagram for S, and hence is a singular link invariant denoted $\widetilde{HFK}(S)$. Singular links also have Alexander polynomials, characterized by either of the skein relations

$$\Delta_{S_+}(t) = \Delta_S(t) + t^{\frac{1}{2}}\Delta_{S_0}(t) \tag{3.14}$$

or

$$\Delta_{S_-}(t) = \Delta_S(t) + t^{-\frac{1}{2}}\Delta_{S_0}(t) \tag{3.15}$$

where S, S_-, S_+ and S_0 are as in Figure 11. The Alexander polynomials of S_+, S_- and S_0 are inductively defined, as each of these potentially singular links will have one fewer singularity than S.

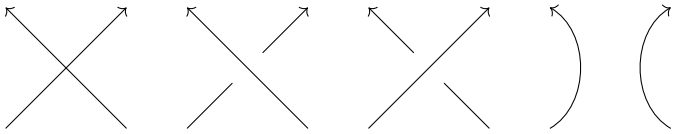

FIGURE 11. S, S_-, S_+ and S_0.

Singular link Floer homology recovers the Alexander polynomial of a singular link as its bi-graded Euler characteristic [OSS09, Theorem 1.1]:

$$\chi(\widehat{HFK}(S)) = \sum_{d,s} t^s \dim(\widehat{HFK}(S), s) = \Delta_S(t). \tag{3.16}$$

In direct analogy to the skein triangle of link Floer homology of [OS04b, Section 8] which categorifies the skein relation Equation (3.8) , there are *singular skein exact triangles* that recover the singular skein relations Equations (3.14) and (3.15) upon taking bi-graded Euler characteristics.

Proposition 3.4. [OS09, Theorem 4.1] *Let (S, S_0, S_+) be a positive singular skein triple. Then for m sufficiently large there is an exact triangle*

$$\begin{array}{ccc} \widehat{HFK}(S_0) \otimes V^{\otimes m} & \longrightarrow & \widehat{HFK}(S_+) \otimes V^{\otimes (m-1)} \\ & \nwarrow \quad \swarrow & \\ & \widehat{HFK}(S) \otimes V^{\otimes m} & \end{array} \tag{3.17}$$

Similarly, if (S, S_0, S_-) is a negative singular skein triple, then for m sufficiently large there is an exact triangle

$$\begin{array}{ccc} \widehat{HFK}(S_-) \otimes V^{\otimes (m-1)} & \longrightarrow & \widehat{HFK}(S_0) \otimes V^{\otimes m} \\ & \nwarrow \quad \swarrow & \\ & \widehat{HFK}(S) \otimes V^{\otimes m} & \end{array} \tag{3.18}$$

Proof. The proof is very similar to the ordinary link Floer homology case and may be found in the Appendix. □

3.4. **Grid homology.** Link Floer homology has a combinatorial reformulation, called grid homology. We give a lightning review of grid homology here; for more details the reader is referred to [OSS15]. Grid homology is used in the proof of Proposition 3.4 given in Appendix and in the construction of the spherical grid diagrams of Section 3.5.

A *grid diagram* $\mathbb{G}$ for a possibly singular link L is a Heegaard diagram on the torus with $m = |\boldsymbol{\alpha}| = |\boldsymbol{\beta}|$. Traditionally these diagrams are drawn on an $m \times m$ grid with sides identified, and the α (respectively β) curves are the horizontal (respectively vertical) rulings of this grid. The basepoints $\boldsymbol{w} = \{w_1, \ldots, w_a\}$ are instead written as $\mathbb{O} = \{O_1, \ldots, O_a\}$ markings, and similarly the basepoints $\boldsymbol{z}$ are written as $\mathbb{X} = \{X_1, \ldots, X_n\}$ markings, with z_1^* written instead as XX in the case that L is singular. Recall that $a = n + 1$ if L is singular and $a = n$ otherwise. See Figures 14 and 15 for examples of grid diagrams. A grid diagram is an example of a *nice diagram*, meaning

that all of the elementary regions that don't contain a basepoint are rectangles or bigons. One can compute the differential of the Floer chain complex associated to a nice Heegaard diagram purely combinatorially by work of Sarkar and Wang [SW10]. This incarnation of link Floer homology was elaborated by Manolescu, Ozsváth and Szabó so that many features of link Floer homology have explicit formulas in terms of combinatorics of the grid diagram $\mathbb{G}$. In particular, there are formulas for the Alexander and Maslov grading of grid homology generators *in the case that L is non-singular* as follows. Let x^{NWO} and x^{NWX} denote the grid states obtained by marking the top left corner of each box containing an O or X respectively. Notice that x^{NWO} is only a valid grid state if L is non-singular. Define functions $M_{\mathbb{O}}, M_{\mathbb{X}} : \mathbf{S}(\mathbb{G}) \to \mathbb{Z}$ by setting

$$M_{\mathbb{O}}(x^{NWO}) = M_{\mathbb{X}}(x^{NWX}) = 0 \tag{3.19}$$

,

$$M_{\mathbb{O}}(x) - M_{\mathbb{O}}(y) = 1 - 2|r \cap \mathbb{O}| + 2|x \cap \mathrm{Int}(r)| \tag{3.20}$$

and

$$M_{\mathbb{X}}(x) - M_{\mathbb{X}}(y) = 1 - 2|r \cap \mathbb{X}| + 2|x \cap \mathrm{Int}(r)| \tag{3.21}$$

where x and y are grid states that differ at exactly two points and $r \in Rect(x, y)$ is any rectangle with bottom left and top right corners in x, and bottom right and top left corners in y. Then the Maslov grading $M(x)$ is given by

$$M(x) := M_{\mathbb{O}}(x) \tag{3.22}$$

and if L has ℓ components, the Alexander grading $A(x)$ is given by

$$A(x) := \frac{1}{2}(M_{\mathbb{O}}(x) - M_{\mathbb{X}}(x)) - \frac{m-\ell}{2}. \tag{3.23}$$

Consider an $m \times m$ grid diagram $\mathbb{G}$ for a knot C with a distinguished negative crossing c that is represented in $\mathbb{G}$ by the local picture on the left hand side of Figure 12. Marking the empty square in the center of the distinguished crossing of $\mathbb{G}$ with an XX and relabeling half of the $X's$ and $O's$ of $\mathbb{G}$ as forced by the local picture on the right hand side of Figure 12, we obtain a diagram $\mathbb{G}_S$ for $S = IS_c(C)$, the intravergent singularization of C at c (cf. Definition 2.13). Performing the local modifications in Figure 13 to $\mathbb{G}_S$ yields $(m+1) \times (m+1)$ grid diagrams $\mathbb{G}_-$ and $\mathbb{G}_0$ for S_- and S_0 respectively. This is illustrated in the case of the trefoil in Figures 14 and 15.

Remark 3.5. The reasons we start with C and $\mathbb{G}$ instead of S and $\mathbb{G}_S$ are twofold. Firstly, by specifying that S arises from an intravergent singularization performed at a negative crossing, it is automatically determined that the two "resolutions" of S shown in Figure 13 are in fact S_- and S_0 (rather than S_0 and S_+). Secondly, this is the situation relevant in this paper with $C = \widetilde{K}$ and $S = S^n_b(\widetilde{K})$.

3.5. **Equivariant Heegaard diagrams for strongly invertible knots.** Let $\widetilde{D}_n$ be a $2g-1$ crossing intravergent diagram, as in Definition 2.2 and Remark 2.16, for a DSI $\widetilde{K}$. Assume for simplicity that $\widetilde{D}_n$ has negative central crossing. Let $\mathbb{G}$ be an $(2k+1) \times (2k+1)$ τ-equivariant planar grid realization of $\widetilde{D}_n$ with associated grid diagrams $\mathbb{G}_S$, $\mathbb{G}_0$ and $\mathbb{G}_-$ for $S^n_b(\widetilde{K}), L_b^{n+\frac{1}{2}}(\widetilde{K})$ and $L^n_b(\widetilde{K})$. Recall that performing an intravergent singularization at the central crossing c of $\widetilde{D}_n$ yields a diagram $IS_c(\widetilde{D}_n)$ of $S^n_b(\widetilde{K})$. In this Section we construct the following Heegaard diagrams.

(1) A doubly pointed genus $2g$ diagram $\widetilde{\mathcal{H}}(\widetilde{D}_n)$ for $\widetilde{K}$.
(2) A triply pointed genus $2g$ diagram $\widetilde{\mathcal{H}}_S(\widetilde{D}_n)$ for $S^n_b(\widetilde{K})$.

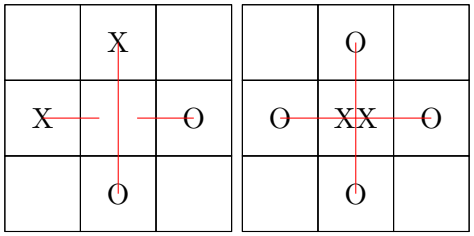

FIGURE 12. Left: The grid diagram $\mathbb{G}$ for C at the distinguished negative crossing c. Right: The modification to move from $\mathbb{G}$ to a grid diagram $\mathbb{G}_S$ for $IS_c(C)$.

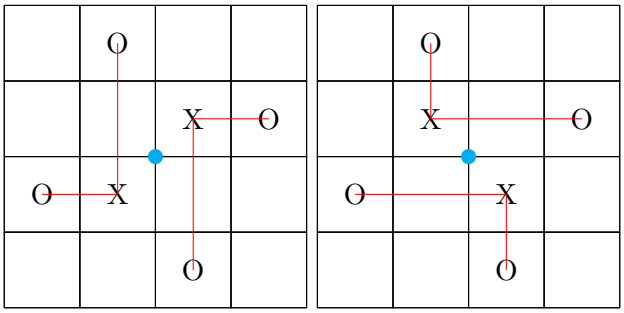

FIGURE 13. Left: Local modifications to move from $\mathbb{G}_S$ to a diagram $\mathbb{G}_-$ for S_-. Right: Local modifications to move from $\mathbb{G}_S$ to a diagram $\mathbb{G}_0$ for S_0.

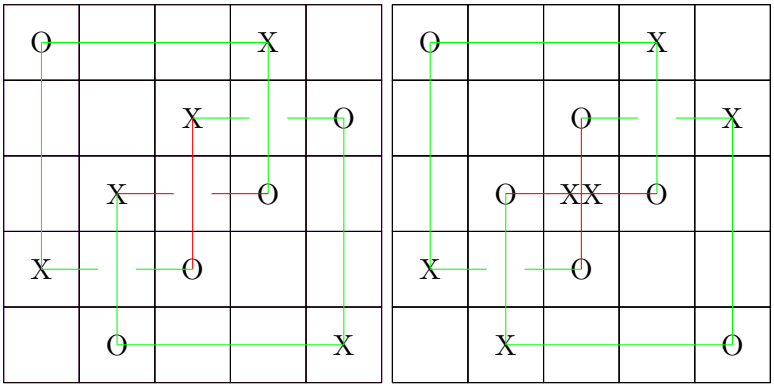

FIGURE 14. Left: A grid diagram $\mathbb{G}$ for an intravergent picture of 3_1^+. Right: A grid diagram $\mathbb{G}_S$ for $S_b^1(3_1^+)$ formed from $\mathbb{G}$ by marking the center square with an XX and swapping the labeling of half of the existing X's and $O's$.

(3) A multi-pointed genus 0 diagram $\mathbb{G}_S^{\text{sphere}}$ for $S_b^n(\widetilde{K})$.
(4) For $* = 0, -$, multipointed genus 0 diagrams $Ax\mathbb{G}_*^{\text{sphere}}$ for $S_b^n(\widetilde{K})_* \cup \widetilde{A}$. The prefix Ax stands for axis, as these are diagrams for butterfly links along with their orientation reversed symmetry axes.

We also describe the quotient diagrams associated to the τ-action.

3.5.1. *A doubly pointed Heegaard diagram for a strongly invertible knot.* Briefly, the doubly pointed Heegaard diagram $\widetilde{\mathcal{H}}(\widetilde{D}_n)$ for $\widetilde{K}$ is the same as the "pringle chip" Heegaard diagram derived from a

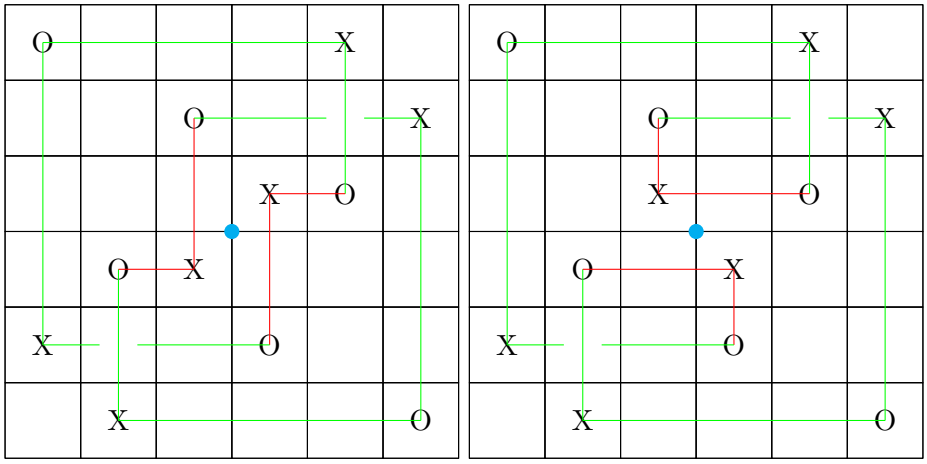

FIGURE 15. Left: The grid diagram $\mathbb{G}_-$ for the Hopf link $L^1_b(\widetilde{K})$. Right: The grid diagram $\mathbb{G}_0$ for the unknot $L^{\frac{3}{2}}_b(\widetilde{K})$

knot diagram in [OS04a, Proposition 12.1] except at the central crossing where we instead use the placement of basepoints and β curves seen in Figure 16. We now explain this in more detail. Ignore the crossing data on $\widetilde{D}_n$ to obtain an immersed curve in the plane C with $2g-1$ double points. Let $\widetilde{\Sigma}$ be the boundary of a τ-equivariant regular neighborhood of C in S^3. For each of the $2g$ bounded regions in the complement of C, put attaching curves $\widetilde{\boldsymbol{\alpha}} = \{\widetilde{\alpha}_1, \dots, \widetilde{\alpha}_{2g}\}$ on $\widetilde{\Sigma}$. Pick the labels on the $\widetilde{\alpha}$ circles so that $\tau(\widetilde{\alpha}_i) = \widetilde{\alpha}_{g+i}$ for $i = 1, \dots, g$. Corresponding to the central crossing in $\widetilde{D}_n$, in the Heegaard diagram label two meridians for $\widetilde{K}$ as $\widetilde{\beta}_1$ and $\widetilde{\beta}_{g+1}$, and place two basepoints $\widetilde{w}$ and $\widetilde{z}$ in such a way that $\tau(\widetilde{w}) = \widetilde{z}$ as indicated in Figure 16. Notice that $\tau(\widetilde{\beta}_1) = \widetilde{\beta}_{g+1}$. For each

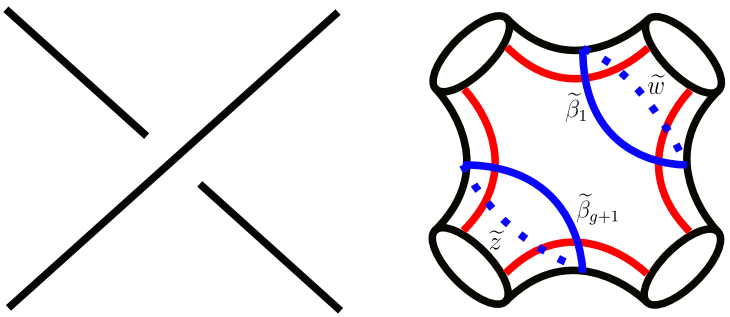

FIGURE 16. The placement of β curves for the Heegaard diagram $\widetilde{\mathcal{H}}(\widetilde{D}_n)$ near the central crossing.

of the non-central $2g-2$ crossings in $\widetilde{D}_n$, insert a $\widetilde{\beta}$ curve on $\widetilde{\Sigma}$ as shown in Figure 17 labeled as $\widetilde{\beta}_2, \dots, \widetilde{\beta}_g, \widetilde{\beta}_{g+2}, \dots, \widetilde{\beta}_{2g}$ in such a way that $\tau(\widetilde{\beta}_i) = \widetilde{\beta}_{g+i}$ for $i = 2, \dots, g$. Then we define

$$\widetilde{\mathcal{H}}(\widetilde{D}_n) := (\widetilde{\Sigma}, \widetilde{\boldsymbol{\alpha}} = \{\widetilde{\alpha}_1, \dots, \widetilde{\alpha}_{2g}\}, \widetilde{\boldsymbol{\beta}} = \{\widetilde{\beta}_1, \dots, \widetilde{\beta}_{2g}\}, \widetilde{\boldsymbol{w}} = \{\widetilde{w}\}, \widetilde{\boldsymbol{z}} = \{\widetilde{z}\}).$$

An example of a Heegaard diagram thus constructed for $\widetilde{D}_n$ the intravergent diagram (5) of Figure 6 is shown on the left side of Figure 4.

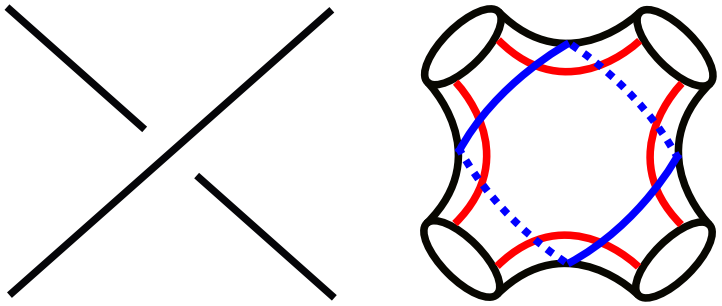

FIGURE 17. The placement of β curves for the Heegaard diagrams $\widetilde{\mathcal{H}}(\widetilde{D}_n)$ and $\widetilde{\mathcal{H}}_S(\widetilde{D}_n)$ near a non-central crossing.

Let Σ be the closed orientable genus g surface obtained by quotienting $\widetilde{\Sigma}$ by τ, and let $\ell_\tau : \widetilde{\Sigma} \to \Sigma$ denote the quotient map. Defining $z := \ell_\tau(\widetilde{w}) = \ell_\tau(\widetilde{z})$, the restriction of ℓ_τ to $\widetilde{\Sigma}\backslash\{\widetilde{w}, \widetilde{z}\}$ has image the once punctured genus g surface $\Sigma\backslash\{z\}$. The quotient of $\mathcal{H}(\widetilde{D}_n)$ by τ is a genus g singly pointed Heegaard diagram

$$\widetilde{\mathcal{H}}(\widetilde{D}_n)/\tau := (\Sigma, \boldsymbol{\alpha} := \ell_\tau(\widetilde{\boldsymbol{\alpha}}), \boldsymbol{\beta} := \ell_\tau(\widetilde{\boldsymbol{\beta}}), z).$$

For an argument that $\widetilde{\mathcal{H}}(\widetilde{D}_n)/\tau$ is a Heegaard diagram for S^3 see Remark 3.6.

3.5.2. *A triply pointed Heegaard diagram for the singularized n-butterfly link.* The first Heegaard diagram $\widetilde{\mathcal{H}}_S(\widetilde{D}_n)$ that we construct for $S^n_b(\widetilde{K})$ will have the same underlying surface $\widetilde{\Sigma}$ and the same set of $\widetilde{\alpha}$ and $\widetilde{\beta}$ curves as the Heegaard diagram $\widetilde{\mathcal{H}}(\widetilde{D}_n)$. The only difference is the number, placement and labeling of basepoints; near the central singular crossing, we have the corresponding piece of the Heegaard diagram shown in Figure 18.

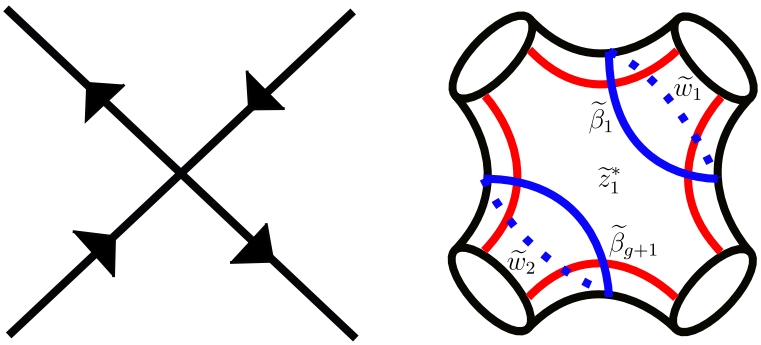

FIGURE 18. The placement of $\widetilde{\beta}$ curves for the Heegaard diagram $\widetilde{\mathcal{H}}_S(\widetilde{D}_n)$ near the central singular crossing.

In summary, we define

$$\widetilde{\mathcal{H}}_S(\widetilde{D}_n) := (\widetilde{\Sigma}, \widetilde{\boldsymbol{\alpha}} = \{\widetilde{\alpha}_1, \ldots, \widetilde{\alpha}_{2g}\}, \widetilde{\boldsymbol{\beta}} = \{\widetilde{\beta}_1, \ldots, \widetilde{\beta}_{2g}\}, \widetilde{\boldsymbol{w}} = \{\widetilde{w}_1, \widetilde{w}_2\}, \widetilde{\boldsymbol{z}} = \{\widetilde{z}_1^*\}).$$

An example of a Heegaard diagram thus constructed for the intravergent diagram (7) of Figure 6 is shown on the right of Figure 4, which we produce again in this Section for the readers convenience.

Remark 3.6. The quotient of $\widetilde{\mathcal{H}}_S(\widetilde{D}_n)$ by τ is the doubly pointed Heegaard diagram for the quotient knot K one would obtain by following the prescription of Proposition 12.1 in [OS04a] for the quotient

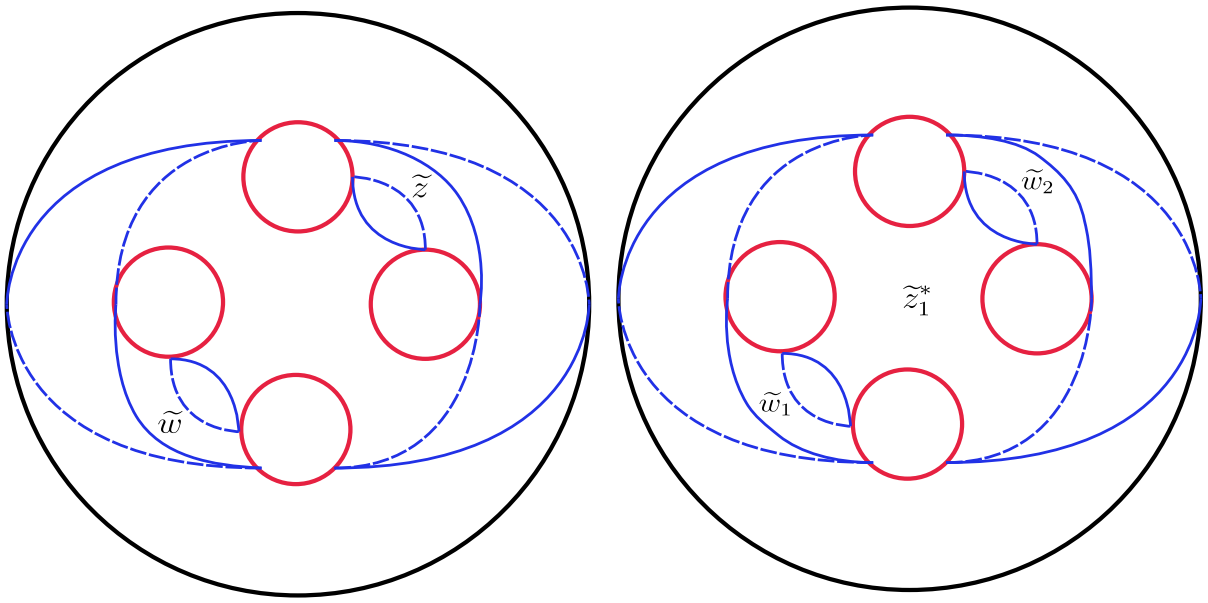

diagram D_n for K. The quotient of $\widetilde{\mathcal{H}}(\widetilde{D}_n)/\tau$ is the same quotient Heegaard diagram but with only one basepoint and hence is a Heegaard diagram for S^3.

3.5.3. *Spherical grid diagrams.* Let $\mathbb{G}$ be any $m \times m$ grid diagram. We construct the *spherical grid diagram* $\mathbb{G}^{\text{sphere}}$ in the following way.

- Place $(m-1)$ α and β curves that intersect in two $(m-2) \times (m-2)$ grids on the top and bottom of the sphere.
- The bottom grid contains no markings.
- The top grid is marked with basepoints according to $\mathbb{G}$. More precisely, the markings in rows and columns 1 and m of $\mathbb{G}$ are placed to the left, right, top and bottom of β_1, β_{m-1}, α_1 and α_{m-1} respectively as indicated by the pink shading in Figure 19, and the center $(m-2) \times (m-2)$ subgrid of $\mathbb{G}$ gets placed in the top $(m-2) \times (m-2)$ grid of $\mathbb{G}_S^{\text{sphere}}$.

3.5.4. *Spherical grid diagrams for links with an axis.* In this Subsection $*$ stands for either 0 or $-$. Recall the grid diagrams $\mathbb{G}_*$, pictured in the case of 3_1^+ in Figure 15. Noticing that the grid number $2k+2$ of $\mathbb{G}_*$ is even, let $\mathbb{G}_*^{\text{I}}$, $\mathbb{G}_*^{\text{II}}$, $\mathbb{G}_*^{\text{III}}$ and $\mathbb{G}_*^{\text{IV}}$ denote the four quadrants of $\mathbb{G}_*$. To construct $Ax\mathbb{G}_*^{\text{sphere}}$, place $(2k+2)$ α and β curves that interlace in two $(2k+1) \times (2k+1)$ grids on the top and bottom of the sphere, and decorate these grids as follows. The bottom grid is empty besides a z marking in the center. The top grid has a w marking in the center, and the remaining grid formed by removing the central row and column of the top grid is filled in with $\mathbb{G}_*^{\text{I}}$, $\mathbb{G}_*^{\text{II}}$, $\mathbb{G}_*^{\text{III}}$ and $\mathbb{G}_*^{\text{IV}}$. The result is a Heegaard diagram compatible with the link

$$S_b^n(\widetilde{K})_* \cup \widetilde{A} = \begin{cases} L_b^{n+\frac{1}{2}}(\widetilde{K}) \cup \widetilde{A} & \text{when } * = 0 \\ L_b^n(\widetilde{K}) \cup \widetilde{A} & \text{when } * = - \end{cases}.$$

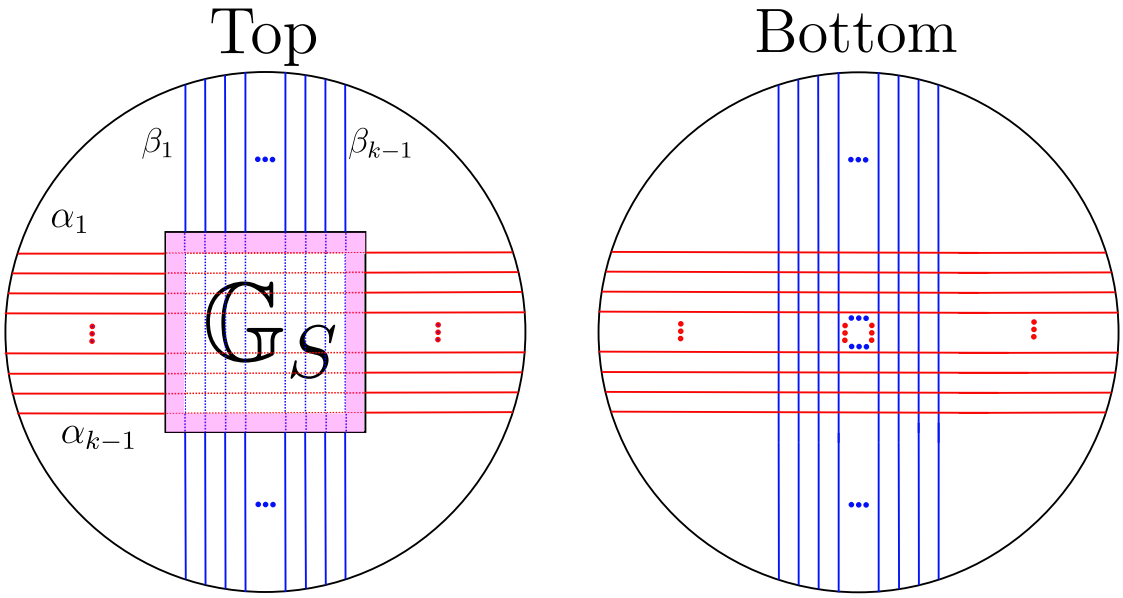

FIGURE 19. The Heegaard diagram $\mathbb{G}_S^{\text{sphere}}$ for the singular link consisting of $S_b^n(\widetilde{K})$ and a separated unknotted component.

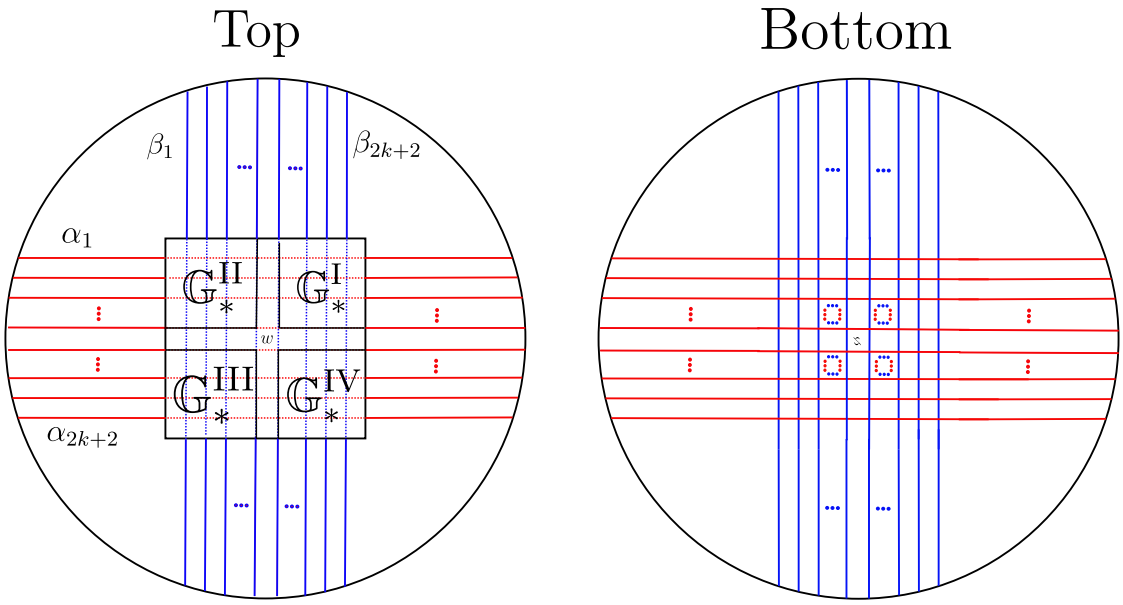

FIGURE 20. The Heegaard diagram $Ax\mathbb{G}_*^{\text{sphere}}$ for the link $(S_b^n(\widetilde{K}))_* \cup \widetilde{A}$.

3.5.5. *The action on gradings.* The strong inversion τ on $\widetilde{K}$ induces $\mathbb{Z}/2\mathbb{Z}$ actions on the equivariant Heegaard diagrams $\widetilde{\mathcal{H}}(\widetilde{D}_n)$ and $\widetilde{\mathcal{H}}_S(\widetilde{D}_n)$ which in turn induce $\mathbb{Z}/2\mathbb{Z}$ actions

$$\tau_* : \widehat{HFK}(\widetilde{K}) \to \widehat{HFK}(\widetilde{K})$$

and

$$\tau_* : \widehat{HFK}(S^n_b\widetilde{K}) \to \widehat{HFK}(S^n_b\widetilde{K}).$$

Proposition 3.7. *The τ_* action on $\widehat{HFK}(\widetilde{K})$ has the following properties:*

(1) For a homogeneous element $x \in \widehat{HFK}(\widetilde{K})$,

$$A(\tau_*(x)) = -A(x).$$

(2) If y is a homogeneous τ-equivariant element of $\widehat{HFK}(\widetilde{K})$ then $A(y) = 0$.

(3) For a homogeneous element $x \in \widehat{HFK}(\widetilde{K})$ with $A(x) = 0$,

$$M(\tau_*(x)) = M(x).$$

Proof. Let x and y be any two homogeneous elements of $\widehat{HFK}(\widetilde{K})$. Then if ϕ is a Whitney disk connecting x and y, $\tau(\phi)$ is a Whitney disk connecting $\tau_*(x)$ and $\tau_*(y)$. Furthermore, since τ switches the z and w basepoints of $\widetilde{\mathcal{H}}(\widetilde{D}_n)$, we have that

$$A(x) - A(y) = n_z(\phi) - n_w(\phi) = n_w(\tau(\phi)) - n_z(\tau(\phi)) = A(\tau_*(y)) - A(\tau_*(x))$$

and therefore

$$A(x) + A(\tau_*(x)) = A(y) + A(\tau_*(y)).$$

Therefore $A(x)+A(\tau_*(x))$ is a constant independent of the choice of x. The symmetry $\widehat{HFK}_*(\widetilde{K}, A) \cong \widehat{HFK}(\widetilde{K}, -A)$ forces this constant to be equal to 0. The second claim follows immediately from the first. For the last claim, let y be a τ-equivariant generator, and let ϕ be a Whitney disk from x to y. Then since $A(x) = A(y) = 0$,

$$n_z(\phi) = n_w(\phi) = n_z(\tau(\phi)) = n_w(\tau(\phi)).$$

Therefore,

$$M(x) - M(y) = \mu(\phi) - 2n_w(\phi) = \mu(\tau(\phi)) - 2n_w(\tau(\phi)) = M(\tau_*(x)) - M(\tau_*(y)) = M(\tau_*(x)) - M(y)$$

which proves the third claim. □

We have the analogous proposition for the τ_* action on $\widehat{HFK}(S^n_b(\widetilde{K}))$ which follows because τ preserves the $\mathbf{w}$ and $\mathbf{z}$ sets of $\widetilde{\mathcal{H}}_S(\widetilde{D}_n)$.

Proposition 3.8. *For a homogeneous element $x \in \widehat{HFK}(S^n_b(\widetilde{K}))$,*

$$A(x) = A(\tau_*(x))$$

and

$$M(x) = M(\tau_*(x)).$$

4. Proofs of the main theorems

Section 4.1 lays out hypotheses which, when met, allow for the application of Large's localization theorem for Lagrangian Floer homology, recapped in Theorem 4.4. In Section 4.2, we apply Theorem 4.4 *under the assumption that its technical hypotheses are met* to derive Theorems 1.1 and 1.2. Sections 6 and 7 are devoted to demonstrating that the hypotheses of Theorem 4.4 are met in our setup.

4.1. Polarization data and Large's localization theorem.

The following definitions and theorem originate from Section 3.2 of Large's paper [Lar19].

Definition 4.1. Let (M, L_0, L_1) be a symplectic manifold equipped with two Lagrangian submanifolds. A set of *polarization data for* (M, L_0, L_1) is a triple $\mathfrak{p} = (E, F_0, F_1)$ where $E \twoheadrightarrow M$ is a symplectic vector bundle and F_i is a Lagrangian subbundle of $E|_{L_i}$ for $i = 0, 1$.

Letting $\underline{\mathbb{C}}$ and $\underline{\mathbb{R}}$ denote the trivial dimension 1 complex and real vector bundles over M, we may *stabilize* polarization data $\mathfrak{p} = (E, F_0, F_1)$ by direct summing with $(\underline{\mathbb{C}}, \underline{\mathbb{R}}, i\underline{\mathbb{R}})$ to obtain

$$\mathfrak{p} \oplus (\underline{\mathbb{C}}, \underline{\mathbb{R}}, i\underline{\mathbb{R}}) := (E \oplus \underline{\mathbb{C}}, F_0 \oplus \underline{\mathbb{R}}, F_1 \oplus i\underline{\mathbb{R}}).$$

Definition 4.2. Let $\mathfrak{p} = (E, F_0, F_1)$ and $\mathfrak{p}' = (E', F_0', F_1')$ be two sets of polarization data for (M, L_0, L_1). An *isomorphism of polarization data* is a symplectic vector bundle isomorphism $\alpha : E \to E'$ such that $\alpha(F_i)$ is homotopic through Lagrangian subbundles to F_p for $i = 0, 1$. Equivalently, this is an isomorphism $\beta : \pi^*E \to \pi^*E'$ where $\pi : M \times [0, 1] \to M$ is the projection map onto the first factor and $\beta|_{L_i \times i}$ is an isomorphism from $F_i \to F_p$ for $i = 0, 1$. We say that polarization data $\mathfrak{p}$ and $\mathfrak{p}'$ are *stably isomorphic* if $\mathfrak{p} \oplus (\underline{\mathbb{C}}, \underline{\mathbb{R}}, i\underline{\mathbb{R}})^{\oplus k}$ and $\mathfrak{p}' \oplus (\underline{\mathbb{C}}, \underline{\mathbb{R}}, i\underline{\mathbb{R}})^{\oplus k'}$ are isomorphic polarization data for some $k, k' \in \mathbb{N}$.

Definition 4.3. Let M be a symplectic manifold equipped with two Lagrangians L_0 and L_1. Suppose $\tau : (M, L_0, L_1) \to (M, L_0, L_1)$ is a symplectic involution with $\tau-$invariant sets

$$(M^{\text{inv}}, L_0^{\text{inv}}, L_1^{\text{inv}}) \subset (M, L_0, L_1).$$

Define the *tangent polarization*

$$\mathfrak{p}_T := (TM^{\text{inv}}, TL_0^{\text{inv}}, TL_1^{\text{inv}}) \tag{4.1}$$

and the *normal polarization*

$$\mathfrak{p}_N := (NM^{\text{inv}}, NL_0^{\text{inv}}, NL_1^{\text{inv}}). \tag{4.2}$$

Then a *stable tangent normal isomorphism* is a stable isomorphism of the polarization data $\mathfrak{p}_T$ and $\mathfrak{p}_N$.

The following theorem is mainly due to Large [Lar19]. The fact that the spectral sequence splits along components of the path space $P(L_0, L_1)$ was first observed in [HLL22].

Theorem 4.4. *Suppose that*

1. *M is an exact symplectic manifold and convex at infinity, and L_0, L_1 are compact exact Lagrangians.*
2. *There is a symplectic involution $\tau : (M, L_0, L_1) \to (M, L_0, L_1)$ and an associated stable tangent normal isomorphism from $\mathfrak{p}_T$ to $\mathfrak{p}_N$.*

Then there is a spectral sequence with E_1 page equal to $HF(L_0,L_1)\otimes\mathbb{F}[\theta,\theta^{-1}]$ and E_∞ page isomorphic to $HF(L_0^{\mathrm{inv}},L_1^{\mathrm{inv}})\otimes\mathbb{F}[\theta,\theta^{-1}]$. This spectral sequence can be refined as follows. If $P(L_0,L_1)$ denotes the space of paths between L_0 and L_1, $\iota: P(L_0^{\mathrm{inv}},L_1^{\mathrm{inv}})\hookrightarrow P(L_0,L_1)$ is the inclusion map and $\widetilde{\mathfrak{s}}\in\pi_0P(L_0,L_1)$ is some component of $P(L_0,L_1)$ then there is a spectral sequence

$$HF(L_0,L_1;\widetilde{\mathfrak{s}})\otimes_{\mathbb{F}}\mathbb{F}[\theta,\theta^{-1}]\Rightarrow\bigoplus_{\mathfrak{s}\in(\iota^*)^{-1}(\widetilde{\mathfrak{s}})}HF(L_0^{\mathrm{inv}},L_1^{\mathrm{inv}};\mathfrak{s})\otimes_{\mathbb{F}}\mathbb{F}[\theta,\theta^{-1}]. \tag{4.3}$$

Remark 4.5. The relevance to our paper of the splitting of the spectral sequence over spaces of paths between Lagrangians is because of the following identifications which allow us to say that the spectral sequence of Theorem 1.2 splits over Alexander gradings. All of the spaces referenced below are defined in Section 3.5.

- Given $L_0=\mathbb{T}_{\widetilde{\boldsymbol{\alpha}}}$ and $L_1=\mathbb{T}_{\widetilde{\boldsymbol{\beta}}}$ considered as Lagrangians in $M=\mathrm{Sym}^{2g}(\widetilde{\Sigma}\backslash\{\widetilde{w}_1,\widetilde{w}_2,\widetilde{z}^*\})$, $\pi_0(P(L_0,L_1))$ is canonically identified with the set $\underline{\mathrm{Spin}}^c(S^3-\nu(S^n_b(\widetilde{K})),\partial(S^3-\nu(S^n_b(\widetilde{K}))))$ of relative Spin^c structures on S^3 without a neighborhood of $S^n_b(\widetilde{K})$. There is again a map
$$\mathfrak{s}_{\widetilde{w}_1,\widetilde{w}_2,\widetilde{z}^*}:\mathbb{T}_{\widetilde{\boldsymbol{\alpha}}}\cap\mathbb{T}_{\widetilde{\boldsymbol{\beta}}}\to\underline{\mathrm{Spin}}^c(S^3-\nu(S^n_b(\widetilde{K})),\partial(S^3-\nu(S^n_b(\widetilde{K}))))$$
but this only a relatively defined map, i.e only the differences $\mathfrak{s}_{\widetilde{w}_1,\widetilde{w}_2,\widetilde{z}^*}(x)-\mathfrak{s}_{\widetilde{w}_1,\widetilde{w}_2,\widetilde{z}^*}(y)$ are well defined. This information is, however, enough to determine the relative Alexander gradings $A(x)-A(y)$ [HO17, Section 6.3].
- Identify the fixed point set
$$(\mathrm{Sym}^{2g}(\widetilde{\Sigma}\backslash\{\widetilde{w}_1,\widetilde{w}_2,\widetilde{z}^*\})^{\mathrm{inv}},\mathbb{T}^{\mathrm{inv}}_{\widetilde{\boldsymbol{\alpha}}},\mathbb{T}^{\mathrm{inv}}_{\widetilde{\boldsymbol{\alpha}}})$$
with
$$(\mathrm{Sym}^{g}(\Sigma\backslash\{z,w\}),\mathbb{T}_{\boldsymbol{\alpha}},\mathbb{T}_{\boldsymbol{\beta}}).$$
This identification is elaborated upon in the proof of Theorem 1.2. Assuming this identification, $\pi_0(P(L_0^{\mathrm{inv}},L_1^{\mathrm{inv}}))$ corresponds to $\pi_0(P(L_0',L_1'))$, which is in turn canonically identified with the set $\underline{\mathrm{Spin}}^c(S^3-\nu(K),\partial(S^3-\nu(K)))$. The image $\mathfrak{s}_{w,z}(x)\in\underline{\mathrm{Spin}}^c(S^3-\nu(K),\partial(S^3-\nu(K)))$ of a generator $x\in\mathbb{T}_{\widetilde{\boldsymbol{\alpha}}}\cap\mathbb{T}_{\widetilde{\boldsymbol{\beta}}}$ determines the Alexander grading $A(x)$.

4.2. **Spectral sequences for strongly invertible knots.** Let $\widetilde{D}_n$ be a $2g-1$ crossing intravergent diagram for the DSI $\widetilde{K}$. Recalling the genus $2g$ τ-equivariant Heegaard diagrams constructed in Section 3.5, for ease of notation we set
$$\widetilde{\mathcal{H}}:=\widetilde{\mathcal{H}}(\widetilde{D}_n)=(\widetilde{\Sigma},\widetilde{\boldsymbol{\alpha}},\widetilde{\boldsymbol{\beta}},\widetilde{z},\widetilde{w})\text{ and }\mathcal{H}_S:=\widetilde{\mathcal{H}}_S(\widetilde{D}_n)=(\widetilde{\Sigma},\widetilde{\boldsymbol{\alpha}},\widetilde{\boldsymbol{\beta}},\widetilde{z}_1^*,\{\widetilde{w}_1,\widetilde{w}_2\})$$
for the strongly invertible knot $\widetilde{K}$ and the singularized n-butterfly link $S^n_b(\widetilde{K})$ respectively, and we also set
$$\mathcal{H}:=\widetilde{\mathcal{H}}/\tau=(\Sigma,\boldsymbol{\alpha},\boldsymbol{\beta},z)\text{ and }\mathcal{H}_S:=\widetilde{\mathcal{H}}_S/\tau=(\Sigma,\boldsymbol{\alpha},\boldsymbol{\beta},w,z)$$
for the induced genus g quotient diagrams of S^3 and K respectively. The following lemma will be useful when proving invariance of both spectral sequences.

Lemma 4.6. *Let $\widetilde{\mathcal{H}}$ and $\widetilde{\mathcal{H}}'$ be τ-equivariant Heegaard diagrams for $\widetilde{K}$ with the same number of basepoints, and which induce intravergent knot diagrams $\widetilde{D}_n$ and $\widetilde{D}_n'$. Also let $\mathcal{H}:=\widetilde{\mathcal{H}}/\tau$ and $\mathcal{H}'=\widetilde{\mathcal{H}}'/\tau$ be the induced quotient Heegaard diagrams for S^3. Recall from Section 3.5 that q_τ denotes the quotient map $\widetilde{\Sigma}\twoheadrightarrow\Sigma$ associated to a τ-equivariant Heegaard surface. Then there is a sequence of Heegaard moves interpolating between $\mathcal{H}$ and $\mathcal{H}'$ that avoids basepoints and $\ell_\tau(Fix(\tau))$. These Heegaard moves therefore lift to τ-equivariant Heegaard moves interpolating between $\widetilde{\mathcal{H}}$ and $\widetilde{\mathcal{H}}'$.*

Proof. Consider the Heegaard diagrams $s\widetilde{\mathcal{H}}$ and $s\widetilde{\mathcal{H}}'$ obtained by

(1) converting $\widetilde{H}$ and $\widetilde{H}'$ into Heegaard diagrams $\widetilde{H}_S$ and $\widetilde{H}'_S$ for $S^n_b(\widetilde{K})$ by adding a new w basepoint at one of the fixed points of τ and relabeling half of the existing basepoints as outlined in Section 3.5.
(2) Adding another new w basepoint at the second fixed point of τ.

The diagrams $s\mathcal{H} = s\widetilde{\mathcal{H}}/\tau$ and $s\widetilde{\mathcal{H}}'/\tau$ are Heegaard diagrams for the same singular link. In particular, $s\mathcal{H}$ and $s\mathcal{H}'$ are related by a sequence of Heegaard moves avoiding their basepoints [OSS09, Theorem 2.4]. The set of basepoints for $s\mathcal{H}$ is the same as the set of basepoints for $\mathcal{H}$ unioned with $\ell_\tau(\mathrm{Fix}(\tau))$. □

Remark 4.7. The proof given above also shows that the same sequence of τ-equivariant Heegaard moves interpolates between $\widetilde{\mathcal{H}_S}$ and $\widetilde{\mathcal{H}_S}'$.

4.2.1. *Proof of Theorem 1.1.* We work in the symmetric product

$$M := \mathrm{Sym}^{2g}(\widetilde{\Sigma}\backslash\{\widetilde{z}, \widetilde{w}\}) \tag{4.4}$$

equipped with submanifolds

$$L_0 := \mathbb{T}_{\widetilde{\boldsymbol{\alpha}}} = \widetilde{\alpha}_1 \times \ldots \times \widetilde{\alpha}_{2g} \text{ and } L_1 := \mathbb{T}_{\widetilde{\boldsymbol{\beta}}} = \widetilde{\beta}_1 \times \ldots \times \widetilde{\beta}_{2g}. \tag{4.5}$$

Let $\tau : (M, L_0, L_1) \to (M, L_0, L_1)$ be the involution

$$\tau((x_1 \ldots x_{2g})) := (\tau(x_1) \ldots \tau(x_{2g})). \tag{4.6}$$

The τ on the right hand side of this equation is the involution on the Heegaard surface $\widetilde{\Sigma}$ induced by the involution τ on $(S^3, \widetilde{K})$. As explained in Section 3, the work of Perutz shows that M carries a symplectic form $\omega' \in \Omega^2(M)$ that agrees with the product symplectic form induced by an area form on $\Sigma\backslash\{z\}$ away from the fat diagonal of $\mathrm{Sym}^g(\Sigma\backslash\{z\})$, and with respect to which L_0 and L_1 are Lagrangians [Per08]. The techniques of [Hen12, Section 4] – there applied to the case of symmetric products of multi-punctured spheres corresponding to weakly admissible genus 0 Heegaard diagrams for branched double covers of three manifolds – generalize to show that ω' can be modified to a τ-equivariant symplectic form $\omega \in \Omega^2(M)$ with respect to which M is convex at infinity and L_0 and L_1 are still Lagrangians. The proof given in [HLL22, Proposition 4.2] then shows that there exists a primitive of ω that demonstrates exactness of L_0 and L_1. These remarks tell us that (1) of Theorem 4.4 is satisfied for $(M, L_0, L_1, \omega, \tau)$. The proof that (2) of Theorem 4.4 is also satisfied in this setup is the subject of Sections 6 and 7. From here, we proceed assuming that this assumption is satisfied.

In order to better understand the fixed point sets $(M^{\mathrm{inv}}, L_0^{\mathrm{inv}}, L_1^{\mathrm{inv}})$, we define

$$M' = \mathrm{Sym}^g(\Sigma\backslash\{z\}), \tag{4.7}$$

$$L'_0 := \mathbb{T}_{\boldsymbol{\alpha}} = \alpha_1 \times \ldots \times \alpha_g \text{ and } L'_1 := \mathbb{T}_{\boldsymbol{\beta}} = \beta_1 \times \ldots \times \beta_g. \tag{4.8}$$

Recall the quotient map $\ell_\tau : \widetilde{\Sigma} \to \Sigma$ defined in Section 3.5. The map $\phi : (M', L'_0, L'_1) \to (M^{\mathrm{inv}}, L_0^{\mathrm{inv}}, L_1^{\mathrm{inv}})$ defined by

$$\phi((\ell_\tau(x_1) \ldots \ell_\tau(x_g))) = (x_1\tau(x_1) \ldots x_g\tau(x_g)) \tag{4.9}$$

identifies (M', L'_0, L'_1) with $(M^{\mathrm{inv}}, L_0^{\mathrm{inv}}, L_1^{\mathrm{inv}})$; specifically, ϕ is a biholomorphic map – see [Hen12, Appendix 1] for a proof in local charts of this fact. Letting $\phi^*(\omega|_{M^{\mathrm{inv}}})$ be the symplectic form on M', the Lagrangian intersection Floer homologies $HF(L_0^{\mathrm{inv}}, L_1^{\mathrm{inv}})$ and $HF(L'_0, L'_1)$ are isomorphic.

Applying Theorem 4.4 along with the isomorphisms $HF(L_0^{\text{inv}}, L_1^{\text{inv}}) \cong HF(L_0', L_1')$ gives us a spectral sequence with E_1 page equal to

$$HF(L_0, L_1) \otimes \mathbb{F}[\theta, \theta^{-1}] = \widehat{HFK}(\widetilde{K}) \otimes \mathbb{F}[\theta, \theta^{-1}]$$

and E_∞ page isomorphic to

$$HF(L_0', L_1') \otimes \mathbb{F}[\theta, \theta^{-1}] = \widehat{HF}(S^3) \otimes \mathbb{F}[\theta, \theta^{-1}].$$

Now we prove that this spectral sequence is independent of the τ-equivariant Heegaard diagram inducing it, and in particular is independent of the intravergent diagram $\widetilde{D}_n$ for $\widetilde{K}$ that we start with. By [HLS16, Proposition 4.3] along with the identification of Large's $\mathbb{Z}/2\mathbb{Z}$-equivariant Floer homology with Seidel-Smith's $\mathbb{Z}/2\mathbb{Z}$-equivariant Floer homology, the spectral sequence above is the same as the spectral sequence induced by $CF_{\mathbb{Z}/2}(\mathbb{T}_{\widetilde{\boldsymbol{\alpha}}}, \mathbb{T}_{\widetilde{\boldsymbol{\beta}}})$, the equivariant complex from non-invariant complex structures defined in Section 3 of [HLS16]. The aforementioned identification is nicely summarized in the proof of [HLL22, Theorem 2.4]. By Propositions 3.23 and 3.24 of [HLS16], this spectral sequence is independent of the choices in its construction and is invariant under equivariant Hamiltonian isotopies of the Lagrangians. Lemma 4.6 shows that the Heegaard diagrams $\widetilde{\mathcal{H}}(\widetilde{D}_n)$ and $\widetilde{\mathcal{H}}(\widetilde{D}_n')$ are related by a sequence of τ-equivariant Heegaard moves. These moves are realized as equivariant Hamiltonian isotopies in $\text{Sym}^{2g}(\Sigma_g \backslash \{\widetilde{w}, \widetilde{z}\})$.

The key observation to reduce the E_1 page of this spectral sequence to $\widehat{HFK}(K, 0) \otimes \mathbb{F}[\theta, \theta^{-1}]$ is that any generator in Alexander grading not equal to 0 must be killed by the d^2 differential. In some more detail, by the invariance proved above we can start with a *nice* τ-equivariant diagram for $\widetilde{K}$, and the arguments given in [HLS16, Section 5.1] show that for such a diagram the spectral sequence can be computed from the Leray spectral sequence induced from the vertical filtration of the double complex

$$\begin{array}{ccccc}
\vdots & & \vdots & & \\
\downarrow & & \downarrow & & \\
\cdots \longrightarrow CF(\mathbb{T}_{\widetilde{\boldsymbol{\alpha}}}, \mathbb{T}_{\widetilde{\boldsymbol{\beta}}}) & \xrightarrow{1+\tau_\#} & CF(\mathbb{T}_{\widetilde{\boldsymbol{\alpha}}}, \mathbb{T}_{\widetilde{\boldsymbol{\beta}}}) & \xrightarrow{1+\tau_\#} & \cdots \\
\downarrow \partial & & \downarrow \partial & & \\
\cdots \longrightarrow CF(\mathbb{T}_{\widetilde{\boldsymbol{\alpha}}}, \mathbb{T}_{\widetilde{\boldsymbol{\beta}}}) & \xrightarrow{1+\tau_\#} & CF(\mathbb{T}_{\widetilde{\boldsymbol{\alpha}}}, \mathbb{T}_{\widetilde{\boldsymbol{\beta}}}) & \xrightarrow{1+\tau_\#} & \cdots \\
\downarrow & & \downarrow & & \\
\vdots & & \vdots & &
\end{array}.$$

In particular, the d_2 differential is given by $1 + \tau_*$ acting on $HF(\mathbb{T}_{\widetilde{\boldsymbol{\alpha}}}, \mathbb{T}_{\widetilde{\boldsymbol{\beta}}}) = \widehat{HFK}(\widetilde{K})$. If x is an element of $\widehat{HFK}(\widetilde{K})$ with $A(x) \neq 0$, then since $A(\tau_*(x)) = -A(x)$ by Proposition 3.7, it must be the case that $x \neq \tau_*(x)$ and hence if a sum of homology classes $x + ...$ is in the kernel of τ_*, then $\tau_*(x)$ must also appear with a coefficient of 1 in that linear combination. □

From Theorem 1.1 we can define a numerical invariant associated to any strongly invertible knot.

Definition 4.8. Let $(\widetilde{K}, \tau)$ be a strongly invertible knot. The Maslov grading of the Alexander grading 0 generator that generates the $\mathbb{F}_2$ of the E_∞ page in the spectral sequence of Theorem 1.1 is an invariant of $(\widetilde{K}, \tau)$ which we denote s_τ.

That s_τ thus defined is an invariant of $(\widetilde{K},\tau)$ follows In a sequel to this paper we hope to return to the following conjecture along with computations of s_τ for non-δ-thin strongly invertible knots.

Conjecture 1. *The number s_τ is an equivariant concordance invariant.*

The most mainstream definition of equivariant concordance is the following:

Definition 4.9. We say that two directed strongly invertible knots $(\widetilde{K}_i,\tau_i,h_i)$, $i=0,1$ (where h_i denotes the half-axis), are *equivariantly concordant* if there exists a smooth properly embedded annulus $C\cong S^1\times[0,1]\subset S^3\times[0,1]$, invariant with respect to some involution τ of $S^3\times[0,1]$ such that:

- $\partial(S^3\times[0,1],C)=(S^3,K_0)\cup-(S^3,K_1)$
- τ is an extension of the strong inversion $\tau_i: S^3\times\{i\}\to S^3\times\{i\}$
- the orientations of h_0 and $-h_1$ induce the same orientation on the annulus $Fix(\tau)$, and h_0 and h_1 are contained in the same component of $Fix(\tau)\backslash C$.

There is a slightly different notion of equivariant concordance where the extension τ is required to be isotopic to rotation by π along a fixed axis in each slice $S^3\times\{t\}$. Whether these two definitions of equivariant concordance induce the same equivalence relation on the set of directed strongly invertible knots is an open question. We expect s_τ to be an equivariant concordance invariant with respect to the second notion, and therefore hope that it may shed some light on the aforementioned question.

4.2.2. *Proof of Theorem 1.2.* Now we work in the symmetric product

$$\overline{M}:=\mathrm{Sym}^{2g}(\widetilde{\Sigma}\backslash\{\widetilde{w}_1,\widetilde{w}_2,\widetilde{z}^*\}) \tag{4.10}$$

equipped with the same submanifolds

$$L_0:=\mathbb{T}_{\widetilde{\boldsymbol{\alpha}}}=\widetilde{\alpha}_1\times\ldots\times\widetilde{\alpha}_{2g} \text{ and } L_1:=\mathbb{T}_{\widetilde{\boldsymbol{\beta}}}=\widetilde{\beta}_1\times\ldots\times\widetilde{\beta}_{2g}. \tag{4.11}$$

Recall that $\widetilde{z}=\widetilde{w}_1$ and $\widetilde{w}=\widetilde{w}_2$, so that we can think of $\overline{M}$ as a subset of M. Pulling back the form ω constructed on $M=\mathrm{Sym}^{2g}(\widetilde{\Sigma}\backslash\{\widetilde{w},\widetilde{z}\})$ to $\overline{M}$ tells us that (1) of Theorem 4.4 is satisfied for $(\overline{M},L_0,L_1,\omega,\tau)$. As mentioned before, the proof that (2) of Theorem 4.4 is also satisfied in this setup is the subject of Sections 6 and 7, and so we assume for this Section that this assumption is satisfied.

In order to better understand the fixed point sets $(\overline{M}^{\mathrm{inv}},L_0^{\mathrm{inv}},L_1^{\mathrm{inv}})$, we define

$$\overline{M}'=\mathrm{Sym}^{g}(\Sigma\backslash\{z,w\}), \tag{4.12}$$

and define L_0' and L_1' as in Equation 4.8.

We again have that the map $\phi:(\overline{M}',L_0',L_1')\to(\overline{M}^{\mathrm{inv}},L_0^{\mathrm{inv}},L_1^{\mathrm{inv}})$ defined by

$$\phi((\ell_\tau(x_1)\ldots\ell_\tau(x_g)))=(x_1\tau(x_1)\ldots x_g\tau(x_g)) \tag{4.13}$$

is biholomorphic. And, again letting $\phi^*(\omega|_{\overline{M}^{\mathrm{inv}}})$ be the symplectic form on $\overline{M}'$, the Lagrangian intersection Floer homologies $HF(L_0^{\mathrm{inv}},L_1^{\mathrm{inv}})$ and $HF(L_0',L_1')$ are isomorphic.

Applying Theorem 4.4 along with the isomorphism $HF(L_0^{\mathrm{inv}},L_1^{\mathrm{inv}})\cong HF(L_0',L_1')$ gives us a spectral sequence with E_1 page equal to $HF(L_0,L_1)\otimes\mathbb{F}[\theta,\theta^{-1}]=\widehat{HFK}(S^n_b(\widetilde{K}))$ and E_∞ page isomorphic to $HF(L_0',L_1')\otimes\mathbb{F}[\theta,\theta^{-1}]=\widehat{HFK}(K)\otimes\mathbb{F}[\theta,\theta^{-1}]$.

That this spectral sequence is invariant under choice of τ-equivariant Heegaard diagram for $S^n_b(\widetilde{K})$, and in particular under the choice of the intravergently singularized diagram $IS_c(\widetilde{D}_n)$ for

$S^n_b(\widetilde{K})$, is an identical argument to the invariance proof of the spectral sequence of Theorem 1.1 given in the last Subsection with Remark 4.7 in place of Lemma 4.6.

By the same argument given in [HLS16, Section 5.3], if a τ-equivariant Heegaard diagram for $S^n_b(\widetilde{K})$ with more basepoints (such as $\mathbb{G}^{\text{sphere}}_S$) was used to construct a spectral sequence, the resulting spectral sequence would be the same as the aforementioned spectral sequence arising from the triply pointed Heegaard diagram tensored with the complex $X = \{xx, yy, xy, yx\}$ with τ action $\tau(xx) = xx$, $\tau(yy) = yy$, $\tau(xy) = yx$ and $\tau(yx) = xy$. In particular, if we can determine the relation between the Alexander grading of a τ-equivariant generator for $\widetilde{CFL}(\mathbb{G}^{\text{sphere}}_S)$ with the Alexander grading of its projection to a generator in $\widetilde{CFL}(\mathbb{G}^{\text{sphere}}_S/\tau)$ this will be the same relation between the Alexander gradings of a τ-equivariant generator in $\widehat{CFK}(\widetilde{\mathcal{H}}_S(\widetilde{D}_n))$ and its projection to a generator in $\widehat{CFK}(\widetilde{\mathcal{H}}_S(\widetilde{D}_n)/\tau)$.

Consider a τ-equivariant generator $\widetilde{\mathbf{x}} \in \mathbb{G}^{\text{sphere}}_S$ and its projection $\mathbf{x} \in \mathbb{G}^{\text{sphere}}_S/\tau$ (c.f Section 3.5). According to Propositions A.6 and A.7 we have the following commutative diagram

$$\begin{array}{ccc} \widetilde{CFL}(\mathbb{G}^{\text{sphere}}_S) & \xrightarrow[-\frac{1}{2}]{\Phi} & \widetilde{CFL}(Ax\mathbb{G}^{\text{sphere}}_0, \partial_{\widetilde{A}}) \\ \pi\downarrow & & \downarrow\pi \\ \widetilde{CFL}(\mathbb{G}^{\text{sphere}}_S/\tau) & \xrightarrow[0]{\mathcal{P}} & \widetilde{CFL}(Ax\mathbb{G}^{\text{sphere}}_0/\tau, \partial_A) \end{array}$$

where Φ and $\mathcal{P}$ have associated Alexander grading shifts of $-\frac{1}{2}$ and 0 respectively. The proof of [Hen15, Theorem 1.3] shows that if $\lambda = lk(L_b^{n+\frac{1}{2}}(\widetilde{K}), \widetilde{A})$ and $A(\widetilde{\mathbf{x}}) = 2a + \frac{1-\lambda}{2}$, then $A(\pi(\mathbf{x})) = a + \frac{1-\lambda}{2}$. The grading shifts associated to Φ and $\mathcal{P}$ then tell us that if $\mathbf{y}$ is a τ-equivariant generator in $\widetilde{CFL}(\mathbb{G}^{\text{sphere}}_S)$ with Alexander grading $A(\mathbf{y}) = 2a + \frac{2-\lambda}{2}$, then $A(\pi(\mathbf{y})) = a + \frac{1-\lambda}{2}$. To recover the grading statement in the statement of Theorem 1.2 in terms of $\widetilde{lk}(\widetilde{K})$, specialize this argument to $n = 0$ and apply Equation (2.1). □Theorem 1.2 is demonstrated in the case of 3_1^+ in Example 5.0.1, 3_1^- (the directed strong inversion on the trefoil with trefoil quotient) in Example 5.0.2 and in the case of 4_1^- (the directed strong inversion on the figure 8 knot with cinquefoil quotient) in Example 5.0.3. In this last example, while we do not compute the full spectral sequence, we argue that the spectral sequence of Theorem 1.2 has the property that $E_2 \neq E_\infty$.

Remark 4.10. The value of n associated to the diagram $\widetilde{D}_n$ only changes the resulting spectral sequence

$$\widehat{HFK}(S^n_b(\widetilde{K})) \otimes \mathbb{F}[\theta, \theta^{-1}] \Rightarrow \widehat{HFK}(K) \otimes \mathbb{F}[\theta, \theta^{-1}]$$

by an overall shift of Alexander grading. This follows from the fact (c.f Remark 2.15) that the transverse spatial graph associated to $S^n_b(\widetilde{K})$ is independent of n, and the equivalence (modulo absolute Alexander gradings) via sutured Floer homology of singular knot Floer homology with the Heegaard Floer homology of the associated spatial graph. See [HO17, Section 6], [Ali22, Section 2] for discussions of this equivalence. The effect on Floer homology of applying $R\overline{V}$ from [HO17, Figure 4] to the singularity of $S^n_b(\widetilde{K})$ to obtain $S^{n\pm\frac{1}{2}}(\widetilde{K})$ is to shift the absolute Alexander grading up or down by $\frac{1}{2}$ by [BW20, Theorem 4.1].

5. Examples

Before analyzing specific examples, we first record some general facts about the behavior of the spectral sequences of Theorem 1.1 and 1.2. A knot K is said to be Floer δ-thin if the difference

$\delta := M - A$ between the Maslov and Alexander gradings of any homogeneous element of $\widehat{HFK}(K)$ is a constant δ. We remind the reader that for a Floer δ-thin knot, δ is equal to equivalently (suitably normalized versions of) the classical knot signature, Ozsvath-Szabo's concordance homomorphism τ [OS03], or Manolescu-Owens' concordance homomorphism δ [MO05]:

$$\delta = -\frac{\sigma(K)}{2} = -\frac{\tau(K)}{2} = \delta(K).$$

By a similar token, we will say that a singular knot S is Floer δ-thin if the same condition holds on $\widehat{HFK}(S)$.

Proposition 5.1. *If $(\widetilde{K}, \tau)$ is a Floer δ-thin or L-space strongly invertible knot, then $E_2 = E_\infty$ for the spectral sequence of Theorem 1.1. Furthermore, in this case the invariant s_τ is equal to δ.*

Proof. The assumptions that $\widetilde{K}$ is Floer δ-thin or L-space both imply that $\widehat{HFK}(\widetilde{K})$ has exactly one occupied Maslov grading in Alexander grading 0. Every differential d_k for $k \geq 2$ does not preserve the Maslov grading because ∂, the vertical differential, lowers the Maslov grading by one, and $1 + \tau_\#$, the horizontal differential, preserves the Maslov grading by Proposition 3.7. Hence by the assumption, these higher differentials must be identically 0. The unique occupied Maslov grading in Alexander grading 0 is clearly δ, and so the generator that survives the spectral sequence must have Maslov grading δ. □

There is an analogous statement for the spectral sequence of Theorem 1.2 which follows by the same proof using Proposition 3.8 in place of Proposition 3.7.

Proposition 5.2. *If $(\widetilde{K}, \tau)$ is a strongly invertible knot such that $S^n_b(\widetilde{K})$ is Floer δ-thin, then $E_2 = E_\infty$ for the spectral sequence of Theorem 1.2.*

Remark 5.3. Using Proposition 5.1, computations of $\widehat{HFK}$ from [BG07], computations of the CFK^∞ type of non-δ-thin strongly invertible knots from [AP23], and properties of the map $\tau_{\widetilde{K}}$ on $CFK^\infty(\widetilde{K})$ from [DMS22, Theorem 1.7], the author was able to conclude that the spectral sequence of Theorem 1.1 collapses on the E_2 page for all strongly invertible knots with at most 11 crossings.

Despite this, we state the following conjecture:

Conjecture 2. *There exists a strongly invertible knot $\widetilde{K}$ such that the spectral sequence of Theorem 1.1 collapses on the E_k page for some $k \geq 3$.*

In the examples below we content ourselves with analyzing the spectral sequence associated to $S^n_b(\widetilde{K})$ for n associated to any convenient intravergent diagram $\widetilde{D}_n$ of $\widetilde{K}$ in light of Remark 4.10; to obtain the spectral sequence of Theorem 1.2, just perform an overall Alexander grading shift of n.

5.0.1. *The trefoil with unknotted quotient.* The spectral sequence of Theorem 1.1 collapses on the E_1 page as $dim(\widehat{HFK}(3_1, 0)) = 1 = dim(\widehat{HF}(S^3))$. The singular skein triple associated to $S^1_b(3^+_1)$ includes the positive Hopf link and the unknot, and completely determines the singular knot Floer homology of $S^1_b(3^+_1)$:

$$\widehat{HFK}(S^1_b(3^+_1)) \cong \mathbb{F}_{(0,\frac{1}{2})} \oplus \mathbb{F}^2_{(-1,-\frac{1}{2})}.$$

The linking number of $(S^1_b(3^+_1))_0 = L^{\frac{3}{2}}_b(3^+_1) = 0_1$ with the reversed symmetry axis is

$$\lambda = lk(L^{\frac{3}{2}}_b(3^+_1), \widetilde{A}) = 1.$$

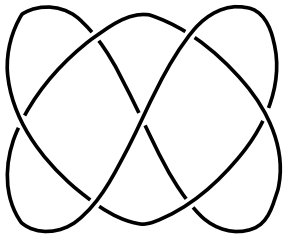

FIGURE 21. An intravergent diagram $\widetilde{D}_3$ for 3_1^-

Therefore, the proof of Theorem 1.2 implies that Alexander grading $2a+\frac{2-1}{2} = 2a+\frac{1}{2}$ of $\widehat{HFK}(S^1_b(3_1^+))$ gets sent under the spectral sequence to Alexander grading $a + \frac{1-1}{2} = a$ of $\widehat{HFK}(0_1) \cong \mathbb{F}_{(0,0)}$. The only occupied Alexander grading in the knot Floer homology of the quotient unknot is $a = 0$ which corresponds to Alexander grading $2 \cdot 0 + \frac{1}{2} = \frac{1}{2}$ in the singular knot Floer homology of $S^1_b(3_1^+)$. This tells us that the two generators in grading $(-1, -\frac{1}{2})$ must be swapped by τ_* so that the $1 + \tau_*$ differential on the E_1 page kills both of them, and the generator in grading $(0, \frac{1}{2})$ survives the spectral sequence and gets sent to the non-zero element of the $E_\infty = E_2$ page. This can all be seen explicitly from the Heegaard diagrams of Figure 4 as well.

5.0.2. *The trefoil with trefoil quotient.* If we consider the same strong inversion on the trefoil but with the opposite choice of half-axis, we obtain a DSI that we denote 3_1^-; it is pictured in Figure 21. Notice that 3_1^- is a right handed trefoil with quotient equal to a left handed trefoil, while 3_1^+ was a left handed trefoil with unknotted quotient. We choose to use the right hand trefoil for 3_1^- so as to have a convenient intravergent diagram with negative central crossing. The spectral sequence of Theorem 1.1 does not depend on the choice of half axis and will therefore be the same as described in the last example up to mirroring. The singular skein triple associated to $\widetilde{D}_3$ consists of $S^3_b(3_1^-)$, $L^3_b(3_1^-) = T(2,6)$ and $L^{\frac{7}{2}}_b(3_1^-) = (3_1)_L \# (3_1)_L$, where the subscript L's denote that we are taking a connect sum of *left hand* trefoils. The skein exact triangle associated to this triple along with the Alexander polynomial $\Delta_{S^3_b(3_1^-)}$ completely determine the singular knot Floer homology of $S^3_b(3_1^-)$:

$$\widehat{HFK}(S^3_b(3_1^-)) \cong \mathbb{F}_{(5,\frac{5}{2})} \oplus \mathbb{F}_{(2,\frac{1}{2})} \oplus \mathbb{F}^2_{(1,-\frac{1}{2})} \oplus \mathbb{F}_{(0,-\frac{3}{2})}.$$

This singular knot is not Floer δ-thin, but nonetheless we will see that the spectral sequence of Theorem 1.2 dies on the E^2 page. From the diagram obtained by doing a resolution to $\widetilde{D}_3$ it can be see that $\lambda = lk(L^{\frac{7}{2}}_b(3_1^-), \widetilde{A}) = -1$ which means that

- Alexander grading $2 \cdot 2 + \frac{-1-2}{2} = \frac{5}{2}$ of $\widehat{HFK}(S^3_b(3_1^-))$ gets sent to Alexander grading $2 + \frac{-1-1}{2} = 1$ of $\widehat{HFK}((3_1)_L) \cong \mathbb{F}_{(2,1)} \oplus \mathbb{F}_{(1,0)} \oplus \mathbb{F}_{(0,-1)}$
- Alexander grading $2 \cdot 1 + \frac{-1-2}{2} = \frac{3}{2}$ of $\widehat{HFK}(S^3_b(3_1^-))$ gets sent to Alexander grading $1 + \frac{-1-1}{2} = 0$ of $\widehat{HFK}((3_1)_L)$
- Alexander grading $2 \cdot 0 + \frac{-1-2}{2} = \frac{5}{2}$ of $\widehat{HFK}(S^3_b(3_1^-))$ gets sent to Alexander grading $0 + \frac{-1-1}{2} = -1$ of $\widehat{HFK}((3_1)_L)$
- Alexander grading $\frac{3}{2}$ of $\widehat{HFK}(S^3_b(3_1^-))$ is not of the form $2a + \frac{\lambda-2}{2}$ and hence dies in the spectral sequence.

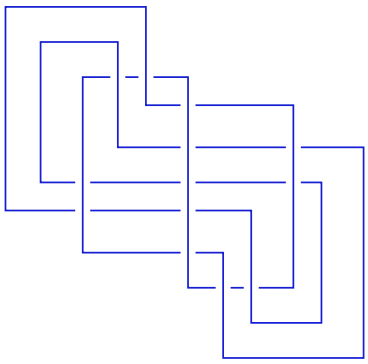

FIGURE 22. An intravergent diagram $\widetilde{D}_n$ for 4_1^-

These observations together tell us that three generators in Alexander grading not equal to $-\frac{1}{2}$ of of $\widehat{HFK}(S^3_b(3_1^-))$ abut to the generators of the quotient left hand trefoil homology in the spectral sequence, while the two generators in Alexander grading $-\frac{1}{2}$ must be swapped by the τ_* action so that they cancel each other out in homology on the E_2 page.

5.0.3. *The figure 8 with cinquefoil quotient.* The unique strong inversion on 4_1 yields quotient knot equal to the unknot or the cinquefoil 5_2 depending on which half axis is chosen. Here we analyze the choice of half axis that yields a 5_2 quotient, denoted by 4_1^-. This is displayed as a transvergent symmetry in Figure 22. We have no need to determine the number n and so we will leave it as an abstract label.

While we do not attempt to discern the precise behavior of the spectral sequence of Theorem 1.2 for this DSI, we can argue that $E_2 \neq E_\infty$, thus demonstrating an answer in the affirmative to the analog of Conjecture 2 for Theorem 1.2. The two other members of the negative skein triple associated to the diagram $\widetilde{D}$ are the knot 12_{n725}, found using Miller's Knotfol.io website [kno], and the link pictured in Figure 23 which we shall just denote $S^n_b(4_1^-)_0$. We used the knot Floer homology calculations in [BG07] along the formula for the knot Floer homology of a mirror knot to find $\widehat{HFK}(12_{n725})$, and a modification of the grid homology program from that paper to find $\widehat{HFK}(S^n_b(4_1^-)_0)$. These computations lead us to the following skein exact triangle:

$$\begin{array}{ccc} \mathbb{F}_{(10,5)}\oplus\mathbb{F}^2_{(9,4)}\oplus\mathbb{F}_{(9,3)}\oplus\mathbb{F}_{(8,3)}\oplus \\ \mathbb{F}^4_{(8,2)}\oplus\mathbb{F}^6_{(7,1)}\oplus\mathbb{F}^6_{(6,0)}\oplus\mathbb{F}^6_{(5,-1)}\oplus \\ \mathbb{F}^4_{(4,-2)}\oplus\mathbb{F}_{(3,-3)}\oplus\mathbb{F}_{(2,-3)}\oplus\mathbb{F}^2_{(1,-4)}\oplus\mathbb{F}_{(0,-5)} & \xrightarrow{(0,0)} & \mathbb{F}_{(10,5)}\oplus\mathbb{F}^2_{(9,4)}\oplus\mathbb{F}_{(8,3)}\oplus\mathbb{F}_{(6,2)}\oplus \\ & & \mathbb{F}^3_{(5,1)}\oplus\mathbb{F}^5_{(4,0)}\oplus\mathbb{F}^5_{(3,-1)}\oplus\mathbb{F}^3_{(2,-2)}\oplus \\ & & \mathbb{F}_{(1,-4)}\oplus\mathbb{F}_{(1,-3)}\oplus\mathbb{F}^2_{(0,-5)}\oplus\mathbb{F}_{(-1,-6)} \end{array}$$

$$(0,0) \qquad\qquad (-1,0)$$

$$(\widehat{HFK}(S^n_b(4_1^-))\otimes V)[[0,-\tfrac{1}{2}]]$$

Observe that $\mathbb{F}_{(9,3)} \oplus \mathbb{F}^4_{(8,2)}$ necessarily maps to 0 under the top horizontal map since that map has bidegree $(0,0)$ and there are not generators in gradings $(9,3)$ or $(8,2)$ on the top right. Therefore $\mathbb{F}_{(9,3)} \oplus \mathbb{F}^4_{(8,2)}$ is in the image of the right diagonal arrow of bidegree $(0,0)$ which implies that $\widehat{HFK}(S^n_b(4_1^-)) \otimes V)[[0,-\frac{1}{2}]]$ contains a $\mathbb{F}_{(9,3)} \oplus \mathbb{F}^4_{(8,2)}$ direct summand. Notice also that there is no generator in grading $(10,4)$ in the top left or in grading $(11,4)$ in the top right, and hence

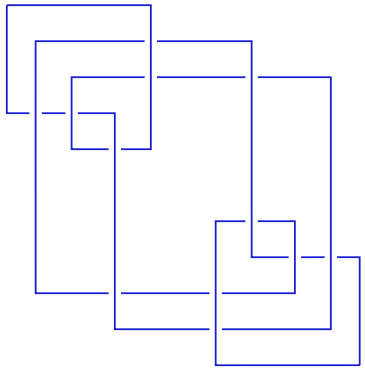

FIGURE 23. The two component two periodic butterfly link $S^n_b(4_1^-)_0$

there is no $(10,4)$ graded generator in $\widehat{HFK}(S^n_b(4_1^-)) \otimes V)[[0,-\frac{1}{2}]]$. This implies that there is a generator in grading $(9,3)$ in $\widehat{HFK}(S^n_b(4_1^-))[[0,-\frac{1}{2}]]$. Similarly, we see that one of the four $\mathbb{F}_{(8,2)}$ summands in $\widehat{HFK}(S^n_b(4_1^-))\otimes V)[[0,-\frac{1}{2}]]$ comes from the $F_{(9,3)} \otimes F_{(-1,-1)}$ tensor product occurring in $\widehat{HFK}(S^n_b(4_1^-)) \otimes V)[[0,-\frac{1}{2}]]$, while the other three must belong to $\widehat{HFK}(S^n_b(4_1^-))[[0,-\frac{1}{2}]$. We have shown there is exactly one generator in grading $(9,\frac{7}{2})$ and three generators in grading $(8,\frac{5}{2})$ in $\widehat{HFK}(S^n_b(4_1^-))$. Taking homology under the $1+\tau_*$ differential, which preserves both Alexander and Maslov gradings by Proposition 3.8, must leave an odd (and in particular positive) number of generators in gradings $(9,\frac{7}{2})$ and $(8,\frac{5}{2})$ on the E_2 page. By Theorem 1.2, generators that survive the spectral sequence must have an even difference in Alexander gradings, and hence not both of these generators persist to the E_∞ page.

6. Geometry of the symmetric product

In analogy to the subspace $X = (L_0^{\text{inv}} \times \{0\}) \cup (L_1^{\text{inv}} \times \{1\})$ of $M^{\text{inv}} \times [0,1]$ define

$$X' := (L_0' \times \{0\}) \cup (L_1' \times \{1\}) \subset M' \times [0,1]. \tag{6.1}$$

In this Section we analyze the (co)homology of the spaces $M' \times [0,1]$, X' and $M' \times [0,1]/X'$. The goal is to prove the following proposition.

Proposition 6.1. *The reduced cohomology $\widetilde{H}^*(M' \times [0,1]/X')$ is a free abelian group of finite rank.*

Let $\nu_1, \dots, \nu_{2g} : [0,1] \to \Sigma\backslash\{z\}$ be parameterizations of simple closed curves with the following properties.

(1) The ν_i all start at the same point, which we think of as their wedge point:
$$\nu_1(0) = \dots = \nu_{2g}(0).$$
(2) The ν_i are disjoint besides at the wedge point: for $t_1, t_2 > 0$ and $i \neq j$
$$\nu_i(t_1) \neq \nu_j(t_2).$$
(3) The ν_i generate the first homology of $\Sigma\backslash\{z\}$:
$$H_1(\Sigma\backslash\{z\}) = \mathbb{Z}\langle [\nu_1], \dots, [\nu_{2g}] \rangle.$$
(4) The punctured surface $\Sigma\backslash\{z\}$ deformation retracts onto the wedge product $\bigvee_{j=1}^{2g} \nu_j$.

Taking symmetric products preserves homotopy equivalence, and so $M' = \mathrm{Sym}^g(\Sigma\backslash\{z\})$ deformation retracts onto $\mathrm{Sym}^g(\bigvee_{j=1}^{2g} \nu_j)$. The following lemma of Ong, proved in detail in [Hen12], describes the homotopy type of this space.

Lemma 6.2. [Hen12, Lemma 5.1] *The r^{th} symmetric product of a wedge of k circles $\mathrm{Sym}^r(\bigvee_{j=1}^{k} S_j^1)$ is homotopy equivalent to the r-skeleton of the k torus $\prod_{j=1}^{k} S_j^1$, where each circle is given a CW structure consisting of the wedge point and a single one-cell, and the torus has the natural product CW structure.*

To understand this homotopy equivalence

$$F : \mathrm{Sym}^r(\bigvee_{j=1}^{k} S_j^1) \to \text{r-skeleton of } \prod_{j=1}^{k} S_j^1,$$

define coordinates $S_j^1 = \{z_j \in \mathbb{C} || z_j| = 1\}$ on each S_j^1 in such a way that the wedge point of each S_j^1 is $z_j = 1$. Then the j^{th} coordinate F_j of the homotopy equivalence F is defined on the tuple $(z_{j_1} \dots z_{j_r}) \in \mathrm{Sym}^r(\bigvee_{j=1}^{k} S_1^j)$ by

$$F_j((z_{j_1} \dots z_{j_r})) := \prod_{j_i = j} z_{j_i} \in S_j^1.$$

The image of F is $\{(z_1, \dots, z_k) | \text{at most r of the } z_j \neq 1\} \subset \prod_{j=1}^{k} S_i^1$ which is indeed the r-skeleton of $\prod_{j=1}^{k} S_j^1$.

Composing the homotopy equivalence of Lemma 6.2 with the deformation retraction $M' \approx \mathrm{Sym}^g(\bigvee_{i=1}^{2g} \nu_i)$ gives a homotopy equivalence G of M' with the g-skeleton of $\prod_{i=1}^{2g} \nu_i$. Define

$$\bar{\nu}_i = G_*^{-1}([t \to (1, \dots, \nu_i(t), \dots, 1)]) \in H_1(M').$$

Then the first homology of M' is

$$H_1(M') = \mathbb{Z}\langle \bar{\nu}_1, ..., \bar{\nu}_{2g} \rangle. \tag{6.2}$$

Applying the Kunneth theorem and the fact that M' is homotopy equivalent to the g-skeleton of $\prod_{i=1}^{2g} \nu_i$, for $m = 1, ..., g$ the homology group $H_m(M')$ is spanned by m-tensors of the $\bar{\nu}_i$ with no repeated indices; we will write this as

$$H_m(M') \cong \Lambda^m H_1(M) = \Lambda^m \mathbb{Z}\langle \bar{\nu}_1, ..., \bar{\nu}_{2g} \rangle. \tag{6.3}$$

The first homology of M' has an alternative description [OS04c, Lemma 2.6]

$$H_1(\Sigma\backslash\{z\}) \cong H_1(\mathrm{Sym}^g(\Sigma\backslash\{z\})) = H_1(M'). \tag{6.4}$$

The homology classes of the attaching curves

$$\boldsymbol{\alpha} \cup \boldsymbol{\beta} = \{\alpha_1, ..., \alpha_g, \beta_1, ..., \beta_g\}$$

form a basis for $H_1(\Sigma\backslash\{z\})$ since they specify a Heegaard decomposition for S^3. Let $\bar{\alpha_i}$ and $\bar{\beta_i}$ denote the images in $H_1(M')$ of $[\alpha_i]$ and $[\beta_i]$ under the isomorphism of Equation 6.4. Explicitly, letting $\alpha_i(t)$ be a parameterization of α_i, then $\bar{\alpha}_i = [t \to (\alpha_i(t)x...x)]$ where x is any point in $\Sigma\backslash\{z\}$. We recast Equation (6.3) as

$$H_m(M' \times [0,1]) \cong H_m(M') \cong \Lambda^m \mathbb{Z}\langle \bar{\alpha}_1, ..., \bar{\alpha}_g, \bar{\beta}_1, ..., \bar{\beta}_g \rangle \text{ for } m = 1, \dots, g, \tag{6.5}$$

and

$$H_m(M' \times [0,1]) = 0 \text{ for } m > g. \tag{6.6}$$

Next we consider the homology of the tori $L_0' = \mathbb{T}_{\boldsymbol{\alpha}} = \alpha_1 \times \ldots \times \alpha_g$ and $L_1' = \mathbb{T}_{\boldsymbol{\beta}} = \beta_1 \times \ldots \times \beta_g$. Choosing basepoints x_i on each α_i and y_i on each β_i for $i = 1, \ldots, g$, and defining

$$\hat{\alpha}_i = [t \to (x_1 \ldots x_{i-1} \alpha_i(t) x_{i+1} \ldots x_g)] \in H_1(L_0') \text{ and} \tag{6.7}$$

$$\hat{\beta}_i = [t \to (y_1 \ldots y_{i-1} \beta_i(t) y_{i+1} \ldots y_g)] \in H_1(L_1'), \tag{6.8}$$

the homology groups of L_0' and L_1' for $m = 1, \ldots, g$ are

$$H_m(L_0') = \Lambda^m \mathbb{Z}\langle \hat{\alpha}_1, \ldots, \hat{\alpha}_g \rangle, \tag{6.9}$$

$$H_m(L_1') = \Lambda^m \mathbb{Z}\langle \hat{\beta}_1, \ldots, \hat{\beta}_g \rangle, \tag{6.10}$$

and are zero for $m > g$. Abusing notation, we then write the homology of $X' = (L_0' \times \{0\}) \cup (L_1' \times \{1\})$ as

$$H_m(X') = \Lambda^m \mathbb{Z}\langle \hat{\alpha}_1, \ldots, \hat{\alpha}_g \rangle \oplus \Lambda^m \mathbb{Z}\langle \hat{\beta}_1, \ldots, \hat{\beta}_g \rangle \text{ for } m = 1, \ldots, g \text{ and} \tag{6.11}$$

$$H_m(X') = 0 \text{ for } m > g. \tag{6.12}$$

Letting $I : X' \hookrightarrow M' \times [0,1]$ denote the inclusion map (lowercase i is reserved for a different inclusion map in Section 7), then the homology pushforward

$$I_* : H_m(X') \to H_m(M' \times [0,1])$$

admits the following description:

$$I_*(\Lambda_{t=1}^m \hat{\alpha}_{j_t} \oplus \Lambda_{t=1}^m \hat{\beta}_{j_t'}) = \Lambda_{t=1}^m \bar{\alpha}_{j_t} + \Lambda_{t=1}^m \bar{\beta}_{j_t'} \tag{6.13}$$

where $(j_1, ..., j_k)$ and $(j_1', ..., j_k')$ are any collection of distinct integers between 1 and g inclusive. Notice that $\Lambda_{t=1}^m \bar{\alpha}_{j_t} = \Lambda_{t=1}^m \bar{\alpha}_{p_t}$ if and only if $(j_1, ..., j_t) = (p_1, ..., p_t)$, and similarly for wedges of the $\hat{\beta}_i$. Since $\Lambda_{t=1}^m \hat{\alpha}_{j_t} \oplus \Lambda_{t=1}^m \hat{\beta}_{j_t'}$ is a generic basis element of $H_m(X')$, and $\Lambda_{t=1}^m \bar{\alpha}_{j_t}$, and $\Lambda_{t=1}^m \bar{\beta}_{j_t'}$ are basis elements of $H_1(M' \times [0,1])$ we have showed the following.

Lemma 6.3. *The homology push-forward map $I_* : H_m(X') \to H_m(M' \times [0,1])$ is an injection for $m \geq 1$.*

We have also showed that $H_*(X')$ and $H_*(M' \times [0,1])$ are free abelian of finite rank because X' is a disjoint union of tori and $M' \times [0,1]$ has the homotopy type of a skeleton of a torus. Every homology and cohomology group in sight will have finite rank from these observations combined with universal coefficients and the (co)homology long exact sequence, so from now on we do not mention rank. From the universal coefficient theorem the cohomology groups $H^*(X')$ and $H^*(M' \times [0,1])$ are free abelian as well. These observations tell us that in the commutative square

$$\begin{array}{ccc} H^m(M' \times [0,1]) & \longrightarrow & \mathrm{Hom}(H_m(M' \times [0,1]), \mathbb{Z}) \\ \downarrow{\scriptstyle I^*} & & \downarrow{\scriptstyle (I_*)^T} \\ H^m(X') & \longrightarrow & \mathrm{Hom}(H_m(X'), \mathbb{Z}) \end{array}$$

the horizontal arrows are isomorphisms. The fact that the homology groups are free abelian further tells us that injectivity of p_* implies surjectivity of $(I_*)^T$. Surjectivity of $(I_*)^T$ along with the fact that the above commutative square has isomorphisms for horizontal arrows yields the following lemma.

Lemma 6.4. *The cohomology pullback map induced by inclusion*

$$I^* : H^m(M' \times [0,1]) \to H^m(X')$$

is a surjection for $m \geq 1$.

Lemma 6.4 is of course equivalent to the same statement for reduced cohomology: the map $I^* : \widetilde{H}^m(M' \times [0,1]) \to \widetilde{H}^m(X')$ for $m \geq 1$ is a surjection.

We are now ready to prove Proposition 6.1.

Proof of Proposition 6.1. In the following we use Q instead of q, again because the lowercase letter is reserved for Section 7. Surjectivity of I^* for $m \geq 1$ tells us that the cohomology long exact sequence of the pair $(M' \times [0,1], X')$

$$\ldots \to \widetilde{H}^m(M' \times [0,1]/X') \xrightarrow{Q^*} \widetilde{H}^m(M' \times [0,1]) \xrightarrow{I^*} \widetilde{H}^m(X') \xrightarrow{\partial} \widetilde{H}^{m+1}((M' \times [0,1]/X') \to \ldots$$

breaks up into short exact sequences

$$0 \to \widetilde{H}^m(M' \times [0,1]/X') \hookrightarrow \widetilde{H}^m(M' \times [0,1]) \twoheadrightarrow \widetilde{H}^m(X') \to 0$$

for $m \geq 2$. So, for $m \geq 2$, $\widetilde{H}^m(M' \times [0,1]/X')$ injects into the free abelian group $\widetilde{H}^m(M' \times [0,1])$, and hence is free abelian itself. All that is left is to analyze $\widetilde{H}^1(M' \times [0,1]/X')$. To do this, we look at the beginning of the cohomology long exact sequence

$$\ldots \to 0 = \widetilde{H}^0(M' \times [0,1]) \xrightarrow{p^*} \widetilde{H}^0(X') \xrightarrow{\partial} \widetilde{H}^1(M' \times [0,1]/X') \xrightarrow{Q^*} \widetilde{H}^1(M' \times [0,1]) \to \ldots$$

and use it to write the short exact sequence

$$0 \to \widetilde{H}^0(X') \hookrightarrow \widetilde{H}^1(M' \times [0,1]/X) \twoheadrightarrow im(Q^*) \to 0.$$

Now $\widetilde{H}^0(X') \cong \mathbb{Z}$ since X' has two connected components, and $im(Q^*)$ is free abelian since it is a subgroup of $\widetilde{H}^m(M' \times [0,1])$. Since the abelian group $\widetilde{H}^1(M' \times [0,1]/X')$ admits a homomorphism with free kernel and image, it must be free itself. We remind the reader that the finite rank condition was verified earlier. □

7. Stable tangent normal isomorphism

In order to make use of Theorem 4.4, we need some method of producing stable tangent normal isomorphisms. If $\pi : M^{\text{inv}} \times [0,1] \to M^{\text{inv}}$ is the projection map, define

$$E_N := \pi^*(NM^{\text{inv}}) = N(M^{\text{inv}}) \times [0,1] \tag{7.1}$$

$$E_T := \pi^*(TM^{\text{inv}}) = T(M^{\text{inv}}) \times [0,1] \tag{7.2}$$

$$X := (L_0^{\text{inv}} \times \{0\}) \cup (L_1^{\text{inv}} \times \{1\}) \subset M^{\text{inv}} \times [0,1] \tag{7.3}$$

and let J denote the complex structure on M^{inv}. We prove for later convenience the following proposition which is an analog of a result alluded to in [SS10, Section 3d] and proven in detail in [Hen12, Proposition 7.1].

Proposition 7.1. *Let*

$$f_N, f_T : (M^{\text{inv}} \times [0,1], X) \to (BU, BO)$$

be the classifying maps of the (complex bundle ξ over $M^{\text{inv}} \times [0,1]$, real subbundle of $\xi|_X$) pairs

$$(E_N, (N(L_0^{\text{inv}}) \times \{0\}) \cup (JN(L_1^{\text{inv}}) \times \{1\})) \twoheadrightarrow (M^{\text{inv}}, X)$$

and

$$(E_T, (T(L_0^{\text{inv}}) \times \{0\}) \cup (JT(L_1^{\text{inv}}) \times \{1\})) \twoheadrightarrow (M^{\text{inv}}, X)$$

respectively. Then a homotopy between f_N and f_T implies the existence of a stable tangent normal isomorphism. That is, to demonstrate a stable tangent normal isomorphism it suffices to produce a stable complex isomorphism between E_N and E_T that restricts to a stable real isomorphism of $(N(L_0^{\text{inv}}) \times \{0\}) \cup (JN(L_1^{\text{inv}}) \times \{1\})$ and $(T(L_0^{\text{inv}}) \times \{0\}) \cup (JT(L_1^{\text{inv}}) \times \{1\})$ over X.

The following proof is identical to the one given in Proposition 7.1 of [Hen12] except necessary modifications to talk about a stable tangent normal isomorphism instead of a stable normal trivialization.

Proof. The structure group of complex vector bundles $GL(n,\mathbb{C})$ deformation retracts onto the unitary group $U(n)$. The unitary group can be written as an intersection

$$U(n) = O(2n) \cap Sp(2n,\mathbb{R}) \subset GL(n,\mathbb{C})$$

of the orthogonal and symplectic groups, and hence every complex vector bundle acquires in particular a symplectic structure. In addition, a symplectic vector bundle has a unique up to homotopy compatible complex structure. Moreover, two symplectic vector bundles are isomorphic if and only if their underlying complex vector bundles are isomorphic, and isomorphisms of symplectic vector bundles map Lagrangian subbundles to Lagrangian subbundles (see McDuff and Salamon [MD95, Theorem 2.62]). Let ω_N and ω_T be the natural symplectic structures on $N(M^{\text{inv}})$ and $T(M^{\text{inv}})$ coming from the symplectic structure on TM. Let the dimension $N(M^{\text{inv}})$ and $T(M^{\text{inv}})$ be $k \in \mathbb{N}$, and let

$$\zeta_k \colon EU_k \to BU_k$$

be the complex k–dimensional universal bundle, and similarly take

$$\eta_k \colon EO_k \to BO_k$$

to be the real k–dimensional universal bundle. Equip EU_k with a symplectic structure ω_ζ such that $\eta_k \subset \zeta_k$ is a Lagrangian subbundle. Then the bundles $(E_N, \widetilde{\omega}_M := \pi^*(\omega_N))$ and $(E_N, f_N^*(\omega_\zeta))$ are equal as complex vector bundles, so there is a symplectic vector bundle isomorphism

$$\widetilde{\chi}_N \colon (E_N, \widetilde{\omega}_M) \to (E_N, f_N^*(\omega_\zeta)),$$

Similarly we have a symplectic vector bundle isomorphism

$$\widetilde{\chi}_T \colon (E_T, \widetilde{\omega}_T) \to (E_T, f_T^*(\omega_\zeta)),$$

The symplectic forms are the pullbacks of the original symplectic forms on $N(M^{\text{inv}})$ or $T(M^{\text{inv}})$ to E_N or E_T, and therefore constant with respect to the interval $[0,1]$, as are the maps $\widetilde{\chi}_N$ and $\widetilde{\chi}_T$. From now on assume that we have first applied isomorphisms of this form to E_N and E_T so that the maps $f_N \colon E_N \to BU$ and $f_T \colon E_T \to BU$ are symplectic classifying maps. We can if necessary pre- and post compose the resulting stable tangent normal isomorphism with $\widetilde{\chi}_T$ and $\widetilde{\chi}_N^{-1}$.

Consider a homotopy H of between f_N and f_T

$$\begin{aligned} H \colon (M^{\text{inv}} \times [0,1], L_0^{\text{inv}} \times \{0\} \cup L_1^{\text{inv}} \times \{1\}) \times [0,1] &\to (BU, BO) \\ (x,t,s) &\mapsto h_s(x,t) \end{aligned}$$

Here the map h_0 is equal to f_N and the map h_1 is equal to f_T.

Since M^{inv} is homotopy equivalent to a compact subspace of itself, we may assume there is some $K > 0$ such that if $s = k + K$, the image of H lies inside (BU_s, BO_s). Let $\zeta_s \colon EU_s \to BU_s$ be the complex s–dimensional universal bundle with subbundle $\eta_s \colon EO_s \to BO_s$ the real s–dimensional universal bundle. Consider the following pullbacks of ζ_s and η_s along h_1 and h_0.

$$\begin{aligned} h_0^*(\zeta_s) &= (E_N \oplus \mathbb{C}^K, h_0^*\omega_\zeta) \\ h_1^*(\zeta_s) &= (E_T \oplus \mathbb{C}^K, h_1^*\omega_\zeta) \\ (h_0|_{L_0^{\text{inv}} \times \{0\}})^*(\eta_s) &= ((N(L_0^{\text{inv}}) \times \{0\}) \oplus \mathbb{R}^K \\ (h_0|_{L_1^{\text{inv}} \times \{1\}})^*(\eta_s) &= (J(N(L_1^{\text{inv}}) \times \{1\}) \oplus \mathbb{R}^K \end{aligned}$$

$$(h_1|_{L_0^{\mathrm{inv}}\times\{0\}})^*(\eta_s) = ((T(L_0^{\mathrm{inv}})\times\{0\})\oplus\mathbb{R}^K$$
$$(h_1|_{L_1^{\mathrm{inv}}\times\{1\}})^*(\eta_s) = (J(T(L_1^{\mathrm{inv}}))\times\{1\})\oplus\mathbb{R}^K$$

Here $\mathbb{R}^K$ is the canonical real subspace in $\mathbb{C}^K$.

Since H is a homotopy, it induces a stable isomorphism ψ of E_N with E_T. Write an arbitrary vector in $E_N\oplus\mathbb{C}^K$ as (x,t,v) where $(x,t)\in M^{\mathrm{inv}}\times[0,1]$ and v is an element of the fiber over (x,t):

$$\psi\colon E_N\oplus\mathbb{C}^K = h_0^*(\zeta_s)\xrightarrow{\sim} h_1^*(\zeta_s) = E_T\oplus\mathbb{C}^K$$
$$(x,t,v)\mapsto\psi(x,t,v).$$

The restrictions of ψ to $N(L_0^{\mathrm{inv}})\times\{0\}\oplus\mathbb{R}^K$ and $J(N(L_1^{\mathrm{inv}})\times\{1\})\oplus\mathbb{R}^K$,

$$\psi|_{N(L_0^{\mathrm{inv}})\times\{0\}\oplus\mathbb{R}^K} : ((N(L_0^{\mathrm{inv}})\times\{0\})\oplus\mathbb{R}^K)\to((T(L_0^{\mathrm{inv}})\times\{0\})\oplus\mathbb{R}^K)$$

and

$$\psi|_{J(N(L_1^{\mathrm{inv}}))\times\{1\}\oplus\mathbb{R}^K} : ((J(N(L_1^{\mathrm{inv}}))\times\{1\})\oplus\mathbb{R}^K)\to(J(T(L_1^{\mathrm{inv}})\times\{1\})\oplus\mathbb{R}^K),$$

are isomorphisms of trivial real bundles.

Since E_N is the pullback of $N(M^{\mathrm{inv}})$ to $M^{\mathrm{inv}}\times[0,1]$, the map $h_0 = f_N$ is constant with respect to the interval $[0,1]$. That is, $h_0(x,t_1) = h_0(x,t_2)$ for all $x\in M^{\mathrm{inv}}$ and $t_1,t_2\in[0,1]$. Then each $\psi_t = \psi|_{M^{\mathrm{inv}}\times\{t\}}$ is a stable isomorphism of $N(M^{\mathrm{inv}})\times\{t\} = N(M^{\mathrm{inv}})$ with $T(M^{\mathrm{inv}})\times\{t\} = T(M^{\mathrm{inv}})$. More concretely, we have symplectic isomorphisms

$$\psi_t\colon N(M^{\mathrm{inv}})\oplus\mathbb{C}^K\to T(M^{\mathrm{inv}})\oplus\mathbb{C}^K$$
$$(x,v)\mapsto\psi(x,t,v).$$

Consider a map ϕ

$$\phi\colon E_N\oplus\mathbb{C}^K\to E_T\oplus\mathbb{C}^K$$
$$(x,t,v)\mapsto\psi_0((x,v)) = \psi(x,0,v).$$

This is a stable isomorphism of E_N with E_T. Because the symplectic structures on E_N and E_T are constant with respect to the interval $[0,1]$, ϕ is a symplectic isomorphism of vector bundles. Consider the following Lagrangian subbundles of $E_N|_{L_0^{\mathrm{inv}}\times[0,1]}$ and $E_N|_{L_1^{\mathrm{inv}}\times[0,1]}$

$$\Lambda_0|_{L_0^{\mathrm{inv}}\times\{t\}} := (N(L_0^{\mathrm{inv}})\times\{t\})\oplus\mathbb{R}^K$$
$$\Lambda_1|_{L_1^{\mathrm{inv}}\times\{t\}} := \psi_0^{-1}\circ\psi_t(N(L_1^{\mathrm{inv}})\times\{t\}\oplus i\mathbb{R}^K).$$

Since the maps ψ_t form a homotopy, Λ_1 is a smooth subbundle. Both subbundles are Lagrangian since their restriction to each $L_i^{\mathrm{inv}}\times\{t\}$ is Lagrangian. The restriction of Λ_i to $L_i^{\mathrm{inv}}\times\{0\}$ for $i=0,1$ is

$$\Lambda_0|_{L_0^{\mathrm{inv}}\times\{0\}} = (N(L_0^{\mathrm{inv}})\times\{0\})\oplus\mathbb{R}^K \tag{7.4}$$
$$\Lambda_1|_{L_1^{\mathrm{inv}}\times\{0\}} = \psi_0^{-1}\circ\psi_0((N(L_1^{\mathrm{inv}})\times\{0\})\oplus i\mathbb{R}^K) = (N(L_1^{\mathrm{inv}})\times\{0\})\oplus i\mathbb{R}^K. \tag{7.5}$$

Also notice that

$$\begin{aligned}\phi(\Lambda_0|_{L_0^{\mathrm{inv}}\times\{1\}}) &= \psi_0((N(L_0^{\mathrm{inv}})\times\{0\})\oplus\mathbb{R}^K) \\ &= \psi((N(L_0^{\mathrm{inv}})\times\{0\})\oplus\mathbb{R}^K) \\ &= T(L_0^{\mathrm{inv}})\oplus\mathbb{R}^K\subset E_T\oplus\mathbb{C}^K\end{aligned} \tag{7.6}$$
$$\phi(\Lambda_1|_{L_1^{\mathrm{inv}}\times\{1\}}) = \psi_0(\psi_0^{-1}\circ\psi_1((N(L_1^{\mathrm{inv}})\times\{1\})\oplus i\mathbb{R}^K) \tag{7.7}$$

$$= \psi_1(J(J((N(L_1^{\text{inv}}) \times \{1\}) \oplus i\mathbb{R}^K)))$$
$$= J(\psi_1(J(N(L_1^{\text{inv}}) \times \{1\}) \oplus \mathbb{R}^k))$$
$$= J(J(T(L_1^{\text{inv}}) \times \{1\}) \oplus \mathbb{R}^K) = (T(L_1^{\text{inv}}) \times \{1\}) \oplus i(\mathbb{R}^K) \subset E_T \oplus \mathbb{C}^K$$

It follows from Equations (7.4), (7.5), (7.6) and (7.7) that applying ϕ to each slice of these subbundles $\Lambda_i|_{L_i^{inv} \times \{t\}}$ yields homotopies through Lagrangians of $\phi(N(L_0^{\text{inv}}) \oplus \mathbb{R}^K)$ with $T(L_0^{\text{inv}}) \oplus \mathbb{R}^K$ and $\phi(N(L_1^{\text{inv}}) \oplus i(\mathbb{R}^K))$ with $T(L_1^{\text{inv}}) \oplus i(\mathbb{R}^K)$. □

We show that the stable tangent normal isomorphism hypothesis of Theorem 4.4 is met for (M, L_0, L_1, τ) defined as in Section 4 by using Proposition 7.1; it will suffice to find a stable complex isomorphism of E_N with E_T that restricts to a stable real isomorphism of

$$(N(L_0^{\text{inv}}) \times \{0\}) \cup J(N(L_1^{\text{inv}}) \times \{1\})$$

with

$$(T(L_0^{\text{inv}}) \times \{0\}) \cup J(T(L_1^{\text{inv}}) \times \{1\}).$$

These are trivializable totally real subbundles of $E_N|_X$ and $E_T|_X$ respectively; see [Hen12, Lemma 7.3] for a proof. After picking real trivializations, we may tensor with $\mathbb{C}$ to obtain complex trivializations

$$\phi_N : E_N|_X \to \mathbb{C}^k$$

and

$$\phi_T : E_T|_X \to \mathbb{C}^k.$$

The composition

$$f := \phi_T^{-1} \circ \phi_N : E_N|_X \to E_T|_X$$

is then an isomorphism of complex bundles over X. We will show that f can be stably extended to all of E_N and E_T, which in particular implies that Proposition 7.1 is satisfied. The strategy for showing that such an extension exists will be to show equality of relative K-theory classes

$$[E_N]_{rel} = [E_T]_{rel} \in \widetilde{K}^0(M^{\text{inv}} \times [0,1], X). \tag{7.8}$$

7.1. **K-theory.** In this Section we recall some results about complex K-theory. Let $\text{Vect}^{\mathbb{C}}(B)$ be the set of all complex finite dimensional vector bundles over a space B. For our purposes it suffices to take B to be a compact manifold, although the following remarks and theorems apply to vector bundles over compact Hausdorff topological spaces. We refer the reader to [Hat03] for a complete treatment of this subject.

Definition 7.2. A stable isomorphism of complex vector bundles $E, E' \in \text{Vect}^{\mathbb{C}}(B)$ is a complex vector bundle isomorphism of $E \oplus \underline{\mathbb{C}}^m \cong E' \oplus \underline{\mathbb{C}}^n$ for some $(m, n) \in \mathbb{Z}^2$. Stable isomorphism is an equivalence relation on $\text{Vect}^{\mathbb{C}}(B)$ which we denote by $\sim$.

Definition 7.3. The 0^{th} (reduced) *complex K-theory group* of a space B is the set of complex vector bundles on B modulo stable isomorphism:

$$\widetilde{K}^0(B) = \text{Vect}^{\mathbb{C}}(B)/\sim . \tag{7.9}$$

The operations of tensor product $\otimes$ and direct sum $\oplus$ on $\text{Vect}^{\mathbb{C}}(B)$ descend to a multiplication and addition on $\widetilde{K}^0(B)$, giving it a ring structure. Complex K-theory can be made into a reduced cohomology theory by defining the higher K theory groups

$$\widetilde{K}^i(B) := \widetilde{K}^0(\Sigma^i(B))$$

where $\Sigma^i(B)$ is the reduced suspension functor applied i times to B (to see that this definition actually yields a reduced cohomology theory *Bott periodicity*, $\widetilde{K}^0(B) \cong \widetilde{K}^0(\Sigma^2(B))$, is employed), and the relative K-theory groups of a pair $X \subset B$

$$\widetilde{K}^i(B, X) := \widetilde{K}^i(B/X)$$

where X is a closed subspace of B. The Brown Representability Theorem then implies that each reduced complex K-theory group can be represented by homotopy classes of maps from X into a classifying space; in particular if BU is the classifying space of the infinite unitary group then

Proposition 7.4. *There is an isomorphism*

$$\widetilde{K}^0(B) \cong [B, BU]. \tag{7.10}$$

This image of the (equivalence class of a) vector bundle under this isomorphism is called the classifying map *of the vector bundle*

The following two propositions relate K-theory to ordinary (singular) cohomology.

Proposition 7.5 (Chern character)**.** *There is a homomorphism*

$$\widetilde{ch} : \widetilde{K}^0(B) \to \widetilde{H}^{even}(B, \mathbb{Q}) \tag{7.11}$$

called the reduced Chern character *between reduced complex K theory and reduced singular cohomology with rational coefficients that enjoys the following properties:*

- *tensoring with $\mathbb{Q}$ makes $\widetilde{ch}$ into an isomorphism (which we will also call $\widetilde{ch}$)*

$$\widetilde{ch} : \widetilde{K}^0(B) \otimes_{\mathbb{Z}} \mathbb{Q} \xrightarrow{\sim} \widetilde{H}^{even}(B, \mathbb{Q}),$$

  and
- *the reduced Chern character $\widetilde{ch}([E])$ is a polynomial in the Chern classes of the (stable equivalence class of) the vector bundle E.*

Proposition 7.6. *If $H^*(B, \mathbb{Z})$ is torsion free and of finite rank, then so is $\widetilde{K}^0(B)$.*

Given a closed subspace X of the compact space B, the K-theory of a quotient space $\widetilde{K}^0(B/X)$ can be thought of as the set of isomorphism classes of vector bundles over B which restrict to a trivial bundle over X. We also denote this space by $\widetilde{K}^0(B, X)$.

Propositions 7.5 and 7.6 along with the fact that the $\widetilde{H}^*(M^{\text{inv}} \times [0, 1], X)$ is torsion free and finite rank (c.f Proposition 6.1) tell us that demonstrating equality of relative Chern classes $c((E_T)_{rel}) = c((E_N)_{rel})$ would in particular imply Equation (7.8), and hence demonstrate the existence of a stable tangent normal isomorphism. This proof is the subject of the next Subsection.

7.2. **Algebraic topology of symmetric products.** Here we show

Proposition 7.7. *The relative Chern classes $c((E_T)_{rel})$ and $c((E_N)_{rel}) \in \widetilde{H}^*(M^{\text{inv}} \times [0, 1], X)$ coincide:*

$$c((E_T)_{rel}) = c((E_N)_{rel}) \in \widetilde{H}^*(M^{\text{inv}} \times [0, 1], X). \tag{7.12}$$

The lemmas and corollaries necessary to prove Proposition 7.7 are collected below.

Lemma 7.8. *The pullback of the total Chern class of M along $i : M^{\text{inv}} \hookrightarrow M$ is the square of the total Chern class of M^{inv} :*

$$c(TM^{\text{inv}})^2 = i^*(c(TM)) = c(i^*(TM)) \in \widetilde{H}^*(M^{\text{inv}}). \tag{7.13}$$

We prove Lemma 7.8 later in this Section. Assuming it, note the following corollary.

Corollary 7.9. *The Chern classes of the tangent and normal bundles of $M^{\text{inv}} \subset M$ coincide:*

$$c(TM^{\text{inv}}) = c(NM^{\text{inv}}) \in \widetilde{H}^*(M^{\text{inv}}). \tag{7.14}$$

Proof of Corollary 7.9. The vector bundle isomorphism $TM^{\text{inv}} \oplus NM^{\text{inv}} \cong i^*(TM)$ implies

$$c(TM^{\text{inv}})c(NM^{\text{inv}}) = c(i^*(TM)) \in \widetilde{H}^*(M^{\text{inv}}).$$

From Lemma 7.8 we then get

$$c(TM^{\text{inv}})c(NM^{\text{inv}}) = c(TM^{\text{inv}})^2 \implies c(TM^{\text{inv}}) = c(NM^{\text{inv}}).$$

We can cancel a factor of $c(TM^{\text{inv}})$ on both sides as there is no torsion in $\widetilde{H}^*(M^{\text{inv}})$. □

Lemma 7.10. *The even degree cohomology map $q^* : \widetilde{H}^{even}(M^{\text{inv}} \times [0,1], X) \to \widetilde{H}^{even}(M^{\text{inv}} \times [0,1])$ is an injection:*

$$q^* : \widetilde{H}^{even}(M^{\text{inv}} \times [0,1], X) \hookrightarrow \widetilde{H}^{even}(M^{\text{inv}} \times [0,1]).$$

Proof. Looking at the cohomology long exact sequence for the pair $(M^{\text{inv}} \times [0,1], X)$

$$\ldots \to \widetilde{H}^{2r-1}(M^{\text{inv}} \times [0,1]) \xrightarrow{\iota^*} \widetilde{H}^{2r-1}(X) \xrightarrow{\delta^*} \widetilde{H}^{2r}(M^{\text{inv}} \times [0,1]/X) \xrightarrow{q^*} \widetilde{H}^{2r}(M^{\text{inv}} \times [0,1]) \to \ldots$$

we see that

$$q^* : \widetilde{H}^{2r}(M^{\text{inv}} \times [0,1]/X) \to \widetilde{H}^{2r}(M^{\text{inv}} \times [0,1])$$

is an injection iff

$$\iota^* : \widetilde{H}^{2r-1}(M^{\text{inv}} \times [0,1]) \to \widetilde{H}^{2r-1}(X)$$

is a surjection. Recall the biholomorphism $\phi : (M', L_0', L_1') \to (M^{\text{inv}}, L_0^{\text{inv}}, L_1^{\text{inv}})$; clearly it induces a biholomorphism

$$\Phi : (M' \times [0,1], X') \to (M^{\text{inv}} \times [0,1], X).$$

Naturality of the cohomology long exact sequence and Lemma 6.4 then tell us that ι^* is a surjection so long as $r \geq 1$. This argument also proves injectivity of q^* on $\widetilde{H}^{2r+1}$ for $r \geq 1$ as well, but we don't have any need for this result. For $r = 0$ injectivity of q^* is immediate since the 0^{th} reduced cohomology of both $M^{\text{inv}} \times [0,1]$ and $M^{\text{inv}} \times [0,1]/X$ is zero. □

Assuming Lemma 7.8 we prove Proposition 7.7.

Proof of Proposition 7.7. From functoriality of Chern classes

$$q^*(c((E_T)_{rel})) = c(E_T) \text{ and } q^*(c((E_T)_{rel})) = c(E_T).$$

By definition, $E_T = \pi^*(TM^{\text{inv}})$ and $E_N = \pi^*(NM^{\text{inv}})$ and so

$$(\pi^*)^{-1} \circ q^*(c((E_T)_{rel})) = (\pi^*)^{-1}(c(E_T)) = (\pi^*)^{-1}c(\pi^*TM^{\text{inv}}) = c(TM^{\text{inv}})$$

and

$$(\pi^*)^{-1} \circ q^*(c((E_N)_{rel})) = (\pi^*)^{-1}(c(E_N)) = (\pi^*)^{-1}c(\pi^*NM^{\text{inv}}) = c(NM^{\text{inv}}).$$

From Corollary 7.9 we know that

$$c(TM^{\text{inv}}) = c(NM^{\text{inv}})$$

and therefore by injectivity of $(\pi^*)^{-1} \circ q^*$ (Lemma 7.10) we conclude

$$c((E_T)_{rel}) = c((E_N)_{rel}).$$

□

In order to establish Proposition 7.7, what remains is to prove Lemma 7.8. To this end, we first record notation for and relations amongst the homology, cohomology and Chern classes of the M and M' in the below proposition. For more about the cohomology ring $H^*(\mathrm{Sym}^{2g}(\widetilde{\Sigma}))$ see [Mac62]. We set $R = \widetilde{\Sigma}\backslash\{z, w\}$ for conciseness.

Proposition 7.11. *Let $\widetilde{s}_1, \ldots, \widetilde{s}_{2g}, \widetilde{m}_1, \ldots, \widetilde{m}_{2g} \in H^1(R)$ be homology classes forming a symplectic basis of $H^1(R)$*

$$\widetilde{s}_i \cup \widetilde{s}_j = \widetilde{m}_i \cup \widetilde{m}_j = 0 \text{ and } \widetilde{s}_i \cup \widetilde{m}_j = \delta_{ij}$$

labeled so that if we take indices modulo $2g$,

$$\tau_*(\widetilde{s}_i) = \widetilde{s}_{i+g}$$

and

$$\tau_*(\widetilde{m}_i) = \widetilde{m}_{i+g}.$$

Let $\widetilde{r} \in H^1(R)$ be the homology class of a small loop about $z \in \widetilde{\Sigma}$. Then the relevant homology and cohomology groups of R, R/τ, M and M' are summarized in the table below

Space	*Homology*	*Cohomology*
$R = \widetilde{\Sigma}\backslash\{z, w\}$	$H_i(R) = \begin{cases} \mathbb{Z} & i = 0 \\ \mathbb{Z}\langle\widetilde{r}\rangle \oplus \bigoplus_{k=1}^{2g} \mathbb{Z}\langle\widetilde{s_i}\rangle \oplus \mathbb{Z}\langle\widetilde{m_i}\rangle & i = 1 \\ 0 & i > 1 \end{cases}$	$H^i(R) = \begin{cases} \mathbb{Z} & i = 0 \\ \mathbb{Z}\langle\widetilde{\rho}\rangle \oplus \bigoplus_{k=1}^{2g} \mathbb{Z}\langle\widetilde{\sigma_i}\rangle \oplus \mathbb{Z}\langle\widetilde{\mu_i}\rangle & i = 1 \\ 0 & i > 1 \end{cases}$
R/τ	$H_i(R/\tau) = \begin{cases} \mathbb{Z} & i = 0 \\ \bigoplus_{k=1}^{g} \mathbb{Z}\langle s_i\rangle \oplus \mathbb{Z}\langle m_i\rangle & i = 1 \\ 0 & i > 1 \end{cases}$	$H^i(R/\tau) = \begin{cases} \mathbb{Z} & i = 0 \\ \bigoplus_{k=1}^{g} \mathbb{Z}\langle\sigma_i\rangle \oplus \mathbb{Z}\langle\mu_i\rangle & i = 1 \\ 0 & i > 1 \end{cases}$
$M = \mathrm{Sym}^{2g}(R)$	–	$H^*(M) \cong (H^*(R)^{\otimes 2g})^{S_{2g}} = \mathbb{Z}[\widetilde{\gamma}] \oplus \bigoplus_{I,J \subset \{1,\ldots,2g\}} \mathbb{Z}\left[\prod_{i\in I} \widetilde{\epsilon_i} \prod_{j\in J} \widetilde{\chi_j}\right]$
$M' = \mathrm{Sym}^{g}(R/\tau)$	–	$H^*(M') \cong (H^*(R/\tau)^{\otimes g})^{S_g} = \bigoplus_{I,J \subset \{1,\ldots,g\}} \mathbb{Z}\left[\prod_{i\in I} \epsilon_i \prod_{j\in J} \chi_j\right]$

where

1. *The cohomology classes $\widetilde{\sigma}_i, \widetilde{\mu}_i$ and $\widetilde{\rho}$ are the algebraic duals of $\widetilde{s}_i$, $\widetilde{m}_i$ and $\widetilde{r}$ respectively under the isomorphism $H^1(R;\mathbb{Z}) \cong \mathrm{Hom}(H_1(R), \mathbb{Z})$.*
2. *The homology classes s_i and m_i for $1 \leq i \leq g$ are defined by*

$$s_i := \ell_*(\widetilde{s}_i) = \ell_*(\widetilde{s}_{i+g})$$

and

$$m_i := \ell_*(\widetilde{m}_i) = \ell_*(\widetilde{m}_{i+g})$$

3. *The cohomology classes σ_i and μ_i are the algebraic duals of s_i and m_i respectively under the isomorphism $H^1(R/\tau;\mathbb{Z}) \cong \mathrm{Hom}(H_1(R/\tau), \mathbb{Z})$.*
4. *The notation $(H^*(R)^{\otimes 2g})^{S_{2g}}$ means the subring of $(H^*(R)^{\otimes 2g})$ that is invariant under the permutation action of the symmetric group S_{2g} on the tensor factors.*

(5) The cohomology class $\widetilde{\gamma}$ is defined as

$$\widetilde{\gamma} := \sum_{k=1}^{2g} 1 \otimes \ldots \otimes \underbrace{\widetilde{\rho}}_{\text{kth slot}} \otimes \ldots \otimes 1,$$

$\widetilde{\epsilon_i}$ is defined as

$$\widetilde{\epsilon_i} := \sum_{k=1}^{2g} = 1 \otimes \ldots \otimes \underbrace{\widetilde{\sigma_i}}_{kth\ slot} \otimes \ldots \otimes 1,$$

and $\widetilde{\chi_j}$ is defined as

$$\widetilde{\chi_i} := \sum_{k=1}^{2g} = 1 \otimes \ldots \otimes \underbrace{\widetilde{\sigma_i}}_{kth\ slot} \otimes \ldots \otimes 1.$$

(6) Similarly for $(H^*(R/\tau)^{\otimes g})^{S_g}$ and the cohomology classes ϵ_i and χ_j.

Furthermore the total Chern classes $c(TM)$ and $c(TM')$ are given by the following formulae.

$$c(TM) = \prod_{i=1}^{2g}(1 - \widetilde{\epsilon_i}\widetilde{\chi_i}) \in H^{even}(M) \tag{7.15}$$

and

$$c(TM') = \prod_{i=1}^{g}(1 - \epsilon_i\chi_i) \in H^{even}(M'). \tag{7.16}$$

Proof. The claims about R and R/τ follow from basic algebraic topology. For the cohomology of M, (1.2) of [Mac62] gives an isomorphism

$$H^*(\mathrm{Sym}^{2g}(R)) \cong (H^*(R))^{S_{2g}}.$$

This isomorphism is stated with cohomology coefficients in a characteristic 0 field K, but it also applies with $\mathbb{Z}$ coefficients so long as the space in question has torsion free cohomology. Using the description of $H^*(R)$ in the table it is then a simple exercise to determine that $\widetilde{\gamma}$, $\widetilde{\epsilon_i}$ and $\widetilde{\chi_i}$ $(1 \leq i \leq 2g)$ form a basis for the S_{2g} invariant tensors in $H^*(R)^{\otimes 2g}$.

In order to establish Equation (7.15), we appeal to [Mac62, (14.5)] which states the following formula for the total Chern class of $\mathrm{Sym}^{2g}(\widetilde{\Sigma})$:

$$c(T\mathrm{Sym}^{2g}(\widetilde{\Sigma})) = (1+\eta)^{n-2g+1}\prod_{i=1}^{2g}(1 + \eta - \xi_i\xi_p)$$

where $\xi_i, \xi_p \in H^1(\mathrm{Sym}^{2g}(\widetilde{\Sigma}))$ for $1 \leq i \leq 2g$ and $\eta \in H^2(\mathrm{Sym}^{2g}(\widetilde{\Sigma}))$ generate $H^*(\mathrm{Sym}^{2g}(\widetilde{\Sigma})) \cong (H^*(\widetilde{\Sigma}))^{\otimes 2g}$. Let $f : \widetilde{\Sigma}\backslash\{z, w\} \hookrightarrow \widetilde{\Sigma}$ denote inclusion; then the induced map $\mathrm{Sym}^{2g}(f)^* : H^*(\mathrm{Sym}^{2g}(\widetilde{\Sigma})) \to H^*(M)$ sends ξ_i to $\widetilde{\epsilon_i}$, ξ_p to $\widetilde{\chi_i}$ and η to 0. Naturality of Chern classes then yields 7.15. The claims about M' follow identically. □

We are now ready to prove Lemma 7.8, thereby establishing Equation (7.12) and verifying the existence of a stable tangent normal isomorphism.

Proof of Lemma 7.8. Pullback along $i \circ \phi : M' \hookrightarrow M$ acts on the generators of $\widetilde{H}^*(M)$ as follows.

- Pullback kills $\widetilde{\gamma}$,

$$(i \circ \phi)^*(\widetilde{\gamma}) = 0.$$

- For $1 \leq i \leq g$ we have
$$(i \circ \phi)^*(\widetilde{\epsilon}_i) = (i \circ \phi)^*(\widetilde{\epsilon}_{i+g}) = \epsilon_i$$
and
$$(i \circ \phi)^*(\widetilde{\chi}_i) = (i \circ \phi)^*(\widetilde{\chi}_{i+g}) = \chi_i.$$

Therefore, from equations 7.15 and 7.16 we see that pullback of the total Chern class of M along $i \circ \phi$ is given by
$$\phi^* i^*(c(TM)) = c((i \circ \phi)^* TM) = c(TM')^2 = \phi^* c(TM^{\text{inv}})^2.$$
The result $i^*(c(TM)) = c(TM^{\text{inv}})^2$ then follows because ϕ^* is invertible. □

Appendix A. Grid homology and Alexander gradings

In this Appendix we review a grid homology based proof of Proposition 3.4, along the way providing a formula for the absolute Alexander grading in a grid diagram for a singular knot. We then modify this proof to provide the analogous result for the spherical grid diagrams of Section 3.5.

Proof of Proposition 3.4. Recall the setup from Section 3.4; we have a grid diagram $\mathbb{G}_S$ for a singular knot S with one singular crossing, and induced grid diagrams $\mathbb{G}_0$ and $\mathbb{G}_-$ for the knots S_0 and S_- obtained by making the local modifications seen in Figure 13. Let $\mathbf{S}_-$ and $\mathbf{S}_0$ denote the set of generators/grid states of $\widetilde{GC}(\mathbb{G}_-)$ and $\widetilde{GC}(\mathbb{G}_0)$ respectively. Partition $\widetilde{GC}(\mathbb{G}_-)$ and $\widetilde{GC}(\mathbb{G}_0)$ as follows: $\widetilde{GC}(\mathbb{G}_-) = I_- \cup N_-$ and $\widetilde{GC}(\mathbb{G}_0) = I_0 \cup N_0$ where I_- and I_0 are generated by those states containing the center point c (marked in blue in Figure 13 and 15), and N_- and N_0 are generated by those states not containing c. The subspaces I_- and N_0 are subcomplexes while the subspaces I_0 and N_- are quotient complexes, and hence all of these subspaces inherit differentials from the complexes $\widetilde{GC}(\mathbb{G}_-)$ and $\widetilde{GC}(\mathbb{G}_0)$; we write the resulting complexes as $(I_-, \partial^{I_-}_{I_-})$, $(N_-, \partial^{N_-}_{N_-})$, $(I_0, \partial^{I_0}_{I_0})$, and $(N_0, \partial^{N_0}_{N_0})$. Consider also the three chain maps
$$\partial^{N_0}_{I_0} : (I_0, \partial^{I_0}_{I_0}) \to (N_0, \partial^{N_0}_{N_0})$$
$$\partial^{I_-}_{N_-} : (N_-, \partial^{N_-}_{N_-}) \to (I_-, \partial^{I_-}_{I_-})$$
$$\psi : (N_0, \partial^{N_0}_{N_0}) \to (N_-, \partial^{N_-}_{N_-})$$
where the first two are induced by the differentials on $\widetilde{GC}(\mathbb{G}_-)$ and $\widetilde{GC}(\mathbb{G}_0)$ respectively while ψ is the map identifying grid states missing c in $\widetilde{GC}(\mathbb{G}_0)$ with grid states missing c in $\widetilde{GC}(\mathbb{G}_-)$. Now compose these chain maps:

$$(I_0, \partial^{I_0}_{I_0}) \xrightarrow[(-1,0)]{\partial^{N_0}_{I_0}} (N_0, \partial^{N_0}_{N_0}) \xrightarrow[(0,0)]{\psi} (N_-, \partial^{N_-}_{N_-}) \xrightarrow[(-1,0)]{\partial^{I_-}_{N_-}} (I_-, \partial^{I_-}_{I_-}) \tag{A.1}$$

The tuples under the arrows indicate the bigraded degree of each chain map. The degree shift associated to $\partial^{N_0}_{I_0}$ and $\partial^{I_-}_{N_-}$ is $(-1, 0)$ because both of these differentials are induced from the standard differential on the grid chain complex which has bi-degree $(-1, 0)$. We use the grid Maslov and Alexander grading formulas, Equations 3.22 and 3.23, to prove the bi-degree of ψ is $(0, 0)$. Let x^{NWX}_- and x^{NWX}_0 be the grid states with markings on the Northwest corner of the X markings in $\mathbb{G}_-$ and $\mathbb{G}_0$ respectively. Notice that x^{NWX}_- is an element of N_0 and N_- because it contains the center point c. Comparing the Alexander and Maslov gradings of x^{NWX}_- considered as an element of $\mathbf{S}_0$ and $\mathbf{S}_-$ will therefore tell us the bi-degree of ψ. Firstly notice that $\mathbb{G}_-$ and

$\mathbb{G}_0$ have the same $\mathbb{O}$ sets and hence $M_{\mathbb{O},-}$ and $M_{\mathbb{O},0}$ (the extra subscript labels the domain of the function, either $\mathbf{S}(\mathbb{G}_-)$ or $\mathbf{S}(\mathbb{G}_0)$) take the same value on x_-^{NWX}. This verifies the claim that the Maslov grading shift of ψ is 0. Next, using equations 3.19, 3.21 and the fact that the 1×1 square NW_c to the Northwest of c is a rectangle going from x_-^{NWX} to x_0^{NWX}, we see that

$$-M_{\mathbb{X},-}(x_0^{NWX}) = M_{\mathbb{X},-}(x_-^{NWX}) - M_{\mathbb{X},-}(x_0^{NWX}) = 1 - 0 + 0 = 1 \implies M_{\mathbb{X},-}(x_0^{NWX}) = -1 \tag{A.2}$$

since NW_c in $\mathbb{G}_-$ contains no X marking, and

$$M_{\mathbb{X},0}(x_-^{NWX}) = M_{\mathbb{X},0}(x_-^{NWX}) - M_{\mathbb{X},0}(x_0^{NWX}) = 1 - 2 \cdot 1 + 0 = -1. \tag{A.3}$$

since NW_c in $\mathbb{G}_0$ contains one X marking. We only need Equation (A.3) to compute the Alexander grading shift of ψ, but Equation (A.2) will be used later in this proof. Now we may compare the Alexander gradings of x_-^{NWX} in $\mathbf{S}(\mathbb{G}_-)$ and $\mathbf{S}(\mathbb{G}_0)$ by using Equation (3.23).

$$A_0(x_-^{NWX}) = \frac{1}{2}(M_{\mathbb{O},0}(x_-^{NWX}) - M_{\mathbb{X},0}(x_-^{NWX})) - \frac{(m+1)-1}{2} \tag{A.4}$$

$$A_-(x_-^{NWX}) = \frac{1}{2}(M_{\mathbb{O},-}(x_-^{NWX}) - M_{\mathbb{X},-}(x_-^{NWX})) - \frac{(m+1)-2}{2} \tag{A.5}$$

Recalling Equations 3.19 and A.3 along with the fact that $M_{\mathbb{O},0}(x_-^{NWX}) = M_{\mathbb{O},-}(x_-^{NWX})$, we have shown $A_{\mathbb{X},0}(x_-^{NWX}) = A_{\mathbb{X},0}(x_-^{NWX})$. The Alexander grading shift of ψ is 0 as claimed.

To produce the skein triangle, we now make use of the following lemma. A singly graded version of this lemma is stated in [OSS15, Lemma A.3.10], but the proof is easily adapted to the bigraded setting.

Lemma A.1. *Suppose that C, C' , and C'' are three bigraded chain complexes, and $f : C' \to C''$ and $g : C \to C'$ are chain maps that are homogeneous of degrees (a, p) and (b, q) respectively. Then, there is a chain map $\Phi : Cone(f) \to Cone(g)$ which is homogeneous of degree $(-a-1, -p)$ and whose induced map on homology fits into the following exact triangle with bidegrees as indicated*

$$\begin{array}{ccc} H(Cone(f)) & \xrightarrow{(-a-1,-p)} & H(Cone(g)) \\ & {\scriptstyle (0,0)} \nwarrow \quad \swarrow {\scriptstyle (a,p)} & \\ & H(Cone(f \circ g)) & \end{array}$$

In Lemma A.1, let $f = \partial_{N_-}^{I_-}$ and $g = \psi \circ \partial_{I_0}^{N_0}$. Then we have $deg(f) = (-1, 0)$, and hence the following exact triangle is established:

$$\begin{array}{ccc} H(\mathrm{Cone}(\partial_{N_-}^{I_-})) & \xrightarrow{(0,0)} & H(\mathrm{Cone}(\psi \circ \partial_{I_0}^{N_0})) \\ & {\scriptstyle (0,0)} \nwarrow \quad \swarrow {\scriptstyle (-1,0)} & \\ & H(\mathrm{Cone}(\partial_{N_-}^{I_-} \circ \psi \circ \partial_{I_0}^{N_0})) & \end{array}$$

There are isomorphisms

$$H(\mathrm{Cone}(\psi \circ \partial_{I_0}^{N_0})) \cong H(\mathrm{Cone}(\partial_{I_0}^{N_0})) \cong \widetilde{GH}(\mathbb{G}_0) \tag{A.6}$$

where the first follows because ψ is an isomorphism of bi-degree $(0,0)$, and the second follows because the differential on $\mathrm{Cone}(\partial_{I_0}^{N_0})$ is by definition $\begin{bmatrix} \partial_{I_0}^{I_0} & 0 \\ \partial_{I_0}^{N_0} & \partial_{N_0}^{N_0} \end{bmatrix}$ which is the full differential on $\widetilde{GH}(\mathbb{G}_0) = I_0 \oplus N_0$ since N_0 is a subcomplex ($\partial_{I_0}^{N_0} = 0$). Similarly there is an isomorphism

$$H(\mathrm{Cone}(\partial_{N_-}^{I_-})) \cong \widetilde{GH}(\mathbb{G}_-). \tag{A.7}$$

Also notice that $\partial_{N_-}^{I_-} \circ \psi \circ \partial_{I_0}^{N_0} : (I_0, \partial_{I_0}^{I_0}) \to \partial_{N_-}^{I_-}(I_-, \partial_{I_-}^{I_-})$ is the zero map and has degree $(-2,0)$. We have the following equalities and isomorphisms of chain complexes:

(A.8)
$$\mathrm{Cone}(\partial_{N_-}^{I_-} \circ \psi \circ \partial_{I_0}^{N_0})_{(d,s)} = (I_0)_{(d+1,s)} \oplus (I_-)_{(d,s)} \cong (I_0)_{(d+1,s)} \oplus (I_0)_{(d,s-1)} = (I_0 \otimes V)[[0,-1]]_{(d,s)}$$

For a bigraded chain complex C, the notation $C[[a,b]]$ denotes the grading shifted complex $C[[a,b]]_{(d,s)} := C_{d+a,b+s}$. The bidegree of the isomorphism $(I_-)_{(d,s)} \cong (I_0)_{(d,s-1)}$ follows from our previous observation that the $\mathbb{O}$ sets of $\mathbb{G}_-$ and $\mathbb{G}_0$ being identical implies $M_{\mathbb{O},-} = M_{\mathbb{O},0}$, and from Equation (A.2). Putting these identifications into the exact triangle yields

$$\begin{array}{ccc} \widetilde{GH}(\mathbb{G}_-) & \xrightarrow{\quad (0,0) \quad} & \widetilde{GH}(\mathbb{G}_0) \\ & {\scriptstyle (0,0)} \nwarrow \quad \swarrow {\scriptstyle (-1,0)} & \\ & (H(I_0) \otimes V)[[0,-1]] & \end{array}$$

Taking bi-graded Euler characteristics (which we denote by the symbol χ) of this exact triangle we get

$$\chi(\widetilde{GH}(\mathbb{G}_-)) = \chi(\widetilde{GH}(\mathbb{G}_0)) + \chi((H(I_0) \otimes V)[[0,-1]]). \tag{A.9}$$

Equations 3.6 and 3.9 tell us that

$$\chi(\widetilde{GH}(\mathbb{G}_-)) = \chi(\widehat{HFK}(S_-) \otimes V^{(m+1)-2}) = \Delta_{S_-}(t)(t^{\frac{1}{2}} - t^{-\frac{1}{2}})(1-t^{-1})^{m-1}$$

and similarly

$$\chi(\widetilde{GH}(\mathbb{G}_0)) = \chi(\widehat{HFK}(S_0) \otimes V^{(m+1)-1}) = \Delta_{S_0}(t)(1-t^{-1})^m.$$

In addition,

$$\chi((H(I_0) \otimes V)[[0,-1]]) = \chi(H(I_0))(1-t^{-1}) \cdot t.$$

Making these replacements in Equation (A.9) and dividing through by $t^{\frac{1}{2}}(1-t^{-1})^m$ yields

$$\Delta_{S_-}(t) = \frac{t^{\frac{1}{2}}\chi(H(I_0))}{(1-t)^{m-1}} + t^{-\frac{1}{2}}\Delta_{S_0}(t). \tag{A.10}$$

Comparing Equation (A.10) to Equation (3.15) shows that

$$\frac{t^{\frac{1}{2}}\chi(H(I_0))}{(1-t)^{m-1}} = \Delta_S. \tag{A.11}$$

Substituting $t^{\frac{1}{2}}\chi(H(I_0)) = \chi(H(I_0)[[0,-\frac{1}{2}]])$ and $\chi(\widetilde{GH}(\mathbb{G}_S)) = \Delta_S(t)(1-t^{-1})^{m-1}$ into Equation (A.11) we conclude

$$\chi(H(I_0)[[0,-\frac{1}{2}]]) = \chi(\widetilde{GH}(\mathbb{G}_S)). \tag{A.12}$$

The complex $\widetilde{GC}(\mathbb{G}_S)$ is, up to a bidegree shift, isomorphic to the complex I_0 through an isomorphism

$$F : \widetilde{GC}(\mathbb{G}_S) \to I_0$$

taking a generator in $\widetilde{GC}(\mathbb{G}_S)$ and mapping it to the corresponding generator in I_0 that contains the center point c. More explicitly, we have

$$F(\{(1,x_1),\dots,(m,x_m)\}) = \{(1,x_1),\dots,(\frac{m-1}{2},x_{\frac{m-1}{2}}),(\frac{m+1}{2},\frac{m+1}{2}),(\frac{m+3}{2},x_{\frac{m+1}{2}}),\dots,(m+1,x_m)\}.$$

By Equation (A.12) F increases Alexander grading by $\frac{1}{2}$ and changes Maslov grading by some even integer $2j$. Making the replacement $H(I_0) \cong \widetilde{GH}(\mathbb{G}_S)[[2j,\frac{1}{2}]]$ in the exact triangle gives us

$$\begin{array}{ccc} \widetilde{GH}(\mathbb{G}_-) & \xrightarrow{(0,0)} & \widetilde{GH}(\mathbb{G}_0) \\ & {\scriptstyle (0,0)}\nwarrow \quad \swarrow{\scriptstyle (-1,0)} & \\ & (\widetilde{GH}(\mathbb{G}_S)\otimes V)[[2j,-\tfrac{1}{2}]] & \end{array}$$

which is the exact triangle (3.18) upon identifying grid homology with (singular) knot Floer homology.

□

Remark A.2. With a more careful analysis we could show that $j = 0$ but this is unnecessary for our purposes.

The main reason that we gave a proof of Proposition 3.4 was the following corollary that was shown along the way:

Corollary A.3. *Let $\mathbb{G}_S$ and I_0 be as in the proof of Proposition 3.4. Then there is an isomorphism of chain complexes*

$$I_0 \cong \widetilde{GC}(\mathbb{G}_S)[[2j,\frac{1}{2}]]. \tag{A.13}$$

Now we modify the above proof to work for the spherical grid diagrams of Section 3.5. Performing the construction of Section 3.5.3 three times we obtain spherical grid diagrams $\mathbb{G}_S^{\text{sphere}}$, $\mathbb{G}_0^{\text{sphere}}$ and $\mathbb{G}_-^{\text{sphere}}$ for $S_b^n(\widetilde{K})$, $L_b^{n+\frac{1}{2}}(\widetilde{K})$ and $L_b^n(\widetilde{K})$ respectively. Just as in the proof of Proposition 3.4, let c denote the center point of the top grid of $\mathbb{G}_0^{\text{sphere}}$ and $\mathbb{G}_-^{\text{sphere}}$. Define sub-complexes I_- generated by those states in $\widetilde{CFL}(\mathbb{G}_-^{\text{sphere}})$ that contain c, and N_0 generated those states in $\widetilde{CFL}(\mathbb{G}_0^{\text{sphere}})$ that don't contain c. Also define quotient complexes I_0 generated by those states in $\widetilde{CFL}(\mathbb{G}_-^{\text{sphere}})$ that don't contain c, and N_- generated by those states in $\widetilde{CFL}(\mathbb{G}_0^{\text{sphere}})$ that contain c. We can prove the following analog of Corollary A.3 for spherical diagrams, using almost the same argument.

Proposition A.4. *The map $F(\mathbf{x}) = \mathbf{x} \cup c$ is a chain isomorphism*

$$F : \widetilde{CFL}(\mathbb{G}_S^{sphere})[[2j,\frac{1}{2}]] \cong I_0 \tag{A.14}$$

for some integer j.

Remark A.5. In the proof below of Proposition A.4, we reuse the notation of the proof of Proposition 3.4 to facilitate a direct comparison between the proofs.

Proof. There is an isomorphism $\psi : N_0 \to N_-$ defined as the identity map on tuples of grid intersection points, and isomorphisms $\widetilde{CFL}(\mathbb{G}_S^{\text{sphere}}) \cong I_0$ defined by taking a generator in $\widetilde{CFK}(\mathbb{G}_S^{\text{sphere}})$ and mapping it to the corresponding generator in I_0 containing c. Consider the composition of chain maps

$$(I_0, \partial_{I_0}^{I_0}) \xrightarrow[(-1,0)]{\partial_{I_0}^{N_0}} (N_0, \partial_{N_0}^{N_0}) \xrightarrow{\psi} (N_-, \partial_{N_-}^{N_-}) \xrightarrow[(-1,0)]{\partial_{N_-}^{I_-}} (I_-, \partial_{I_-}^{I_-}) \tag{A.15}$$

If we can show that the bidegree of ψ is $(0,0)$ and that the map $\xi : I_0 \to I_-$ defined as the identity on tuples of grid states containing c has bidegree $(0,1)$, then the argument given in the proof of Proposition 3.4 applies verbatim to prove this proposition as well. In what follows we will make use of the gradings $M = gr_w$ and gr_z which are the direct analogs of $M_{\mathbb{O}}$ and $M_{\mathbb{X}}$ for more general Heegaard diagrams. We see that gr_w is preserved by both ψ and ξ since both spherical diagrams have the same w basepoints. We imitate the grading pinning procedure demonstrated in of [MOS07, Lemma 3.2, Figure 8] to determine for the gr_z grading shift associated to ψ. Consider a state $\mathbf{y} \in \widetilde{CFL}(\mathbb{G}_-^{\text{sphere}})$ and a state $\mathbf{x} \in \widetilde{CFK}(\mathbb{G}_0^{\text{sphere}})$ that differ only in that they contain the intersection points Southwest of the two central z's on their respective diagrams. Then $\mathbf{x}$ and $\mathbf{y}$ must in fact have the same gr_z grading since upon forgetting about $w's$ and handle-sliding all but one of the β curves to become small loops about z's, these two states correspond through empty Maslov index 1 triangles to the *same* bottom-most gr_z state in the complex used to pin down the gr_z grading. This is illustrated in Figure 24. So we see that

$$gr_z(\mathbf{x}) - gr_z(\psi(\mathbf{x})) = gr_z(\mathbf{y}) - gr_z(\psi(\mathbf{x})) = -1.$$

The last equality follows from applying the relative gr_z grading formula, which states that $gr_z(\mathbf{y}) - gr_z(\psi(\mathbf{x})) = \mu(\phi) - 2n_z(\phi)$ with ϕ equal to the one by one square containing a z and connecting $\mathbf{x}$ and $\mathbf{y}$ in $\mathbb{G}_-^{\text{sphere}}$. The Alexander grading is $A = \frac{gr_w - gr_z}{2} - \frac{m-\ell}{2}$ where m is the number of basepoints on the Heegaard diagram and ℓ is the number of link components. Therefore we see that

$$\begin{aligned} A(\mathbf{x}) =& \frac{gr_w(\mathbf{x}) - gr_z(\mathbf{x})}{2} - \frac{(k+1)-1}{2} = \frac{gr_w(\psi(\mathbf{x})) - (gr_z(\psi(\mathbf{x})) - 1))}{2} - \frac{(k+1)-1}{2} = \\ & \frac{gr_w(\psi(\mathbf{x})) - gr_z(\psi(\mathbf{x})))}{2} - \frac{(k+1)-2}{2} = A(\psi(\mathbf{x})) \end{aligned}$$

and hence $deg(\psi) = (0,0)$. A very similar computation shows that $deg(\xi) = (0,0)$. □

Let a and b denote the Northeast and Southwest intersection points of the square containing the central w, and let AxI_0 be the quotient complex of $\widetilde{CFL}(Ax\mathbb{G}_0^{\text{sphere}})$ generated by states containing both a and b. The following proposition follows from a similar argument to the one given in the proof of Proposition A.4.

Proposition A.6. *Then map* $\Phi(\mathbf{x}) := \mathbf{x} \cup a \cup b$ *is a chain isomorphism*

$$\widetilde{CFL}(\mathbb{G}_S^{sphere})[[2j, \frac{1}{2}]] \cong AxI_0. \tag{A.16}$$

In Figure 25, we show the quotient diagram $Ax\mathbb{G}_0^{\text{sphere}}/\tau$, which is a Heegaard diagram for the quotient knot K along with the orientation reversed axis A. Figure 26 shows the same Heegaard diagram after isotopies of α_{k+1} and β_{k+1} that go over the rightmost z. Such isotopies do not affect

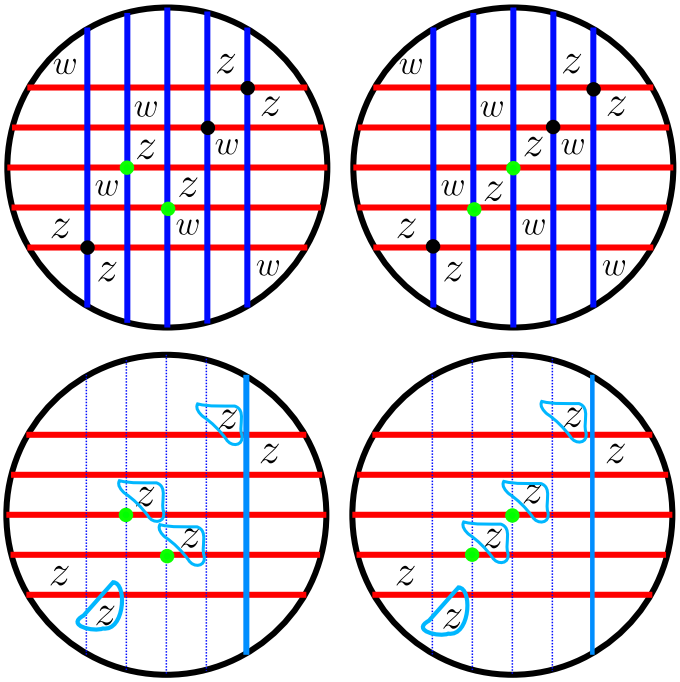

FIGURE 24. Top: The top halves of the diagrams $\mathbb{G}_-^{\text{sphere}}$ and $\mathbb{G}_0^{\text{sphere}}$. Bottom: Both diagrams are the same up to isotopy after deleting w basepoints and performing the displayed handleslides amongst the β curves.

the homology of the complex $(\widetilde{CFL}(Ax\mathbb{G}_*^{\text{sphere}}/\tau), \partial_A)$. This isotoped diagram B *is* the quotient diagram $\mathbb{G}_S^{\text{sphere}}/\tau$ except for the addition of

- the isotoped α_{k+1} and β_{k+1} curves that now meet only each other in the two points p and q,
- the leftmost w basepoint contained in the central bigon formed by α_{k+1} and β_{k+1}, and
- the rightmost z that the differential ∂_A does not see.

With these observations and notation in place, we can state and prove the following proposition

Proposition A.7. *The map*

$$\mathcal{P} : \widetilde{CFL}(\mathbb{G}_S^{sphere}/\tau) \to \widetilde{CFL}(Ax\mathbb{G}_0^{sphere}/\tau)$$

defined by $\mathcal{P}(\mathbf{x}) = \mathbf{x} \cup p$ *preserves Alexander gradings.*

Proof. Since the region that $\alpha_{k+1} \cup \beta_{k+1}$ is contained in also contains a z marking, namely the top left corner of $\mathbb{G}_0^{\text{IV}}$, we obtain a grading preserving isomorphism of chain complexes

$$(\widetilde{CFL}(B), \partial_A) \cong \widetilde{CFL}(\mathbb{G}_S^{\text{sphere}}/\tau) \otimes W.$$

The gradings on the tensor factor of $W = \mathbb{F}_{(0,0)} \oplus \mathbb{F}_{(1,0)}$ (the two summands correspond to those generators in $\widetilde{CFL}(B)$ containing either p or q) are fixed by the homology of the complex $(\widetilde{CFL}(B), \partial_A) \cong (\widetilde{CFL}(\mathbb{G}_0^{\text{sphere}}/\tau), \partial_A)$. In particular,

$$P : \widetilde{CFL}(\mathbb{G}_S^{\text{sphere}}/\tau) \to \widetilde{CFL}(B, \partial_A)$$

defined on a generator $\mathbf{x} \in \widetilde{CFL}(\mathbb{G}_S^{\text{sphere}}/\tau)$ by $P(\mathbf{x}) = \mathbf{x} \cup p$ is an Alexander grading preserving map. The map P' sending a generator containing p in $\widetilde{CFL}(B)$ to the corresponding generator containing p in $\widetilde{CFL}(Ax\mathbb{G}_0^{\text{sphere}}/\tau), \partial_A)$ is also Alexander grading preserving. Finally we have that $\mathcal{P} = P' \circ P$. □

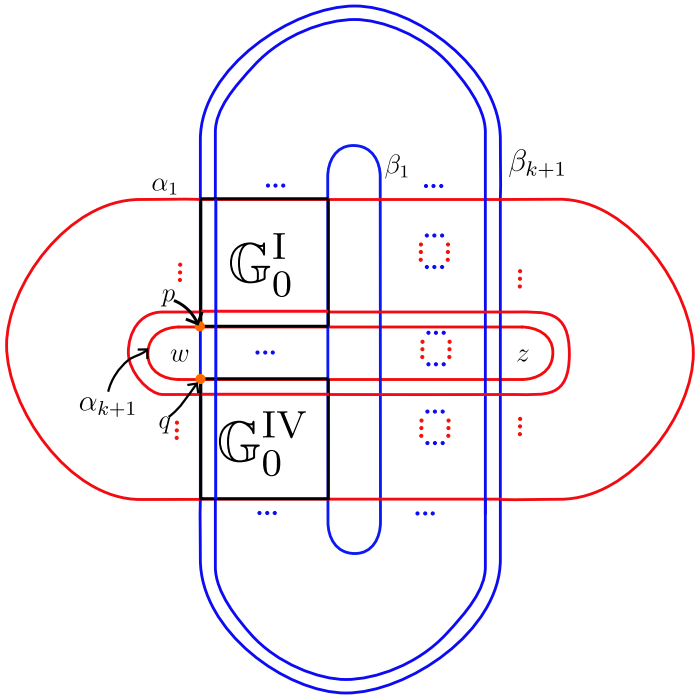

FIGURE 25. The quotient diagram $\mathbb{G}_0^{\text{sphere}}/\tau$.

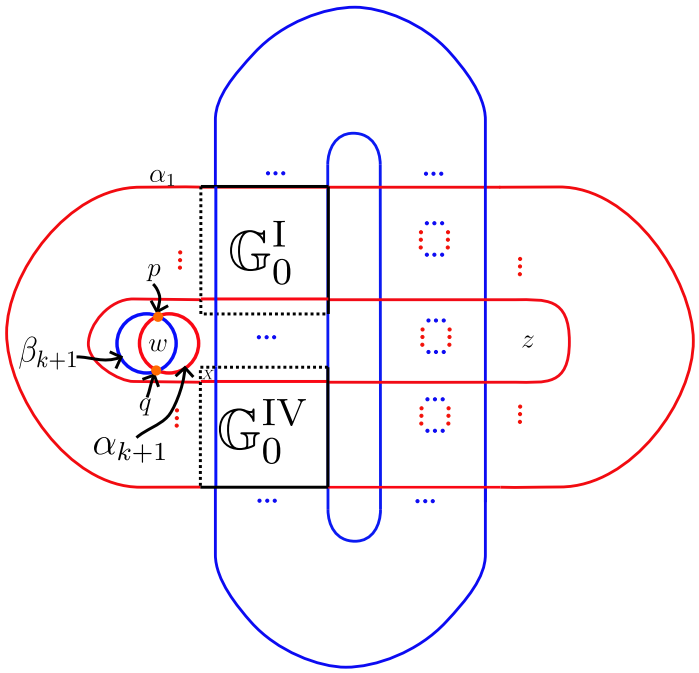

FIGURE 26. The diagram B obtained by isotoping α_{k+1} over the rightmost z and all of the β curves besides β_{k+1} and then isotoping β_{k+1} over the rightmost z and over all the α curves besides α_{k+1}.

REFERENCES

[AB21] Antonio Alfieri and Keegan Boyle, *Strongly invertible knots, invariant surfaces, and the atiyah-singer signature theorem*, 2021.

[Ali22] Akram Alishahi, *Upsilon invariant for graphs and the homology cobordism group of homology cylinders*, 2022.

[AP23] Anna Antal and Sarah Pritchard, *A note on the involutive concordance invariants for certain (1,1)-knots*, 2023.

[BEHY18] Khaled Bataineh, Mohamed Elhamdadi, Mustafa Hajij, and William Youmans, *Generating sets of reidemeister moves of oriented singular links and quandles*, 2018.

[BG07] John A. Baldwin and W. D. Gillam, *Computations of heegaard-floer knot homology*, 2007.

[BI22] Keegan Boyle and Ahmad Issa, *Equivariant 4-genera of strongly invertible and periodic knots*, J. Topol. **15** (2022), no. 3, 1635–1674. MR 4461855

[BW20] Yuanyuan Bao and Zhongtao Wu, *An alexander polynomial for moy graphs*, 2020.

[DMS22] Irving Dai, Abhishek Mallick, and Matthew Stoffregen, *Equivariant knots and knot floer homology*, 2022.

[Hat03] A. Hatcher, *Vector bundles and k-theory*, 2003, http://www.math.cornell.edu/~hatcher.

[Hen12] Kristen Hendricks, *A rank inequality for the knot floer homology of double branched covers*, Algebraic &amp Geometric Topology **12** (2012), no. 4, 2127–2178.

[Hen15] Kristen Hendricks, *Localization of the link Floer homology of doubly-periodic knots*, J. Symplectic Geom. **13** (2015), no. 3, 545–608. MR 3412087

[HHS23] Mikami Hirasawa, Ryota Hiura, and Makoto Sakuma, *The equivariant genera of marked strongly invertible knots associated with 2-bridge knots*, 2023.

[HLL22] Kristen Hendricks, Tye Lidman, and Robert Lipshitz, *Rank inequalities for the heegaard floer homology of branched covers*, 2022.

[HLS16] Kristen Hendricks, Robert Lipshitz, and Sucharit Sarkar, *A flexible construction of equivariant floer homology and applications*, Journal of Topology **9** (2016), no. 4, 1153–1236.

[HMR24] Kristen Hendricks, Cheuk Yu Mak, and Sriram Raghunath, *Symplectic annular khovanov homology and fixed point localizations*, 2024.
[HO17] Shelly Harvey and Danielle O'Donnol, *Heegaard floer homology of spatial graphs*, Algebraic &; Geometric Topology **17** (2017), no. 3, 1445–1525.
[kno] *Knotfolio*, `https://knotfol.io/`, Accessed: 2024-08-20.
[Lar19] Tim Large, *Equivariant floer theory and double covers of three-manifolds*, 2019.
[LS22] Robert Lipshitz and Sucharit Sarkar, *Khovanov homology of strongly invertible knots and their quotients*, 2022.
[LW21] Andrew Lobb and Liam Watson, *A refinement of khovanov homology*, Geometry &; Topology **25** (2021), no. 4, 1861–1917.
[Mac62] I. G. Macdonald, *Symmetric products of an algebraic curve*, Topology **1** (1962), 319–343. MR 151460
[MD95] Salamon Dietmar McDuff Dusa, *Introduction to sympletic topology*, Oxford Mathematical Monographs, The Clarendon Press Oxford University Press, 1995. MR 1373431
[MO05] Ciprian Manolescu and Brendan Owens, *A concordance invariant from the floer homology of double branched covers*, 2005.
[MOS07] Ciprian Manolescu, Peter Ozsvath, and Sucharit Sarkar, *A combinatorial description of knot floer homology*, 2007.
[OS03] Peter Ozsváth and Zoltán Szabó, *Knot Floer homology and the four-ball genus*, Geom. Topol. **7** (2003), 615–639.
[OS04a] ———, *Heegaard diagrams and holomorphic disks*, Different faces of geometry, Int. Math. Ser. (N. Y.), vol. 3, Kluwer/Plenum, New York, 2004, pp. 301–348.
[OS04b] ———, *Holomorphic disks and knot invariants*, Adv. Math. **186** (2004), no. 1, 58–116.
[OS04c] ———, *Holomorphic disks and topological invariants for closed three-manifolds*, Ann. of Math. (2) **159** (2004), no. 3, 1027–1158.
[OS08a] Peter Ozsváth and Zoltán Szabó, *Holomorphic disks, link invariants and the multi-variable Alexander polynomial*, Algebraic & Geometric Topology **8** (2008), no. 2, 615 – 692.
[OS08b] ———, *Holomorphic disks, link invariants and the multivariable alexander polynomial*, Algebraic and Geometric Topology **8** (2008), no. 2, 615–692 (English (US)).
[OS09] Peter Ozsváth and Zoltán Szabó, *A cube of resolutions for knot Floer homology*, J. Topol. **2** (2009), no. 4, 865–910. MR 2574747
[OSS09] Peter Ozsváth, András Stipsicz, and Zoltán Szabó, *Floer homology and singular knots*, J. Topol. **2** (2009), no. 2, 380–404. MR 2529302
[OSS15] Peter Ozsvath, Zoltan Szabo, and Andras Stipsicz, *Grid homology for knots and links*, American Mathematical Society, United States of America, 2015.
[Per08] Tim Perutz, *A remark on kähler forms on symmetric products of riemann surfaces*, 2008.
[Pri22] Alessio Di Prisa, *The equivariant concordance group is not abelian*, 2022.
[Pri23] ———, *Equivariant algebraic concordance of strongly invertible knots*, 2023.
[Ras03] Jacob Andrew Rasmussen, *Floer homology and knot complements*, ProQuest LLC, Ann Arbor, MI, 2003, Thesis (Ph.D.)–Harvard University.
[Ras04] Jacob A. Rasmussen, *Khovanov homology and the slice genus*, 2004.
[Sak86] Makoto Sakuma, *On strongly invertible knots*, Algebraic and topological theories (Kinosaki, 1984), Kinokuniya, Tokyo, 1986, pp. 176–196. MR 1102258
[SS10] Paul Seidel and Ivan Smith, *Localization for involutions in Floer cohomology*, Geom. Funct. Anal. **20** (2010), no. 6, 1464–1501. MR 2739000
[SW10] Sucharit Sarkar and Jiajun Wang, *An algorithm for computing some heegaard floer homologies*, Annals of Mathematics **171** (2010), no. 2, 1213–1236.

Email address: `ap1792@math.rutgers.edu`

Rutgers University, New Brunswick, NJ, USA